

AD-A123 845

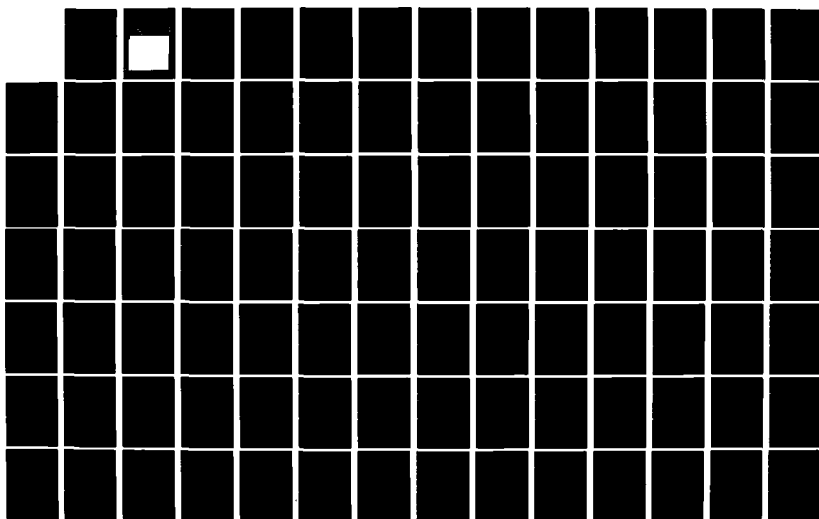
TIME SCALES COHERENCY AND WEAK COUPLING(U) ILLINOIS
UNIV AT URBANA DECISION AND CONTROL LAB B AVRAMOVIC
OCT 88 DC-48 N00014-79-C-0424

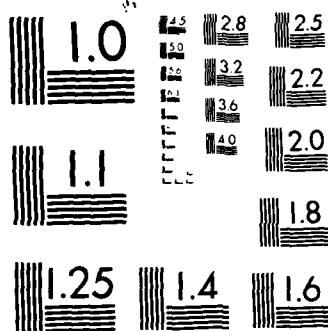
1/2

UNCLASSIFIED

F/G 12/1

NL





MICROCOPY RESOLUTION TEST CHART
NATIONAL BUREAU OF STANDARDS 1963-A

2

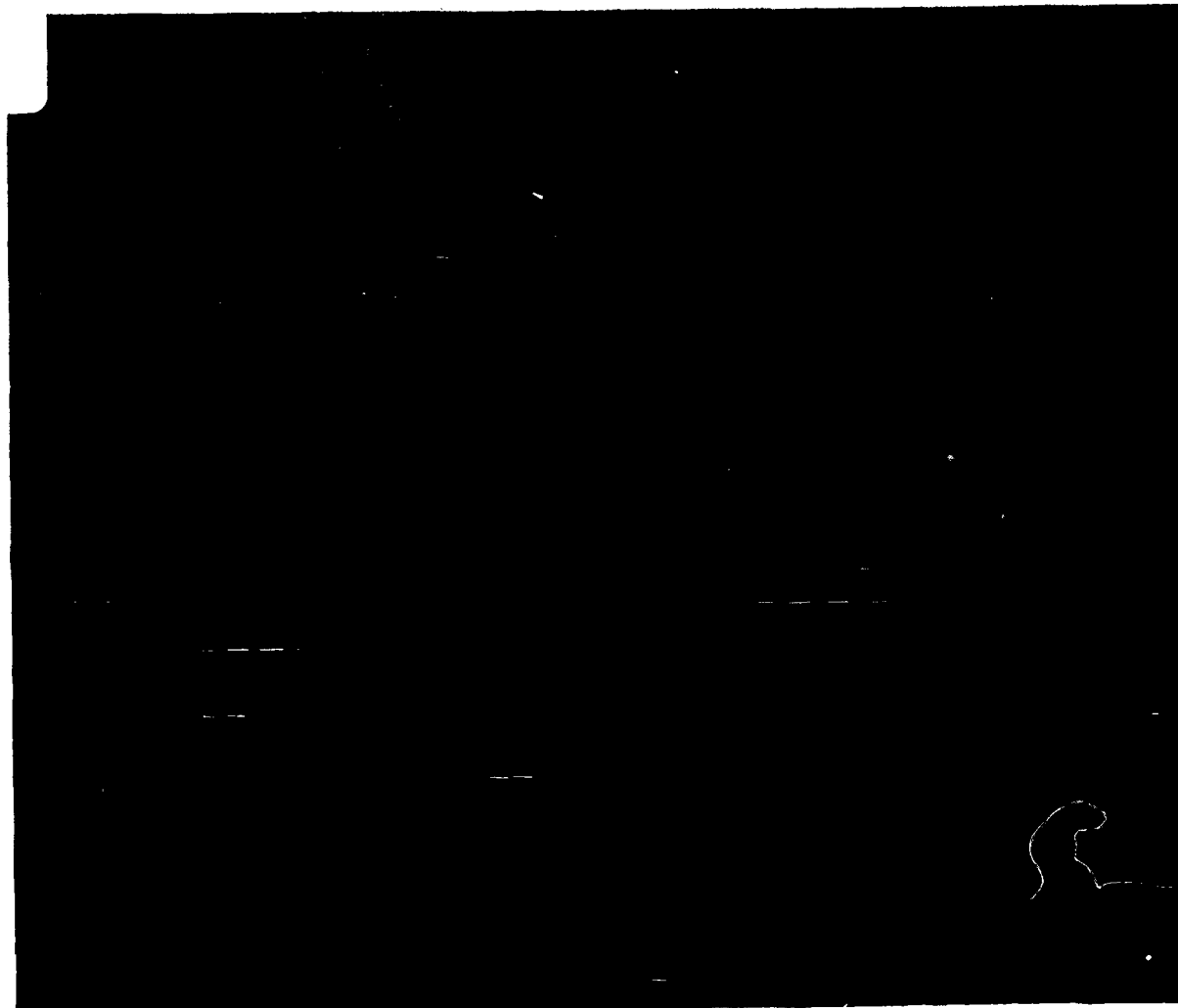
OCTOBER, 1980

COORDINATED SCIENCE LABORATORY
DECISION AND CONTROL LABORATORY

ADA 125845

**TIME SCALES,
COHERENCY,
AND WEAK COUPLING**

DTIC
ELECTE
MAR 21 1983
A



DTIC FILE COPY

UNIVERSITY OF ILLINOIS AT URBANA-CHAMPAIGN

83 03 21 008

UNCLASSIFIED

SECURITY CLASSIFICATION OF THIS PAGE (When Data Entered)

REPORT DOCUMENTATION PAGE		READ INSTRUCTIONS BEFORE COMPLETING FORM
1. REPORT NUMBER	2. GOVT ACCESSION NO.	3. RECIPIENT'S CATALOG NUMBER
	AD-A125 845	
4. TITLE (and Subtitle)		5. TYPE OF REPORT & PERIOD COVERED
TIME SCALES, COHERENCY, AND WEAK COUPLING		Technical Report ^{EN}
		6. PERFORMING ORG. REPORT NUMBER
		R-895(DC-40); UILU-80-2227
7. AUTHOR(s)		8. CONTRACT OR GRANT NUMBER(s)
BOZIDAR AVRAMOVIC		DOE-EX-76-C-01-2088
		NSF-ECS-79-19396
		N00014-79-C-0424
9. PERFORMING ORGANIZATION NAME AND ADDRESS		10. PROGRAM ELEMENT, PROJECT, TASK AREA & WORK UNIT NUMBERS
11. CONTROLLING OFFICE NAME AND ADDRESS		12. REPORT DATE
Joint Services Electronics Program		October 1980
		13. NUMBER OF PAGES
		143
14. MONITORING AGENCY NAME & ADDRESS (if different from Controlling Office)		15. SECURITY CLASS. (of this report)
		UNCLASSIFIED
		15a. DECLASSIFICATION/DOWNGRADING SCHEDULE
16. DISTRIBUTION STATEMENT (of this Report)		
Approved for public release; distribution unlimited.		
17. DISTRIBUTION STATEMENT (of the abstract entered in Block 20, if different from Report)		
18. SUPPLEMENTARY NOTES		
19. KEY WORDS (Continue on reverse side if necessary and identify by block number)		
reduced order modeling direct stability analysis of power systems coherency weak coupling decomposition and aggregation nonlinear system simulation		
20. ABSTRACT (Continue on reverse side if necessary and identify by block number)		
In this thesis we study a relation between time scales and structural properties of a class of systems represented by power systems. First, the time scale decomposition of linear time invariant systems is studied. The properties of the time scale decomposition are shown to be defined by properties of solutions of a generalized matrix Riccati equation. Use of the Riccati equation formulation and a particular method for finding its solution led to the result which shows that the singular perturbation method and modal method for reduced order modeling are two extreme points of an iterative method for the time scale		

UNCLASSIFIED

SECURITY CLASSIFICATION OF THIS PAGE(When Data Entered)

20. Abstract (continued)

decomposition: singular perturbation is its first point and modal method is the limiting point. Convergence properties of a known class of iterative methods for the time scale decomposition are characterized. A method for the time scale decomposition of weakly nonlinear systems is proposed as an extension of linear system analysis to nonlinear systems. Then, for electromechanical model of power systems a connection between its time scales and structural properties is established by showing that the so-called slow coherency can be expressed in terms of the same Riccati equation used for the time scale decomposition. It is shown analytically and then confirmed experimentally on a few realistic size systems, that in the case of slow coherency, the coherent areas are weakly coupled, and hence relatively independent on the fault location. By using the Riccati formulation of coherency, an efficient numerical algorithm for identifying coherent areas is obtained. Finally, a possibility of extending this study to the direct transient stability analysis of power systems is briefly discussed.

SECURITY CLASSIFICATION OF THIS PAGE(When Data Entered)

UILU-80-2227

TIME SCALES, COHERENCY, AND WEAK COUPLING

by

Bozidar Avramovic

This work was supported in part by the U. S. Department of Energy, Electric Energy Systems Division, under Contract EX-76-C-01-2088; in part by the National Science Foundation under Grant ECS-79-19396; and in part by the Joint Services Electronics Program under Contract N00014-79-C-0424.

Reproduction in whole or in part is permitted for any purpose of the United States Government.

Approved for public release. Distribution unlimited.

TIME SCALES, COHERENCY, AND WEAK COUPLING

BY

BOZIDAR AVRAMOVIC

Dipl., University of Belgrade, 1973
M.S., University of Belgrade, 1978

THESIS

Submitted in partial fulfillment of the requirements
for the degree of Doctor of Philosophy in Electrical Engineering
in the Graduate College of the
University of Illinois at Urbana-Champaign, 1980

Thesis Advisor: Professor P. V. Kokotovic

Urbana, Illinois

TIME SCALES, COHERENCY, AND WEAK COUPLING

Bozidar R. Avramovic, Ph.D.
Department of Electrical Engineering
University of Illinois at Urbana-Champaign, 1980

In this thesis we study a relation between time scales and structural properties of a class of systems represented by power systems. First, the time scale decomposition of linear time invariant systems is studied. The properties of the time scale decomposition are shown to be defined by properties of solutions of a generalized matrix Riccati equation. Use of the Riccati equation formulation and a particular method for finding its solution led to the result which shows that the singular perturbation method and modal method for reduced order modeling are two extreme points of an iterative method for the time scale decomposition: singular perturbation is its first point and modal method is the limiting point. Convergence properties of a known class of iterative methods for the time scale decomposition are characterized. A method for the time scale decomposition of weakly nonlinear systems is proposed as an extension of linear system analysis to nonlinear systems. Then, for electromechanical model of power systems a connection between its time scales and structural properties is established by showing that the so-called slow coherency can be expressed in terms of the same Riccati equation used for the time scale decomposition. It is shown analytically and then confirmed experimentally on a few realistic size systems, that in the case of slow coherency, the coherent areas are weakly coupled, and hence relatively independent on

the fault location. By using the Riccati formulation of coherency, an efficient numerical algorithm for identifying coherent areas is obtained. Finally, a possibility of extending this study to the direct transient stability analysis of power systems is briefly discussed.

ACKNOWLEDGMENT

The author would like to express his appreciation to Professors J. B. Cruz, Jr., W. R. Perkins, P. V. Kokotovic, I. N. Hajj, and P. W. Sauer for serving on his doctoral committee.

He would especially like to express his gratitude he feels toward his advisor, Professor P. V. Kokotovic, for his guidance and concern. Most sincere thanks also go to Professor J. V. Medanic, Dr. J. H. Chow, and Dr. J. Winkelman, for numerous hours of fruitful discussions. The author highly regards many stimulating discussions with Dr. J. D. Cobb and Professor A. Sameh. He would also like to thank Mrs. Trudy Little, and especially Mrs. Rose Harris for their excellent typing.

Finally, the author expresses his appreciation to his family for their encouragement and support.

TABLE OF CONTENTS

	Page
1. INTRODUCTION	1
1.1. Methods for Reduced Order Modeling with Applications to Power Systems	1
1.2. Contributions of the Thesis	5
1.3. Chapter Preview	7
2. TIME SCALE DECOMPOSITION VIA RICCATI APPROACH	9
2.1. Problem Formulation	9
2.2. Time Scales and Generalized Riccati Equation	9
2.3. Practical Aspects of the Spectrum Separation Problem	19
2.4. Relation Between Singular Perturbation, Time Scale Decomposition and Modal Methods	21
2.5. Block Diagonalization	34
2.6. Time Scale Separation in Weakly Nonlinear Systems	36
3. PARTIAL COHERENCY	45
3.1. Introduction	45
3.2. Electromechanical Model	47
3.3. Review of Existing Coherency Methods	53
3.4. Partial Coherency	54
3.5. Grouping Algorithm	68
3.6. Area Variables and Intermachine Variables	77
4. SLOW COHERENCY, WEAK COUPLING, AND NONLINEAR EQUIVALENTS	81
4.1. Introduction	81
4.2. Electromechanical Equivalent of Area Dynamics	81
4.3. Structural Conditions for Coherency	86
4.4. Weak Coupling Between Areas	88
4.5. Sensitivity of Area Boundaries to Parameter Changes	94
4.6. Use of Slow Coherency in Nonlinear System Analysis	100
4.7. 48 Machine Example	105
4.8. Numerical Aspects of the Slow Coherency Algorithm	111
4.9. Summary of the Chapter	115
5. SUGGESTIONS AND CONCLUSIONS	117
5.1. Suggestions for Further Research	117
5.2. Conclusions	124
REFERENCES	126

	Page
APPENDIX A. ONE MACHINE INFINITE BUS MODEL [34]	131
APPENDIX B. MATRIX A OF $\ddot{\delta} = A\delta$ FOR THE 48 MACHINE SYSTEM	135
VITA	142
PUBLICATIONS	143

1. INTRODUCTION

1.1. Methods for Reduced Order Modeling with Applications to Power Systems

An object of study in this thesis is the relation between singular perturbation, modal methods and coherency when used for modal order reduction of electromechanical models of power systems. We will show that all these methods are closely related if coherency is suitably defined.

Modal method, originally proposed by Davison [1] and further analyzed by many researchers [2,3] consists of approximating the system

$$\dot{x} = Ax, \quad \dim A = n \quad (1.1)$$

by one of lower order

$$\dot{z} = Fz, \quad \dim F = r. \quad (1.2)$$

It can be shown [4,5] that modal methods can be understood as a particular case of aggregation [6,7], i.e. there exists a matrix K , such that

$$z = Kx \quad (1.3)$$

and

$$FK = KA. \quad (1.4)$$

Aggregation matrix F is then given as

$$F = KAK^+, \quad KK^+ = I \quad (1.5)$$

In [5] it is shown that K has to be of the form

$$K = M(I \ 0)X^{-1} \quad (1.6)$$

where M is an arbitrary nonsingular $r \times r$ matrix and X is the $n \times n$ matrix of right eigenvectors of A . With such K , and $\sigma(\cdot)$ denoting

spectrum of a matrix,

$$\sigma(F) \subset \sigma(A). \quad (1.7)$$

In modal methods of [1] $M = X_{rr}$, which is r -dimensional principal minor of X ordered so that the first r columns correspond to the eigenvalues to be retained in F , and

$$F = A_{11} + A_{12} X_{21} X_{11}^{-1} \quad (1.8)$$

where $X_{11} = X_{rr}$ and X_{21} is "21" block in the matrix X .

In the singular perturbation approach [8], it is assumed that the state vector x consists of subvector x_1 , with r basically slow variables, and of the complementary vector x_2 having variables with mixed fast and slow dynamics. The presense of different speeds of response in these two sets of variables is indicated by writing the model (1.1) in the form

$$\begin{aligned} \dot{x}_1 &= A_{11}x_1 + A_{12}x_2 \\ \varepsilon \dot{x}_2 &= A_{21}x_1 + A_{22}x_2 \end{aligned} \quad (1.9)$$

where $\varepsilon > 0$ is a given small number. The slow behavior of the system is analyzed via the descriptor variable system [9,10]

$$\begin{aligned} \dot{x}_s &= A_{11}x_s + A_{12}x_f \\ 0 &= A_{21}x_s + A_{22}x_f \end{aligned} \quad (1.10)$$

obtained from (1.9) by setting ε to zero. Assuming A_{22}^{-1} exists the slow dynamics is modeled as

$$\dot{x}_s = (A_{11} - A_{12} A_{22}^{-1} A_{21})x_s \quad (1.11)$$

The slow eigenvalues and the corresponding slow eigenspace of (1.9) are continuous in \mathcal{E} [10]. Consequently the slow component of system responses is also continuous in \mathcal{E} [8]. Therefore the slow behavior of (1.9) is used as an approximation of the slow behavior of (1.9), whenever \mathcal{E} is sufficiently small. If

$$\dot{x}_f = \frac{A_{22}}{\mathcal{E}} x_f \quad (1.12)$$

then

$$\begin{aligned} x_1 &= x_s + 0(\mathcal{E}) \\ x_2 &= x_s + x_f - x_s(0) + 0(\mathcal{E}) \end{aligned} \quad (1.13)$$

In the model (1.9) there exists not only an eigenvalue separation (going to infinity as \mathcal{E} tends to zero) [8], but also there is a difference in speed of variables in x_1 and x_2 . Such systems are called [11] state separable systems. Systems which have eigenvalue separation between slow and fast eigenvalues, but state vector can not be separated into x_1 and x_2 based on different speeds of response are called [11] mixed state systems. For such systems and systems with larger \mathcal{E} an iterative separation of time scales of [12,13] can be used.

The problem of the time scale separation consists of finding matrices L and H in the state transformation matrix

$$\begin{bmatrix} y \\ z \end{bmatrix} = T x \equiv \begin{bmatrix} I & -H \\ 0 & I \end{bmatrix} \begin{bmatrix} I & 0 \\ -L & I \end{bmatrix} \begin{bmatrix} x_1 \\ x_2 \end{bmatrix} \quad (1.14)$$

such that L satisfies a generalized matrix Riccati equation

$$R(L) \equiv A_{22}L - LA_{11} - LA_{12}L + A_{21} = 0 \quad (1.15)$$

and H satisfies a Lyapunov type equation

$$P(H) = -B_1H + HB_2 + A_{12} = 0 \quad (1.16)$$

In the above equations B_1 and B_2 are defined via

$$TAT^{-1} = \begin{bmatrix} B_1 & 0 \\ 0 & B_2 \end{bmatrix} \quad (1.17)$$

The solutions L and H have to be such that

$$|\lambda(B_1)| < |\lambda(B_2)|. \quad (1.18)$$

A central problem in so defined time scale decomposition is existence and form of the solution for L. This problem has been studied in [31,14,15,13]. It has been shown that the generalized, like the standard Riccati equation, has many solutions; furthermore, whenever there is a solution for L the existence of a solution for H is guaranteed. Several numerical schemes have been proposed for solving the Riccati equation [12,13]. The typical sequence has the form

$$L_{k+1} = (A_{22} + LA_{12})^{-1} R(L_k) + L_k \quad (1.19)$$

Both modal methods [16,17,18] and the singular perturbation methods [11] have been applied to power system problems. Independently of these general system concepts, in the analysis of power systems a specific method called coherency has been used for model order reduction.

This concept relies on an empirically observed phenomenon that after a disturbance system responds in groups of machines, such that in each group all the machines have the same response. These groups are called coherent groups. A numerical algorithm for identifying coherent groups based on simulation of machine responses after a disturbance and checking which machines satisfy the above property is given in [19]. In [20,21] it is shown that coherency of a group of machines is equivalent to the reachable subspace of the disturbance being in the null space of the output matrix defined to give as output the differences of machine angles in the groups. In [16] it is indicated that coherency can be identified in a special case of the modal method analysis, when $X_{21}X_{11}^{-1}$ of (1.3) has a special structure, namely if each row has all elements zero except for one which is 1. Other approaches to coherency include [22,23]; an extensive list of references is contained in [24].

Having established the connection between modal methods, singular perturbation and iterative time scale decomposition in [14], it is the above result of [16] that motivated the work on defining partial coherency in the framework of the time scale decomposition [25], i.e. in terms of the Riccati equation. The alternative formulation of the coherency led to a number of new results surveyed in the next section.

1.2. Contributions of the Thesis

The major contribution of this thesis is in establishing a link between time scales, coherency and coupling between areas. It is shown that if coherency is defined with respect to the slow modes of the system, resulting areas are weakly coupled. In this case interarea motion

represents the slow dynamics of the system and the intermachine oscillations within coherent groups represent systems fast dynamics. For the first time it is argued analytically and then confirmed experimentally that so defined areas are relatively robust with respect to parameter changes and fault location in the system. The consideration of coherency is completed by presenting a novel algorithm for identifying coherent areas which beneficially exploits an analytical definition of coherency via the Riccati equation.

This work has been motivated by desire to overcome limitations of existing methods for reduced order modeling of power systems. For example, all existing methods for identifying coherency [20,21,19] depend heavily on the fault location, making the identified areas valid only for the particular disturbance. The analytical work of [20,21] qualifies coherency analytically, but suffers from the same fault dependance and lacks an efficient algorithm for identifying areas. The modal method of [18] is based on the linearized model of a part of the system (the one outside of a specified subsystem, usually called the study area). As such the approach can give erroneous results in the case of stronger coupling between the two parts. The other common objection of the method is that the reduced order system loses any physical meaning. In the modal approach of [16] the first objection is eliminated by considering linearized model of the whole system. Furthermore, the connection with coherency is indicated in case of the matrix $X_{21}X_{11}^{-1}$ having the special structure, as discussed earlier. However, neither explicit characterization of this coherency nor the method of manipulating the system so as to achieve this desired form of L given. In [26] coherency is defined as

partial coherency with respect to a desired subset of eigenvalues.

The algorithm for identifying coherent areas and the properties of those are not elaborated on. Furthermore, none of the known works analyses analytically robustness of the area boundaries with respect to parameter and load changes.

1.3. Chapter Preview

Chapter 2 establishes a background for the analysis of coherency in power systems, which is the main theme of this study. This background is found in the spectrum separation problem formulated in terms of a general matrix Riccati equation. Properties of its solution are studied and as a result a relation between singular perturbations, iterative separation of time scales and the modal methods is established. An algorithm for the time scale decomposition of weakly nonlinear systems is proposed.

A short overview of the existing methods for the coherency analysis of power systems is given in Chapter 3. Then a new definition of coherency as a partial coherency with respect to a given subspectrum is given in the framework of the spectrum separation problem. A class of systems called r -decomposable systems is introduced to study the idealized coherency. The gained insight is then used in constructing an algorithm for coherency identification of realistic (large) power systems. An algebraic criterion is given for checking the validity of the use of so called "area" variables, frequently used by power system analysts.

Aggregation of linear and nonlinear power system models based on the partial coherency is studied in Chapter 4. When, instead of an arbitrary partial coherency, the so called slow coherency is used, the resulting areas are insensitive to small variations in network parameters. Furthermore, in this case the areas are weakly coupled. Writing the electromechanical model in terms of the area variables and machine angle differences (the differences of angles within coherent areas) transforms the originally mixed state electromechanical model into the singularly perturbed form. Use of the singular perturbation theory and the weak coupling for the simulation of the systems responses is illustrated on a nontrivial power system example.

Further uses of coherency in the direct transient stability analysis and other possibilities of extending this study are discussed in Chapter 5.

2. TIME SCALE DECOMPOSITION VIA RICCATI APPROACH

2.1. Problem Formulation

In this chapter a group of results will be given concerning linear systems, among which we will have: the form and the properties of solutions of Riccati equation (1.15); a relation between the time scale decomposition, modal methods and singular perturbation methods for reduced order modeling; and convergence properties of a class of iterative algorithms (1.19). For weakly nonlinear systems an algorithm for simulation is proposed, which takes advantage of time scale decomposition of the linear part. The algorithm is related on an example system with an alternative, purely numerical algorithm.

2.2. Time Scales and Generalized Riccati Equation

We will first define a general spectrum separation problem and then as a special case treat the time scale decomposition. We start with the spectrum separation problem as given in [27] and then proceed with physically more meaningful formulation of the same problem via solution of a Riccati equation. The problem of spectrum separation can be defined as one of finding two lower order matrices F_1 and F_2 such that F_1 reproduces a given subspectrum of A , σ_r , and F_2 reproduces the complementary subspectrum σ_r^c , $\sigma_r \cup \sigma_r^c = \sigma(A)$. We further want:

Assumption 2.1: $\sigma_r \cap \sigma_r^c = \emptyset$.

According to [27, first decomposition theorem], the problem of spectrum separation is always solvable under the Assumption 2.1. To each of the subspectra there corresponds a unique A -invariant subspace, $S_r \subset \mathcal{X}$ of dimension r and $S_r^c \subset \mathcal{X}$ of dimension $n - r$, where \mathcal{X} is n -dimensional

vector space^{*}, such that the spectrum of A restricted to S_r is σ_r , and the spectrum of A restricted to S_r^c is σ_r^c . Then A in this new basis is of the form:

$$A_r = \begin{bmatrix} F_1 & 0 \\ 0 & F_2 \end{bmatrix} \quad (2.1)$$

where $\sigma(F_1) = \sigma_r$, $\sigma(F_2) = \sigma_r^c$. To verify above form let us note that for all column vectors in V_1 we have $AV_1 \in S_r$. Hence, there exists a matrix F_1 such that

$$AV_1 = V_1 F_1, \quad (2.2)$$

but this defines eigenvalue-eigenvector problem up to a similarity transformation $V_1 = X_1 K_1$, where X_1 is the matrix of r eigenvectors corresponding to σ_r . Similarly, for all vectors in V_2 , $AV_2 \in S_r^c$ and there exists a matrix F_2 such that

$$AV_2 = V_2 F_2 \quad (2.3)$$

with $\sigma(F_2) = \sigma_r^c$ and $V_2 = X_2 K_2$ for eigenvectors X_2 and some nonsingular K_2 .

The relation between the states of equivalent systems in which A and A_v are state matrices is given by

$$x = V x_v. \quad (2.4)$$

Notice that in order to achieve the spectrum separation it is sufficient to consider only the invariant subspace corresponding to the given subspectrum σ_r , and complement the space by any independent $n-r$ -dimensional subspace. Of course, in this case one gets only a blocktriangular form of A_v .

^{*} $S_r \subset \mathcal{X}$ is A-invariant if $AS_r \subset S_r$

Let us consider now the transformation of (1.1) in the form

$$x = [V_1 \ V_2] x_v \quad (2.5)$$

where $\text{Im } V_1$ is A -invariant r -dimensional subspace of \mathcal{X} corresponding to σ_r , and $\text{Im } V_2$ spans $n-r$ dimensional subspace of \mathcal{X} such that it does not contain any of the vectors in the subspace $\text{Im } V_1$, but otherwise arbitrary.

Remark 2.2: Since V_1 has full rank, there always exists an ordering of states in x for which V_{11} of $V_1 = \begin{bmatrix} V_{11} \\ V_{21} \end{bmatrix}$ is nonsingular. Due to this

remark we assume that x in (2.5) is ordered so that V_{11} is nonsingular. That allows a particularly simple V_2 , $V_2 = \begin{bmatrix} 0 \\ I \end{bmatrix}$. With this choice of V_1 and V_2 the transformation (2.5) can be rewritten as

$$x = \begin{bmatrix} I & 0 \\ V_{21}V_{11}^{-1} & I \end{bmatrix} \begin{bmatrix} V_{11} & 0 \\ 0 & I \end{bmatrix} x_v \quad (2.6)$$

The transformed state matrix is

$$\begin{bmatrix} V_{11}^{-1} & 0 \\ 0 & I \end{bmatrix} \begin{bmatrix} I & 0 \\ -L & I \end{bmatrix} A \begin{bmatrix} I & 0 \\ L & I \end{bmatrix} \begin{bmatrix} V_{11} & 0 \\ 0 & I \end{bmatrix} = \begin{bmatrix} F_1 & A_{12} \\ 0 & F_2 \end{bmatrix} \quad (2.7)$$

where

$$L \equiv V_{21}V_{11}^{-1} \quad (2.8)$$

$$F_1 = V_{11}^{-1}(A_{11} + A_{12}L)V_{11} \equiv V_{11}^{-1}B_1V_{11} \quad (2.9)$$

$$F_2 = A_{22} - LA_{12} \equiv B_2 \quad (2.10)$$

It follows from (2.7) that the spectrum separation can be achieved with the transformation

$$x = \begin{bmatrix} I & 0 \\ L & I \end{bmatrix} x_v \equiv T_L^{-1} x_v \quad (2.11)$$

with the only requirement that $\text{Im} \begin{bmatrix} I \\ L \end{bmatrix}$ is A-invariant corresponding to σ_r . The significance of this transformation is that the states of x_v retain the physical meaning if the spectrum separation problem results in $L=0$, i.e. if the original system consists of two decoupled (through A_{21}) subsystems. In cases of nonzero coupling between the subsystems, the first r states of x_v still retain their meaning, while only the last $n-r$ states are changed. After this transformation is applied, we get

$$A_v = \begin{bmatrix} B_1 & A_{12} \\ 0 & B_2 \end{bmatrix} \quad (2.12)$$

where B_1 and B_2 are defined by (2.9) and (2.10).

From (2.7) it also follows that in solving the spectrum separation problem it is necessary to make "21" block in the transformed matrix equal zero. By writing the equation for "21" block of (2.7) we get

$$R(L) \equiv -LA_{11} + A_{22}L - LA_{12}L + A_{21} = 0 \quad (2.13)$$

This equation has the form of a generalized Riccati equation. In the case when $A_{11} = -A_{22}^T$ it becomes the standard algebraic Riccati equation found in optimal control and estimation theory. For later reference we write this equation in the form [28,29]

$$R_s(L) \equiv -LF - F^T L + LBR^{-1}B^T L - Q \quad (2.14)$$

for which underlining problem is one of finding control u of the system

$$\dot{x} = Ax + Bu \quad (2.15)$$

so as to minimize $J(x,u)$ given by

$$J(x,u) = \int_0^\infty (x^T Q x + u^T R u) dt \quad (2.16)$$

The matrix E associated with (2.14), the same way A is associated to (2.13), has the form

$$E = \begin{bmatrix} A & -BR^{-1}B^T \\ -Q & -A^T \end{bmatrix} \quad (2.17)$$

Therefore equation (2.14) is a special case in the spectrum separation problem. Several standard results of (2.14) will be rephrased in the light of the results on existence, form and uniqueness of the solution of generalized Riccati equation (2.13), which are coming next.

Theorem 2.3:

Let an r -element subspectrum of A , σ_r be given, with no common eigenvalues with its complement σ_r^c , $\sigma_r \cap \sigma_r^c \neq 0$, $\sigma_r \cup \sigma_r^c = \sigma(A)$. Let S_r be the corresponding A -invariant subspace of dimension r with its basis given as columns of a matrix $V \in \mathbb{R}^{n \times r}$, i.e.

$$AV = VF_1 \quad (2.18)$$

implies

$$\sigma(F_1) = \sigma_r \quad (2.19)$$

Then,

(i) the solution L of the Riccati equation (2.13), such that $\sigma(B_1) = \sigma_r$ exist if and only if the matrix V_1 of $V = \begin{bmatrix} V_1 \\ V_2 \end{bmatrix}$ is nonsingular. This solution is then given as

$$L = L_2 V_1^{-1} \quad (2.20)$$

(ii) When columns of V are eigenvectors of A , then columns of V_1 are eigenvectors of B_1 .

Proof: Equation (1.13) can be rewritten as

$$R(L) = \begin{bmatrix} -L & I \end{bmatrix} A \begin{bmatrix} I \\ L \end{bmatrix} = 0 \quad (2.21)$$

The equation will be satisfied if and only if

$$(a) \quad \text{Im} \begin{bmatrix} I \\ L \end{bmatrix} \subset \text{Ker } A, \text{ or}$$

$$(b) \quad \text{Im } A \begin{bmatrix} I \\ L \end{bmatrix} \subset \text{Ker} \begin{bmatrix} -L & I \end{bmatrix} = \text{Im} \begin{bmatrix} I \\ L \end{bmatrix}$$

But since (a) is already included in (b) we proceed with (b).

$$\text{Im } A \begin{bmatrix} I \\ L \end{bmatrix} = A \text{Im} \begin{bmatrix} I \\ L \end{bmatrix} \subset \text{Ker} \begin{bmatrix} -L & I \end{bmatrix} = \text{Im} \begin{bmatrix} I \\ L \end{bmatrix}, \quad (2.22)$$

i.e. for any solution L , $\text{Im} \begin{bmatrix} I \\ L \end{bmatrix}$ must be A -invariant. We now want to relate this subspace to the spectrum σ_r . More specifically we will be given σ_r and the corresponding A -invariant subspace S_r with a basis $V \in \mathbb{R}^{n \times r}$, and we want to see if there exists an L for which $\begin{bmatrix} I \\ L \end{bmatrix}$ will span S_r . Clearly, if and only if V_1 is nonsingular such an L exists, since from the requirement that V and $\begin{bmatrix} I \\ L \end{bmatrix}$ span the same subspace, there exists

a matrix $K \in \mathbb{R}^{r \times r}$ for which

$$\begin{bmatrix} I \\ L \end{bmatrix} = VK. \quad (2.23)$$

From $\text{rank } I = r = \text{rank } V_1 K$ it follows that both V_1 and K have to be of full rank. Then $K = V_1^{-1}$; which proves (2.20). To prove $\sigma(B_1) = \sigma_r$ we write B_1 as

$$B_1 = \begin{bmatrix} I & 0 \end{bmatrix} A \begin{bmatrix} I \\ L \end{bmatrix} \quad (2.24)$$

Due to (2.18) and (2.23) with $K = V_1^{-1}$, we have

$$B_1 = \begin{bmatrix} I & 0 \end{bmatrix} A V V_1^{-1} = \begin{bmatrix} I & 0 \end{bmatrix} V F_1 V_1^{-1} = V_1 F_1 V_1^{-1}$$

which completes the proof of (i) and (ii).

The proof given here is more general than those given in [31,15,14]. In [31] only the case of diagonalizable matrix A has been treated and a particular, eigenvector basis for S_r was assumed. In [14,15] sufficiency has been proved. Namely if V spans an invariant subspace then the solution L is of the form (2.20). Here it is proved that for L to exist it is also necessary that V spans an invariant subspace of A . The form of the solution also applies to the standard Riccati equation (2.14) with E of (2.17) playing the role of A . A different proof for this equation is given in [30].

Remark 2.4: From the geometrical arguments used in the proof of the theorem, it should be clear that L does not depend on the particular choice of basis for an invariant subspace corresponding to a given spectrum. We will however demonstrate this fact in matrix terms, which are more suitable for computational purposes.

Proposition 2.5: Each matrix L solving the Riccati equation (2.7) is independent on the choice of V spanning A -invariant subspace corresponding

to a given spectrum.

Proof: Suppose that V spans A -invariant subspace corresponding to a given spectrum σ_r . By assumption on existence of L , V_1 is invertible and $L = V_2 V_1^{-1}$. If some $V' \neq V$ spans the same subspace, then $V' = \begin{bmatrix} V_1 \\ V_2 \end{bmatrix} K$, for some nonsingular K . In this case

$$L' = (V_2 K)(V_1 K)^{-1} = L, \quad (2.25)$$

which completes the proof. From the theorem it follows that the Riccati equation has many solutions. In fact for any σ_r for which eigenvector basis V has V_1 invertible (due to the Proposition 2.1 any other basis can be assumed) there corresponds one L . For the time scale decomposition of particular interest is the case when $\sigma_r = \sigma_s$, where σ_s contains r smallest in magnitude eigenvalues of A . In this case the eigenvalues of A are divided into the slow eigenvalues contained in B_1 and the fast eigenvalues contained in B_2 . Due to the crucial role of this solution in the most of the results that follow, we introduce

Definition 2.6: The solution of Riccati equation (2.13) for which $|\lambda(B_1)| < |\lambda(B_2)|$ is called dichotomic and is denoted by L_d .

Remark 2.7: In case of the standard Riccati equation (2.14) and (2.17), it is known [29] that under usual controllability - observability assumptions, matrix E has exactly n eigenvalues with strictly negative real parts, whose spectrum we will denote by σ_n^- and, symmetric to those with respect to the imaginary axes, n eigenvalues with positive real part, whose spectrum will be σ_n^+ . Among many solution of (2.14), of particular interest is the one for which $\sigma_r = \sigma_n^-$ and $B_1 = A_F = F - BR^{-1}B^T L$. In this case the Assumption 2.1 is satisfied. By the Theorem 2.3 $\sigma(A_F) = \sigma_n^-$,

i.e. the closed loop system matrix is stable. It is also easy to see that there exists one solution L for which $\sigma(A_F) = \sigma_n^+$. The symmetry of L can be concluded from $R_s(L^T) = [R_s(L)]^T = 0$ and uniqueness of the solution corresponding to the same spectrum.

Remark 2.8: Let X be the matrix of right eigenvectors (and generalized eigenvectors) of A . If V of Theorem 2.1 is $V = \begin{bmatrix} X_{11} \\ X_{21} \end{bmatrix}$, then $L = X_{21}X_{11}^{-1}$ and $B_1 = A_{11} + A_{12}X_{21}X_{11}^{-1}$. But this B_1 has exactly the same form as the aggregated state matrix in modal method approaches. The spectrum separation problem as defined by (2.1) and (2.2) indicates one less known fact, that with almost the same computational expense needed to obtain B_1 in modal method approaches one can get also the matrix B_2 (2.10) which reproduces the complementary spectrum of A .

From the statement of the theorem and when Assumption 2.1 applies it can be seen that the only condition under which the solution of the Riccati equation does not exist is when V_1 is singular. Since at the time when a spectrum σ_r is specified and some basis of the corresponding A -invariant subspace is computed it is not known whether V_1 will be singular or not, the question arises: can the effort spent on computing V (which is considerable as will be discussed in chapter 3 and 4) be still used to achieve the desired spectrum separation, even if V_1 is singular. The answer is yes, due to the following Proposition [31].

Proposition 2.2: If V spans r -dimensional A -invariant subspace corresponding to a given σ_r , then there always exists a state permutation $\hat{x} = Px$, $\hat{A} = PAP^T$ such that $\hat{V} = PV$ is \hat{A} -invariant and \hat{V}_1 is invertible.

Proof: It simply follows from $\text{rank } V = r$. Hence there exist r linearly independent rows in V . From $AV = VK$, where $\sigma(K) = \sigma_r$ it follows that $\hat{V} = PV$.

This result says that with the mere reordering of states, and likewise reordering of rows of V there can always be found V_1 invertible, i.e. the solution of the Riccati equation, now for the redefined system (\hat{x}, \hat{A}) . The singularity of V_1 is related to the controllability and observability of the subsystems of A . From the form of B_1 and B_2 (2.9) and (2.10), in which L appears once as a controller feedback matrix for the pair (A_{11}, A_{12}) and the other time as an observer feedback matrix for the pair (A_{22}, A_{12}) , it can be seen that a necessary condition for V_1 to be invertible (i.e. for L to exist) is that the modes of A_{11} uncontrollable through A_{12} belong to $\sigma_r = \sigma(B_1)$, and the modes of A_{22} unobservable through A_{12} belong to the complementary spectrum $\sigma_r^c = \sigma(B_2)$. This becomes apparent by noting, for example in the case of uncontrollability, that if a $\lambda \in \sigma_r^c$ is an uncontrollable mode of A_{11} , then for any L this λ will be in $\sigma(B_1)$, which is contrary to the requirement that $\lambda \in \sigma_r^c = \sigma(B_2)$. It should be noted that in most applications the approach via reordering rows of V to assure invertibility of V_1 is viable one. However, in the case of standard Riccati equation, because of the structure of E , it is not possible to permute rows of V , except within V_1 and V_2 in which case it does not change singularity of V_1 . However, under usual assumptions on controllability-observability it is known that the unique solution for L exists, which means that V_1 is invertible. For some algorithms for the time scale decomposition, one of which will be presented in the next section, it is important to make reordering of states to assure invertibility of V_1 before the algorithm is applied. From the form of the transformation (2.11) and the requirement that $\lambda(B_1) < \lambda(B_2)$ it can be concluded that the reordering of states should be such that x_1 contains

the slow variables of the model and x_2 predominantly fast variables. For cases in which physical considerations or previous experience cannot help make such ordering, states can be ordered so that the first row of A has the smallest norm, the second row has the next largest norm, and so on.

2.3. Practical Aspects of the Spectrum Separation Problem

In practice $R(L)$ cannot be made zero, except in very special cases. Therefore, it is of interest to see how accurately $\sigma(B_1)$ and $\sigma(B_2)$ of

$$A_V = \begin{bmatrix} B_1 & A_{12} \\ R(L) & B_2 \end{bmatrix}, \quad (2.26)$$

in which $R(L)$ is supposedly small, reproduce σ_r and σ_r^c . Equation (2.26) represents the lefthand side of (2.7) for some L ; we assume it is close to the solution corresponding to a given σ_r . The answer to the above question is given in the following theorem, given in [32].

Theorem 2.10: Let $\|A\|^2 = \text{trace}(A^T A)$ and define $\delta = \inf_P \{\|PB_1 - B_2P\| : P \in \mathbb{R}^{(n-r) \times r}, \|P\| = 1\}$. If

$$\frac{\|R(L)\| \|A_{12}\|}{\delta^2} < \frac{1}{4}, \quad (2.27)$$

then there exists a unique $P \in \mathbb{R}^{(n-r) \times r}$ satisfying

$$\|P\| < 2 \frac{\|R(L)\|}{\delta} \quad (2.28)$$

such that

$$\text{Im} \begin{bmatrix} I \\ P \end{bmatrix} \quad (2.29)$$

is an invariant subspace of A_V . Moreover $\sigma(A_V)$ is the disjoint union

$$\sigma(A_V) = \sigma(B_1 + A_{12}P) \cup \sigma(B_2 - PA_{12}) . \quad (2.30)$$

In practical applications, when $R(L)$ is sufficiently small we approximate A_V with $\begin{bmatrix} B_1 & A_{12} \\ 0 & B_2 \end{bmatrix}$, so that $\sigma(B_1)$ approximates $\sigma(B_1 + A_{12}P)$ and $\sigma(B_2)$ approximates $\sigma(B_2 - PA_{12})$, and, finally, $\text{Im} \begin{bmatrix} I \\ 0 \end{bmatrix}$ approximates $\text{Im} \begin{bmatrix} I \\ P \end{bmatrix}$. The theorem states that the error is directly proportional to P , whose norm is bounded by the norm of $R(L)$. In other words there is a continuity in the change of spectrum and the invariant subspace for small changes in $R(L)$. The number δ in the theorem is a measure of spectrum separation between B_1 and B_2 . If B_1 and B_2 are symmetric this number is equal [32] to the smallest in magnitude difference between any two eigenvalues of B_1 and B_2 . This number is positive, except when B_1 and B_2 contain common eigenvalues, in which case it is equal to zero. However under Assumption 2.1 it will always be positive. Condition (2.27) indicates that the Riccati equation has to be solved more precisely if either there is a strong connection between B_1 and B_2 subsystems through A_{12} or spectrum separation between the two subsystems is small.

We now use the theorem to give an alternative interpretation of some of the standard results in the singular perturbation theory [8].

When the state matrix of (1.9), which is

$$A' = \begin{bmatrix} A_{11} & A_{12} \\ \frac{A_{21}}{\varepsilon} & \frac{A_{22}}{\varepsilon} \end{bmatrix} \text{ is transformed by means of the transformation (2.11),}$$

the corresponding Riccati equation is $R(L) = -LA_{11} + \frac{A_{22}}{\varepsilon}L - LA_{12}L + \frac{A_{21}}{\varepsilon}$

For small ε the dominant terms in the equation are those containing ε .

Hence a natural choice of an approximate L solving the equation is the

one which annihilates \mathcal{E} -dependent terms. This leads to $L = -A_{22}^{-1}A_{21}$, and $B_1 = A_{11} - A_{12}A_{22}^{-1}A_{21} \equiv A_s$, which is the slow state matrix as given by (1.11). To apply the Theorem 2.10 we have to check the condition (2.27). It can be shown that for nonsingular A_{22} and sufficiently small \mathcal{E} , $\delta = O(\frac{1}{\mathcal{E}})$, and hence there exists an \mathcal{E}^* such that for all $\mathcal{E} \in (0, \mathcal{E}^*]$ the condition (2.27) is satisfied. Therefore, there exists a $P = O(\mathcal{E})$, such that the spectrum of A' is given as a disjoint union

$$\sigma(A') = \sigma(A_s + A_{12}P) \cup \sigma\left(\frac{A_{22}}{\mathcal{E}} - A_{22}^{-1}A_{21}A_{12} - PA_{12}\right), \quad (2.30)$$

and the slow eigenspace of A' is spanned by $\begin{bmatrix} I \\ -A_{22}^{-1}A_{21} + P \end{bmatrix}$. Because of

$P = O(\mathcal{E})$ this result exhibits the continuity of the slow eigenvalues and the slow eigenspace with $\mathcal{E} \in (0, \mathcal{E}^*]$. A slight difficulty in extending the argument to hold for $\mathcal{E} = 0$ is avoided in [10], where in addition the continuity of the inverse of the fast eigenvalues and the fast eigenspace with $\mathcal{E} \in [0, \mathcal{E}^*]$ is proved as well.

2.4. Relation Between Singular Perturbation, Time Scale Decomposition and Modal Methods

In the previous section it has been shown that the time scale decomposition and the modal method for reduced order modeling are the same in regard to the slow subsystem. In addition time scale decomposition formulation reveals the fact that with the same expense spent for obtaining the slow subsystem state matrix, the fast state matrix can be obtained as well. For some engineering applications it is not necessary to find exact invariant subspaces, or equivalently the exact solution of

the Riccati equation [11]. Instead, an iterative algorithm for the time scale decomposition is established, whose results after only few iterations are then used. In this section we will relate so defined time scale decomposition with the singular perturbation and the modal methods.

A basis for comparison of the methods is found in the simultaneous iteration method for computing invariant subspaces of general (nonhermitian) matrices (SI for short) [32]. We will first review relevant facts about this method and then establish the relation.

For matrix A let $\lambda_1, \lambda_2, \dots$ be eigenvalues ordered so that

$$|\lambda_1| \geq |\lambda_2| \geq \dots \geq |\lambda_n| \quad (2.31)$$

Let σ_r denote the spectrum consisting of the r largest in magnitude eigenvalues, and let S_r be the corresponding r -dimensional invariant subspace. Furthermore, let Q_r be r -dimensional subspace with nonzero projection on S_r along the complementary invariant subspace. Then, if $|\lambda_r| > |\lambda_{r+1}|$, $A^k Q_r$ tends to S_r as k tends to infinity. For $r = 1$ this corresponds to the well known power method for obtaining the eigenvector for the largest eigenvalue λ_1 .

Before presenting an algorithm which uses this sequence to find a basis of the invariant subspace let us recall the result about Schur-decomposition of a matrix [32,38].

Theorem 2.11: Let $A \in \mathbb{R}^{n \times n}$. Then there is a unitary $X \in \mathbb{C}^{n \times n}$ such that

$$S = X^* A X \quad (2.32)$$

is upper triangular. The matrix X may be chosen so that the diagonal elements of S which are eigenvalues of A are in descending order of absolute value.

For distinct eigenvalues corresponding columns of X are unique up to multiplication with a unit length number; for multiple eigenvalues of multiplicity p , the corresponding p columns in X span unique p -dimensional subspace. If X_r denotes first r columns of X then $A \cdot \text{Im } X_r = \text{Im } X_r$, i.e. these columns span r -dimensional invariant subspace corresponding to σ_r . Column vectors in X are usually called Schur vectors.

Now let us explain one step of SI algorithm for finding a basis of $A^k Q_r$. Define $r \times r$ matrix B as

$$B = V_k^* A V_k \quad (2.33)$$

and apply the decomposition of Theorem 2.3 to B

$$(X_k^B)^* B X_k^B = S_B \quad (2.34)$$

Let $Q_k = V_k X_k^B$, which is obviously a basis for $A^k Q$. A basis for the next step is obtained as

$$Q_{k+1} = A Q_k \quad (2.35)$$

To summarize, the algorithm consists of orthonormalizing an arbitrary basis matrix (Q_{k+1}) , say) to get V , then forming B (2.33), decoupling low order matrix B according to (2.34) and using unitary matrix Q_k to perform the next step (2.35).

Convergence behavior of this algorithm is given in the following lemma due to [32].

Lemma 2.12: Let S be equivalent matrix to A according to Theorem 2.11.

Let E_1 denote the matrix consisting of columns 1 through ℓ of I and E_2 denote the matrix consisting of columns $\ell+1$ through r . If $|\lambda_\ell| > |\lambda_{\ell+1}|$ and $|\lambda_r| > |\lambda_{r+1}|$, then there are matrices, $W_k \in \mathbb{R}^{n \times r}$ with orthonormal columns

divided on $W_k = (W_1, W_2)$, $W_1 \in \mathbb{R}^{n \times \ell}$, $W_2 \in \mathbb{R}^{n \times (r-\ell)}$ such that

$$1. \quad \text{In}(W_k) = S^k Q \quad (2.36)$$

$$2. \quad W_1 = E_1 + O(|\lambda_{r+1}/\lambda_\ell|^k) \quad (2.37)$$

$$3. \quad W_2 = E_2 + O(|\lambda_{r+1}/\lambda_r|^k) \quad (2.38)$$

The lemma shows the speed with which individual columns in Q of (2.35) tend to the corresponding Schur vectors. The speed is linear with the factor ε_i for the i -th Schur vector, defined as

$$\varepsilon_i = \frac{|\lambda_{r+1}|}{|\lambda_i|}, \quad (2.39)$$

and the convergence of the algorithm is global.

Practical details about the realization of the algorithm are contained in [32]. For our purpose we need only the established result about global convergence of the algorithm with the linear speed defined by ε_i .

We also rewrite the algorithm (2.33) - (2.34) in the form

$$A V_{k+1} = V_k \quad (2.40)$$

Using this form of the algorithm we now characterize the convergence properties of a class of iterative algorithms for solving Riccati equation represented by (1.19) [13]. We rewrite it here for convenience

$$L_{k+1} = L_k - (A_{22} - L_k A_{12})^{-1} R(L_k) \quad (2.41)$$

Theorem 2.13: Let r be given such that $|\lambda_r| > |\lambda_{r+1}|$, with the eigen-

values of A ordered according to (2.31). Let $V_k = \begin{bmatrix} v_{1k} \\ v_{2k} \end{bmatrix}$ be an

$n \times r$ matrix with nonzero projection of column vectors on the r -dimensional slow subspace of A . If V_{1k}^{-1} exists, denote $P_k = V_{2k} V_{1k}^{-1}$. Then, if $L_0 = P_0$, the sequences P_k generated by (2.40) and L_k generated by (2.41) are identical. Furthermore, $|\lambda(B_1(L_k))| < |\lambda(B_2(L_k))|$ for sufficiently large k .

Proof: Writing (2.40) in expanded form, substituting $P_k V_{1k}$ for V_{2k} , eliminating V_{1k}^{-1} from the equations and regrouping the terms, directly results in $P_k = L_k$. Since $\text{Im } V_{1k}$ tends to the slow subspace of A , due to the Lemma 2.11, $B_1(L_k)$ will eventually contain the r slow eigenvalues of the system.

This result shows that the Riccati iterations (2.41) have global convergence, with the speed determined by the largest \mathcal{E}_i , i.e. \mathcal{E}_r which corresponds to the slowest converging Schur vector in the SI method. Furthermore the spectrum of $B_1 = A_{11} + A_{12} L_k$ tends to σ_s , which means that L_k tends to L_d . In [15] it is shown that L_d is the only stable equilibrium solution of the matrix differential equation

$$\dot{L} = R(L) \quad (2.42)$$

The following relation between singular perturbation, modal methods and the iterative time scale separation is immediate consequence of the above theorem.

Corollary 2.14:

Let $B_1(k)$ be defined as $B_1(k) = A_{11} + A_{12} L_k$, where L_k is defined by (2.41) for $L_0 = 0$. Then

- (i) $B_1(1)$ is the slow state matrix obtained from singular perturbation approach (1.11)

- (ii) $B_1(k)$, $k \rightarrow \infty$ is the modal method slow state matrix, and
- (iii) $B_1(k)$, $1 \leq k < \infty$, is the slow state matrix of time scale separation.

Proof: Substituting $L_0 = 0$ into (2.41) gives $L_1 = -A_{22}^{-1} A_{21}$ and $B_1(L_1)$ of the form given in (1.11). This proves (i). From Theorem 2.12

$\text{Im} \begin{bmatrix} I \\ L_k \end{bmatrix}$ tends to the invariant slow subspace of A as k goes to infinity, which due to the Remark 2.8 means that $B_1(L_k)$ tends to the slow subsystem matrix obtained from modal methods. The case (iii) is the case in between singular perturbation and modal methods, which offers advantage over the exact modal method when low accuracy is acceptable but \mathcal{E}_r is not sufficiently small that only one iteration of the singular perturbation approach suffices.

This corollary, in view of Lemma 2.11 and Theorem 2.13 gives a numerical interpretation for why the singular perturbation approach is successful in case of small \mathcal{E} : it is simply because the speed of convergence is so high (proportional to \mathcal{E}^{-k}) that only one iteration is needed to make $\frac{R(L)}{\sigma}$ sufficiently small. The corollary also suggests one meaningful interpretation of the small parameter \mathcal{E} , as being the eigenvalue ratio

$$\mathcal{E} = \frac{\lambda_{r+1}}{\lambda_r}.$$

We now give several examples to illustrate properties of the iterative time scale decomposition.

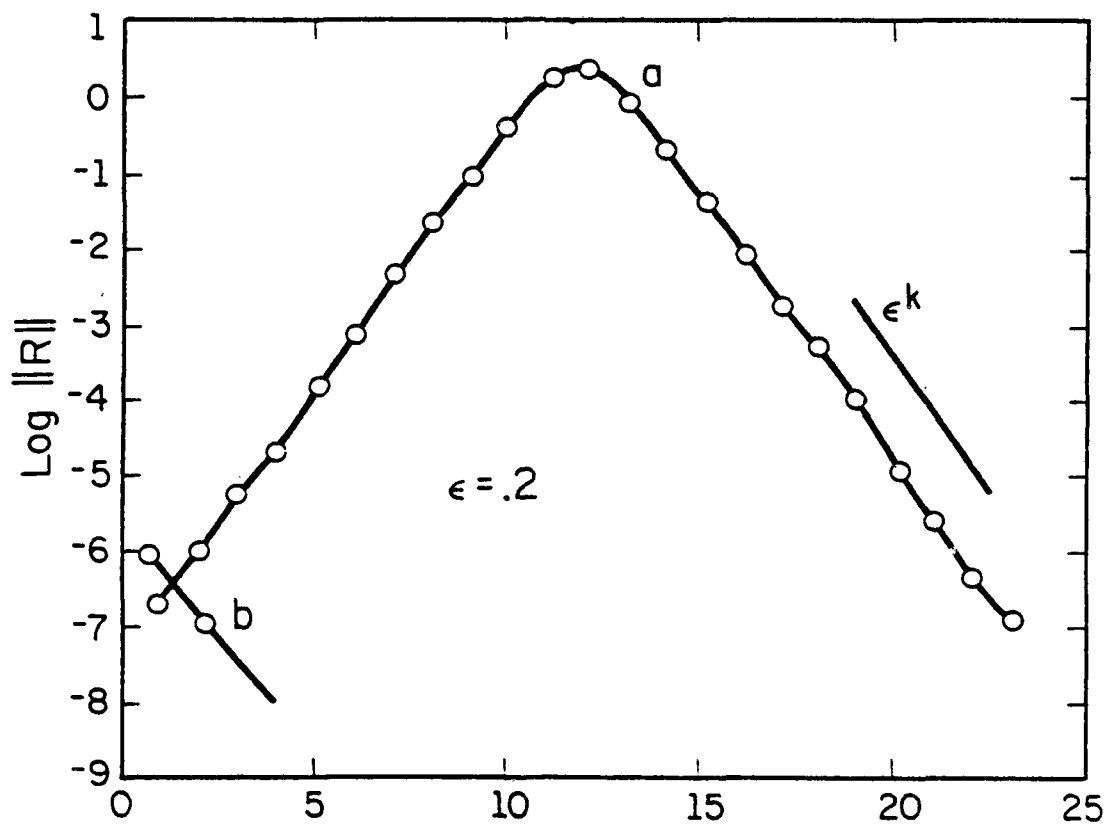
Example 2.15: In this example we demonstrate the importance of the state ordering for the time scale decomposition. Given (2.43) and $r=2$,

$$\dot{X} = \begin{bmatrix} 5 & 0 & 1 \\ 0 & 1 & 1 \\ 0 & 0 & 1 \end{bmatrix} X \quad (2.43)$$

it is evident that the state matrix has two Jordan blocks: one of size 1 corresponding to the simple eigenvalue 5 and the other of size 2 corresponding to the eigenvalue 1. From the triangular structure of this matrix it is evident that the spectrum separation is already achieved for any choice of σ_r . However, the time scale separation is not achieved since the large eigenvalue 5 appears in the "11" block. We specify $r = 2$ and want to find matrix L_d , which is a part of the transformation (2.11) so that $\sigma(B_1) = \{1, 1\}$. The Riccati equation has the form

$$R(L) = - (\ell_1 \ell_2) \cdot 1 + (\ell_1 \ell_2) \begin{pmatrix} 5 & 0 \\ 0 & 1 \end{pmatrix} - (\ell_1 \ell_2) \begin{pmatrix} 1 \\ 1 \end{pmatrix} (\ell_1 \ell_2) = 0$$

from which two solutions can be found easily: $L_1 = (0 \ 0)$ and $L_2 = (-4 \ 0)$. For the first solution B_1 has eigenvalues 5 and 1, i.e. nothing is changed from (2.43). Only the second solution results in the desired spectrum of B_1 , i.e. $L_d = L_2$. Application of the iterative algorithm (2.19) to this system results in the convergence behavior given in fig. 2.1a. After initial divergence the algorithm achieves asymptotic behavior predicted by the Lemma 2.12. To start the algorithm we have perturbed slightly A_{21} , since for the usual initial condition $L_1 = A_{22}^{-1} A_{21}$ the algorithm would stay at the unstable solution $L = 0$. This example shows several interesting points. First, it emphasizes the importance of state ordering, for if the state ordering was such that A_{11} had the eigenvalues close to the eigenvalues of the desired B_1 , the algorithm would have started from the falling side of the curve a, in fig. 2.1. The situation is illustrated by the curve b, which corresponds to the ordering of states (x_2, x_3, x_1) and a small A_{21} . This is also one of the reasons for the success of singular



FP-6959

Figure 2.1. Iterative separation of time scales for the systems of Example 2.15.

perturbation approach, in which it is required that the states be ordered according to their speeds (1.9). This example shows that even though the eigenvalue separation exists, only after the states are properly ordered one step approximation of the singular perturbation approach is successful - as indicated by the curve b as opposed to the curve a. Second characteristic of the example is that it contains multiple eigenvalues, and still achieves the asymptotic behavior predicted by Lemma 2.12. In other words the individual generalized eigenvectors corresponding to multiple eigenvalues may not be unique but the space they span is unique, as discussed in connection with Theorem 2.11.

Example 2.16: With this example we demonstrate applicability of the techniques of this chapter to the solution of the standard Riccati equation (2.14), associated with the optimization on infinite interval. The problem is to find a control u which will minimize criterion (2.16) for the system with

$$A = \begin{bmatrix} 0 & 1 \\ 0 & -2 \end{bmatrix}, \quad B = \begin{bmatrix} 0 \\ 1 \end{bmatrix}, \quad R = 1, \quad Q = \begin{bmatrix} 4 & 0 \\ 0 & 1 \end{bmatrix} \equiv C^T C$$

It is easy to check that (A,B) is controllable pair, and (A,C) is observable pair. In fact the system is stable since eigenvalues are 0 and -2. The objective of the design is to improve its performance. The matrix E (2.17) for this system is

$$E = \begin{bmatrix} 0 & 1 & 0 & 0 \\ 0 & -2 & 0 & -1 \\ -4 & 0 & 0 & 0 \\ 0 & -1 & -1 & 2 \end{bmatrix},$$

whose eigenvalues are $(-2, -1, 1, 2)$. If we define spectrum separation problem for E with $\sigma_2 = (-2, -1)$, then corresponding $B_1 = A - BR^{-1}B^T L$ would be the closed loop feedback matrix whose spectrum would be σ_2 and the feedback gain K from $u = Kx$ would be $K = -R^{-1}B^T L$. The spectrum of B_1 indicates improvement in performance over the open loop system. Now, we want to use globally convergent subspace iteration method for computing the solution L . Since the eigenvalues of σ_2 are not the largest in magnitude eigenvalues of E , we perform bilinear transformation

$$\bar{E} = (E - \phi I)(E + \phi I)^{-1} \quad (2.44)$$

which has the property to preserve the invariant subspace corresponding to σ_r , and has eigenvalues

$$\lambda(E) = \frac{\lambda(E) - \phi}{\lambda(E) + \phi} \quad (2.45)$$

so that the n eigenvalues corresponding to $\operatorname{Re} \lambda(E) < 0$ can be made to be the largest in magnitude eigenvalues of \bar{E} with a suitable choice of ϕ .

A ϕ that suffices is

$$\phi > \sup\{\operatorname{Re} \lambda_i(E), i = 1, 2, \dots, 2n\} \quad (2.46)$$

In this example we estimate $\phi = 5$. We now use subspace iterations (2.40) with \bar{E} and initial guess randomly selected as

$$V_0 = \begin{bmatrix} 1 & -.2 \\ .1 & .7 \\ -.3 & 1 \\ .5 & -.8 \end{bmatrix}$$

After each iteration k we compute $\|R(L_k)\|$, and give it in fig. 2.2 as

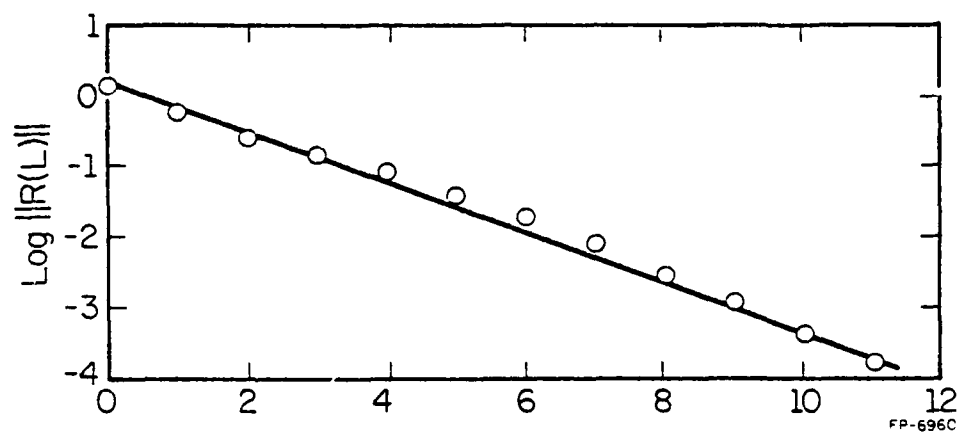
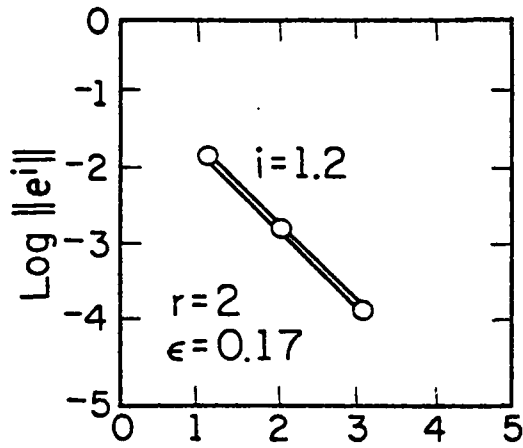


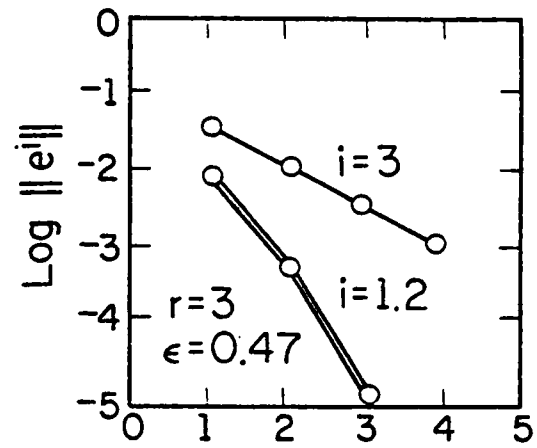
Figure 2.2. Solution process for the standard regulator problem.

a function of the number of iterations. The behavior is as predicted by the Lemma 2.11. After 11 iterations elements of L_{11} differ from the corresponding elements of the exact $L = \begin{bmatrix} 6 & 2 \\ 2 & 1 \end{bmatrix}$ by less than 0.01. Convergence is faster for systems whose closed loop system matrix has larger margin of stability since in this case the eigenvalue separation between the eigenvalues with positive real part and the eigenvalues with negative real part is bigger, and hence $\mathcal{E} = \frac{\lambda_{n+1}(\bar{E})}{\lambda_n(\bar{E})}$ is smaller. This example demonstrates the possibility of using the advantage of having globally convergent algorithm for solving the Riccati equation, for either initializing the faster converging algorithms, such as [33], which require initial guess close to the final solution, or directly use it for, say, large sparse system matrices A . Because of the simplicity of the algorithm it can also be used for smaller order systems when limited computer capabilities are available.

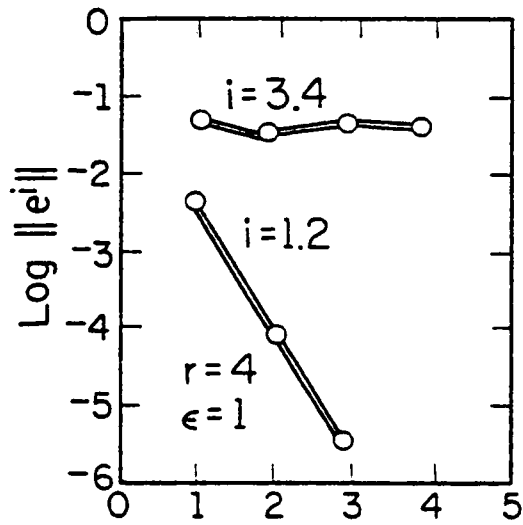
Example 2.17: This example illustrates time scale decomposition of one machine infinite bus power system model. The form of the model and the linearized state matrix [34] are given in Appendix A. The iterative time scale decomposition using the algorithm (2.41) is exhibited in fig. 2.3d, for the case $r=2$, which is the case with the fastest convergence. The behavior of the subspace iterations for the same model and different r is given in fig. 2.3. The convergence criterion for the latter is derived from (2.34) by defining $E = (X_k^B)^* B X^B - S_B \equiv (e^1 e^2 \dots e^r)$. This example will be completed in the next section after the block-diagonalization is discussed, by showing a relation between the number of iterations in the time scale decomposition and the quality of the approximation.



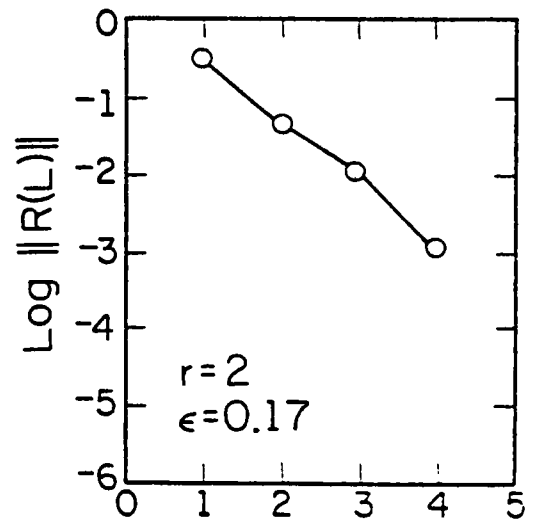
(a)



(b)



(c)



(d)

FP-6961

Figure 2.3. Time scale decomposition of one machine-infinite bus system.

2.5. Block Diagonalization

After the spectrum separation is completed, the system state matrix is in the block triangular form (2.12). For some application it is useful to have the two subsystems, whose dynamics is contained in B_1 and B_2 , completely decoupled. In geometrical terms it amounts to finding a basis for invariant subspace corresponding to the spectrum σ_r^c , as indicated by (2.4). In matrix terms we can apply a similarity transformation to (2.12), similar to (2.11)

$$\begin{bmatrix} y \\ z \end{bmatrix} = \begin{bmatrix} I & H \\ 0 & I \end{bmatrix} x_v = T_H x_v \quad (2.47)$$

which does not change the physical meaning of the last $n - r$ components of x_v . When this transformation is applied to (2.12) it results in

$$T_H \begin{bmatrix} B_1 & A_{12} \\ 0 & B_2 \end{bmatrix} T_H^{-1} = \begin{bmatrix} B_1 & P(H) \\ 0 & B_2 \end{bmatrix} \quad (2.48)$$

where

$$P(H) = HB_2 - B_1H + A_{12}. \quad (2.49)$$

The solution of $P(H) = 0$ is a function of the solution L of $R(L) = 0$.

It is well known that equation (2.49) always has a solution when

Assumption 2.1 is satisfied. In case when $\sigma_r = \sigma(B_1)$ contains r slowest modes of A , this solution can be found as the limit of the sequence

$$H_{k+1} = (B_1 H_k - A_{12}) B_2^{-1}. \quad (2.50)$$

This can be seen by writing (2.50) as

$$h_{k+1} = \tilde{A} h_k + b \equiv (I \otimes B_2)^{-1} [(B_1 \otimes I) h_k - a_{12}] \quad (2.51)$$

where \otimes denotes the Kronecker product. The eigenvalues of \tilde{A} are $\lambda(\tilde{A}) = \lambda(B_1)/\lambda(B_2)$ so that $|\lambda(\tilde{A})| < 1$ and hence H_k converges to a unique solution.

Combining transformations (2.11) and (2.47) we get the complete transformation between x and (y,z) as

$$\begin{bmatrix} y \\ z \end{bmatrix} = \begin{bmatrix} I-HL & H \\ -L & I \end{bmatrix} \begin{bmatrix} x^1 \\ x^2 \end{bmatrix} \equiv T^{-1}x \quad (2.52)$$

where L and H satisfy (2.13) and (2.49), respectively.

For some engineering applications where time scale decomposition is required, only a few iterations of (2.41) and (2.50) for L and H are sufficient. Figure 2.4 is the power system of Example 2.17 where the responses of the system based on subsystem integration of (B_1, y) and (B_2, z) , combined through (2.52) into x are compared with the slow approximation y . The matrices B_1, B_2 and T contain L and H obtained after two iterations of (2.41) and (2.50).

2.6. Time Scale Separation in Weakly Nonlinear Systems

Simulation is still dominant method of analysis for many systems, especially for nonlinear systems. An objective of the analysis is to investigate the effect of parameter changes on system behavior, or to detect system instability. The emphasis is usually on the speed of simulation rather than on accuracy. Yet, the speed of simulation is constrained by the wide range of dynamic phenomena encountered typically in large scale systems. In other words some variables of the system respond much faster than the others (in linear systems this is to say that there is a spread of eigenvalues). We say that system possesses multitime scale property. This property is indicated by writing the

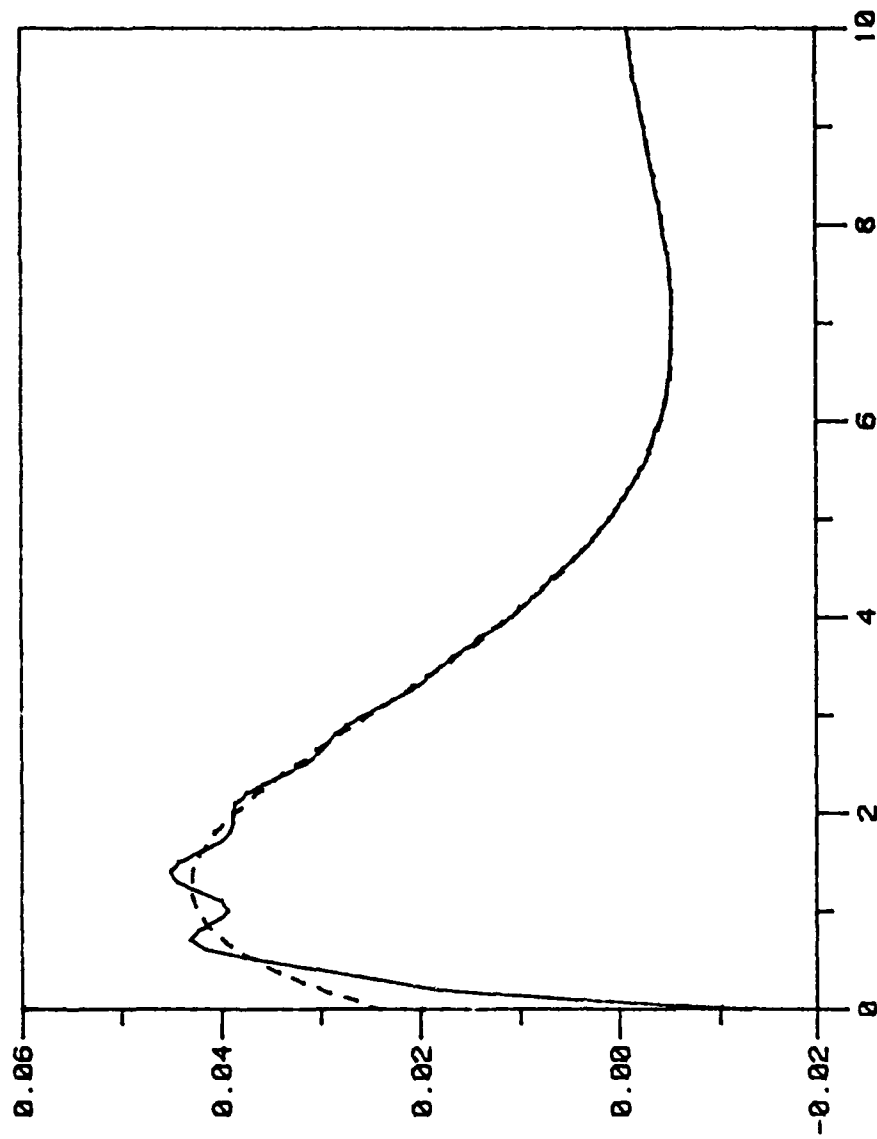


Figure 2.4. Exact e'_q and its slow approximation.

system model in the singularly perturbed form

$$\dot{x}_1 = \varphi_1(x_1, x_2) \quad (2.53)$$

$$\varepsilon \dot{x}_2 = \varphi_2(x_1, x_2) \quad (2.54)$$

for x in some domain D , as in (1.9) for linear systems. Assuming that the fast subsystem is stable along any trajectory initiated in D , [8], the analysis of (2.53), (2.54) is performed in two time scales avoiding so the stiffness of the model, in much the same way as in the analysis of the linear singularly perturbed systems. The problem arises when all states have mixed fast and slow components, i.e. in the mixed state case. In this case meaningful decomposition of the state vector as in (2.53), (2.54) is impossible.

This section addresses the problem of the simulation of two time scale mixed state systems transformable to the form

$$\dot{x} = Ax + f(x), \quad f(0) = 0 \quad (2.55)$$

if $f(x) \in C^{1*}$ and has small Lipschitz constant. We will call such systems weakly nonlinear since basic characteristics of their behavior are determined by the linear part. Hence, two time scale property of (2.55) implies that the matrix A has two groups of eigenvalues widely separated in magnitude. If T is the block diagonalizing transformation (2.52) for the matrix A , such that slow eigenvalues are in B_1 and fast eigenvalues are in B_2 (B_1 and B_2 are defined by (2.9) and (2.10)), then a transformation of variables

* C^1 is a class of functions with continuous first derivative.

$$x = T \begin{bmatrix} y \\ z \end{bmatrix}, \quad \begin{bmatrix} y \\ z \end{bmatrix} = \begin{bmatrix} W_1 \\ W_2 \end{bmatrix} x \quad (2.56)$$

can be used for the nonlinear model as well, in which case (2.55) becomes

$$\begin{bmatrix} \dot{y} \\ \dot{z} \end{bmatrix} = \begin{bmatrix} B_1 & 0 \\ 0 & B_2 \end{bmatrix} \begin{bmatrix} y \\ z \end{bmatrix} + W f(x) \quad (2.57)$$

where W is the inverse of T given explicitly by (2.52). In the above model y and z represent predominantly slow and predominantly fast variables respectively, which are decoupled through linear part, and weakly coupled through the nonlinear part (the weak coupling is the consequence of the assumption on f as having small Lipschitz constant). The system (2.57) is now in singularly perturbed form and the standard singular perturbation approach can be applied:

(i) solve the slow subsystem

$$\dot{\bar{y}} = B_1 \bar{y} + W_1 f(\bar{y}, \bar{z}) \quad (2.58)$$

$$0 = B_2 \bar{z} + W_2 f(\bar{y}, \bar{z}) \quad (2.59)$$

for \bar{y} and \bar{z} , and

(ii) solve the fast subsystem

$$\dot{\tilde{z}} = B_2 \tilde{z} + B_2 \bar{z} + W_2 f\left(T \begin{bmatrix} \bar{y} \\ \bar{z} + \tilde{z} \end{bmatrix}\right) \quad (2.60)$$

for \tilde{z} . Then approximate the solution x by $x = T \begin{bmatrix} \bar{y} \\ \bar{z} + \tilde{z} \end{bmatrix}$.

Implicit assumption in this algorithm is that the fast subsystem Jacobian

$$T_f = B_2 + W_2 \frac{\partial f}{\partial z} \quad (2.61)$$

evaluated along \bar{y} and \bar{z} has $\text{Re}\lambda(T_f) < 0$ and $z(0)$ is in the appropriate domain of attraction [8]. Under this assumption \bar{z} can be expressed as a continuous, unique function of \bar{y} , and hence a unique solution of (2.58) and (2.60) exists in \bar{y} and \bar{z} . Solving this equations can answer the question of slow subsystem stability, and complete system behavior.

If, however, we assume that system is stable and want to observe its slow behavior only, for different initial conditions in the stability domain, or after a change in parameters, then a useful combination of the linear and nonlinear simulation can be achieved if the system is presented in the form (2.57). In this case after some time t_c , such that $f(x)$ is sufficiently small, the simulation can be continued on the low order linear subsystem $\dot{y} = B_1 y$. We illustrate now some of the potentials of this approach, and some differences from other related approaches to simulation, on the one machine infinite bus power system, whose model is given in Appendix A. Let us denote that model as $\dot{x} = \varphi(x)$. For integration we use the predictor-corrector method of [35], but do not investigate which numerical method is the best. We will show a set of figures with responses of x_1 , which is typical of what we want to show. On each figure there are two responses: solid line is always the full system response, i.e. the solution of $\dot{x} = \varphi(x)$. The dashed line corresponds to different approximations of the slow response, each of which will now be explained.

First the system is linearized around the stable equilibrium, and the linearized state matrix A is given in Appendix A. Then $f(x) = \varphi(x) - Ax$. For the block-diagonalization of A we specify $r=2$, $\tau_2 = \sigma_s$ and use T of (2.52), in which L , H , B_1 and B_2 are as obtained

after two iterations of the algorithms (2.41) and (2.50), respectively. Now the model is in the form (2.57). Figure 2.5 gives x_1 as obtained by solving (2.53) and (2.54) with ϵ set to zero. The error is unacceptable. Figure 2.6 shows the nonlinearity present in the slow system response, since the dashed curve is the response of $\dot{y} = B_1 y$. The true nonlinear slow response should be a line which would pass in between the wiggles of the solid curve. Figure 2.7 gives the response of the slow component of x_1 , which result from solving (2.58) and (2.59) for \bar{y} and using the back transformation $x_1 = \bar{y}$ (which comes from $x = T \begin{bmatrix} y \\ 0 \end{bmatrix}$). The improvement of this approach (application of singular perturbation to the transformed system) over the application of singular perturbation to the original model is significant. On the next figure, fig. 2.8 the slow response of x_1 is given as computed by using nonlinear model (2.58), (2.59) for the first two seconds only, and then for the rest of the time using linearized, low order model $\dot{y} = B_1 y$. In addition larger step size is used. Here the nonlinear model is used to initiate properly the slow linear subsystem. The effect of nonlinearities is evident from comparing these responses with fig. 2.6.

In some recent approaches to numerical integration of singularly perturbed and descriptor variable system [36] it has been proposed to integrate the original system (2.53), (2.54) but adjust the step size of integration according to the slow component of the local error (see [50] for numerical integration details). For "filtering" the error in order to get its slow component a matrix very much related to W_1 (2.53) is computed, whenever the step size has to be changed. Based on the power system example only, it seems that that approach may give more accurate response

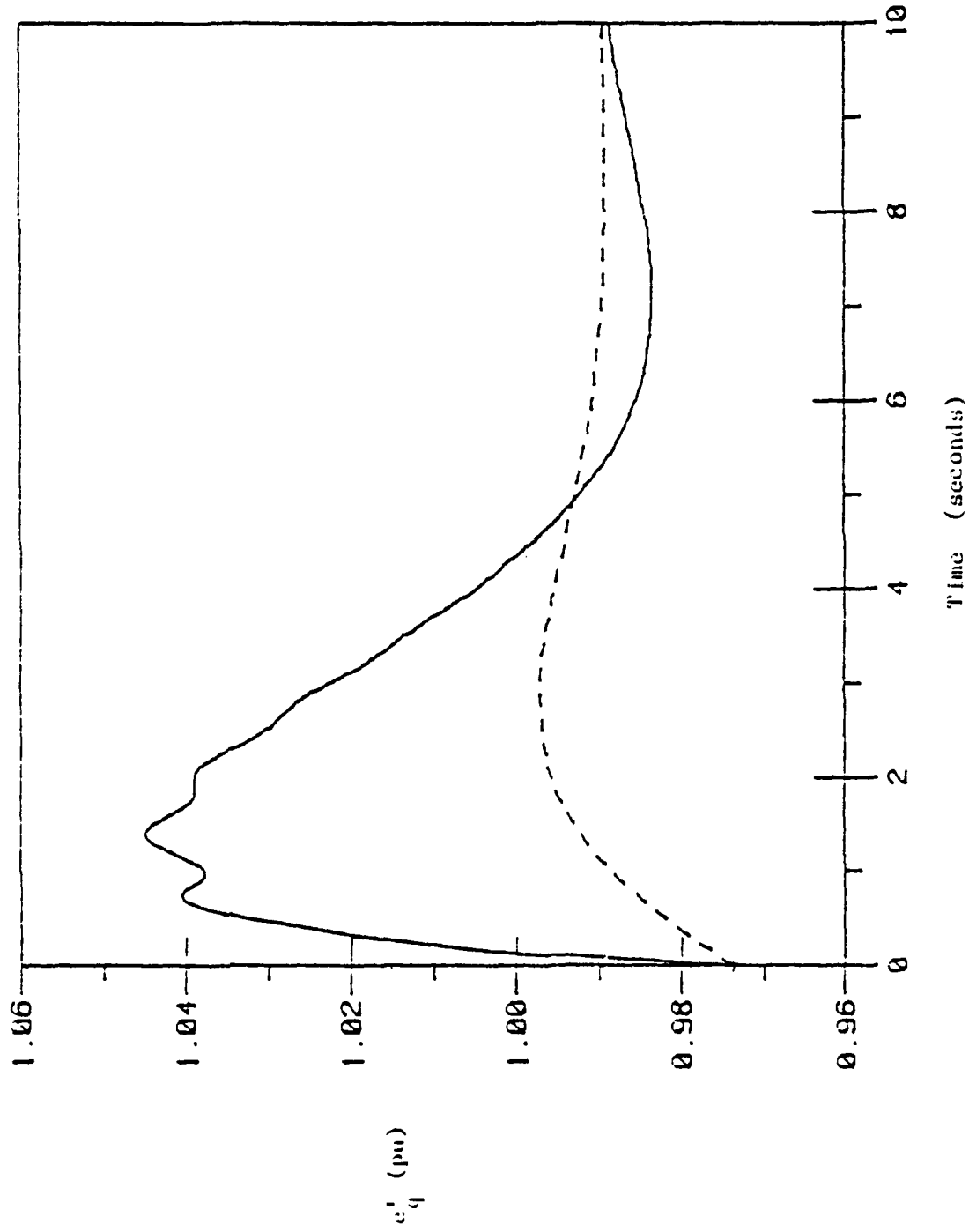


Figure 2.5. Application of the singular perturbation to the nonlinear model of one machine infinite bus system: exact systems response vs. its slow approximation.

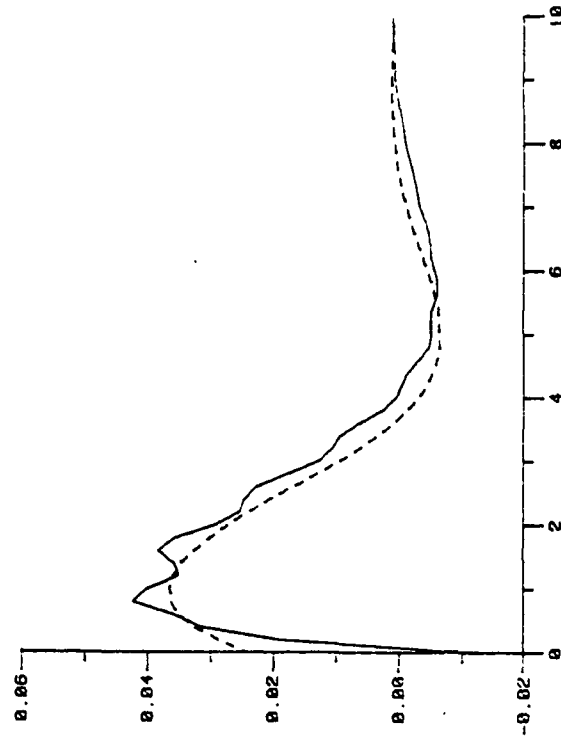


Figure 2.7. Application of the singular perturbation to the transformed model: exact response of e'_q vs. the slow approximation step size 0.2s.

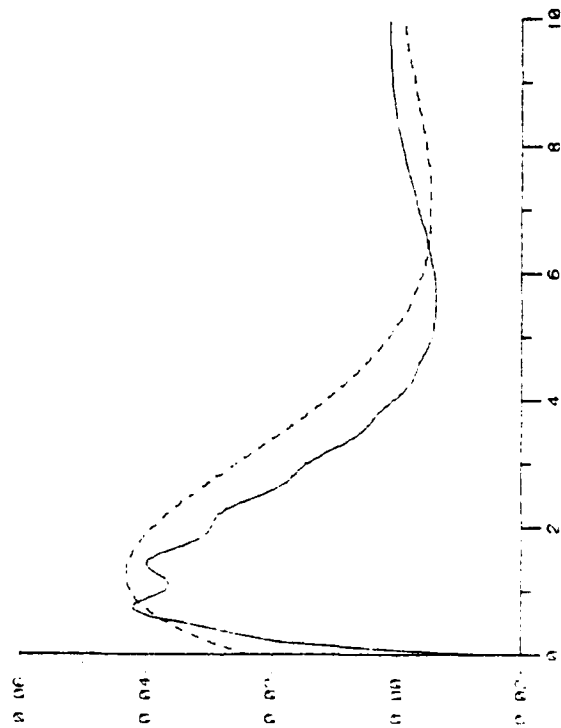


Figure 2.6. Exact response of e'_q vs. the slow approximation of the linearized model.

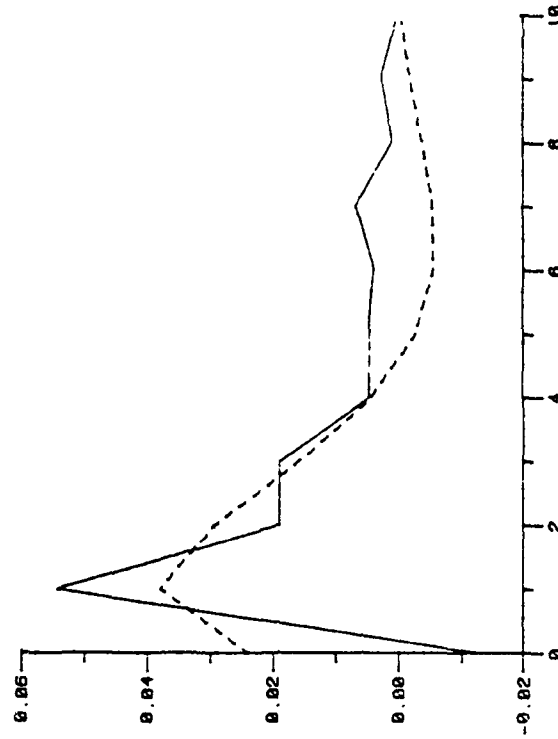


Figure 2.9. Response of e'_q from the full model and the approximation; step size 1s, $t_c=2s$.

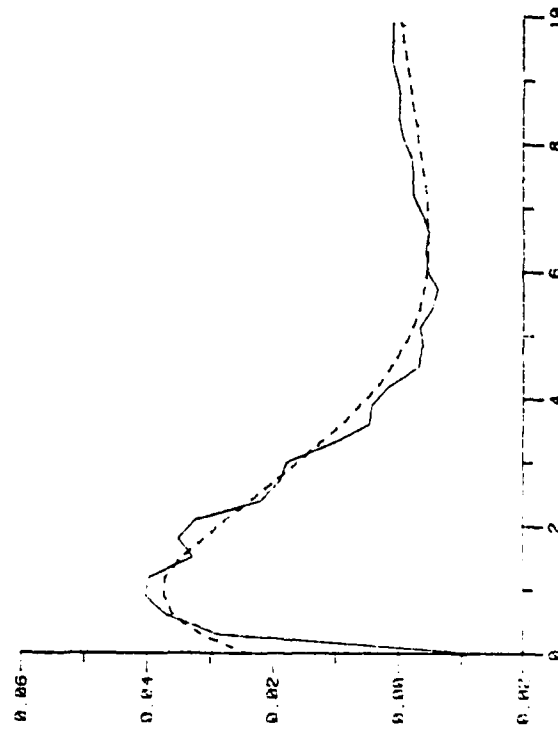


Figure 2.8. Exact response of e'_q vs. its slow approximation; step size 0.3s, $t_c=2s$.

of the slow dynamics if required, then it is possible by solving (2.58) (2.59). However, slow dynamics of (2.58), (2.59) permits much larger step size than in the method of [36]. This is useful when a quick approximate solution is satisfactory. The difference in accuracy between the two methods is illustrated for the case when both are forced to use very large step size, fig. 2.9.

3. PARTIAL COHERENCY

3.1. Introduction

Application of the modal method for the reduction of the multi-machine electromechanical model of power systems, has been tried in [16,18]. However, more successful has been the use of coherency. Two generators, with responses denoted by $x_i(t)$ and $x_j(t)$ are called coherent if

$$x_i(t) - x_j(t) = \text{const.} \quad (3.1)$$

Groups of machines in which any two generators satisfy this criterion are called coherent groups or coherent areas. Once coherent areas are known the reduction of the model order is achieved by replacing all the coherent generators by one. A critical step however, is the grouping of the machines into areas. Coherent machines are identified either from actual or simulated machine responses [17,18], or by an algebraic evaluation of the modes present in the linearized model [16,20,21,23]. Most analytical methods require that machines be coherent throughout the duration of their transients. We propose here a less demanding definition of partial coherency. It may be interpreted as a requirement that the equivalent machines of the areas represent as closely as possible a preselected group of modes. In the next chapter it will be shown that in the particular case, when these modes are the slowest modes of the system, the resulting area decomposition is relatively independent of fault locations and loading conditions. In our approach partial coherency is related to the spectrum separation of the previous chapter. In the ideal partial coherency case the solution L of the suitably formulated Riccati equation has the elements made of zeros and ones,

which unambiguously define coherent areas. The subsystem reproducing complementary subspectrum turns out to model intermachine dynamics, showing that in the case of ideal partial coherency the interarea and intermachine dynamics are decoupled. In a nonideal case our approach is to search for a solution L which can be approximated by the matrix of zeros and ones. In this case areas are made of machines which are near-coherent in the pre-selected modes, and weakly coupled rather than decoupled area and intermachine dynamics.

In connection with power system stability study, there is continuing interest in the development of a systematic area decomposition procedure. Our grouping algorithm reduces the decomposition procedure to the computation of a basis for the invariant subspace corresponding to the given subspectrum, and a Gaussian elimination of a low order matrix.

In the next section we present an electromechanical model and review some of its properties. An overview of existing approaches to coherency will be given in Section 4.3. In Section 4.4 the concept of partial coherency will be introduced and its properties analyzed for ideally decomposable systems. A grouping algorithm developed for near decomposable systems will be given in Section 4.5. The algorithm will be illustrated by a 48 machine example. Physical meaning of the variables associated with the decomposition of a system into coherent areas will be given in Section 4.6.

3.2. Electromechanical Model

The electromechanical model of a power system with n generators labeled from 1 to n and m load buses labeled from $n+1$ to $n+m$ is given by [52]

$$\dot{\delta}_i = \omega_i$$

$$M_i \dot{\omega}_i + D_i \omega_i = P_{m_i} - P_{g_i}$$

$$P_{g_i} = \sum_{\substack{j=1 \\ j \neq i}}^N v_i v_j B_{ij} \sin(\delta_i - \delta_j) + v_i^2 G_{ii} \quad i=1,2,\dots,n \quad (3.2)$$

$$P_{l_i} = \sum_{\substack{j=1 \\ j \neq i}}^N v_i v_j B_{ij} \sin(\delta_i - \delta_j) + v_i^2 G_{ii} \quad i=n+1,\dots,N \quad (3.3)$$

where

$$N = n+m$$

δ_i = for $1 \leq i \leq n$ rotor angle of machine i ; for $n+1 \leq i \leq N$ bus angle of the load bus $i-n$ (radians)

ω_i = speed of machine i (per unit)

P_{m_i} = mechanical input power (per unit)

P_{g_i} = generated electrical power of machine i (per unit)

M_i = moment of inertia of machine i

D_i = Damping constant of machine i (per unit)

P_{l_i} = negative of load consumed at the load bus $i-n$.

B_{ij} = reactive part of the admittance connecting buses i and j

G_{ii} = i -th diagonal entry of the real part of admittance matrix.

Assumptions associated with the model are:

Assumption 3.1: Mechanical input power P_{m_i} and load P_{l_i} are constant.

Assumption 3.2: Active power losses are neglected, i.e. active part of admittance matrix is neglected.

Assumption 3.3: Active and reactive power flow are decoupled, i.e. bus voltages are assumed constant in the model (3.2), (3.3).

Model (3.2) and (3.3) contain both dynamic and static equations. In linear system theory such models are known as descriptor variable systems [9,10]. Study of the descriptor variable system obtained from (3.2) and (3.3) by linearization around a stable equilibrium point reveals to a great extent the intermachine oscillation behavior. The linearized model is

$$\begin{bmatrix} \Delta \dot{\delta} \\ \Delta \dot{\omega} \\ 0 \\ 0 \end{bmatrix} = \begin{bmatrix} 0 & I & 0 & 0 \\ 0 & -M^{-1}D & -M^{-1} & 0 \\ H_{gg} & 0 & -I & H_{gl} \\ H_{\ell\lambda} & 0 & 0 & H_{\ell\ell} \end{bmatrix} \begin{bmatrix} \Delta \delta \\ \Delta \omega \\ \Delta P_g \\ \Delta \theta \end{bmatrix} \quad (3.4)$$

where

$$\Delta \delta^T = (\delta_1 - \delta_1^*, \delta_2 - \delta_2^*, \dots, \delta_n - \delta_n^*)$$

$$\Delta \omega^T = (\dots, \omega_i - \omega_i^*, \dots)$$

$$\Delta \theta^T = (\delta_{n+1} - \delta_{n+1}^*, \dots, \delta_N - \delta_N^*)$$

$$\Delta P_g^T = (\dots, P_{gi} - P_{gi}^*, \dots)$$

$$H = \begin{bmatrix} \frac{\partial P_g}{\partial \delta} & \frac{\partial P_g}{\partial \theta} \\ \frac{\partial P_\ell}{\partial \delta} & \frac{\partial P_\ell}{\partial \theta} \end{bmatrix} = \begin{bmatrix} H_{gg} & H_{gl} \\ H_{\ell g} & H_{\ell\ell} \end{bmatrix} = (h_{ij}) \quad (3.5)$$

$$h_{ij} = \begin{cases} -\sum_{j \neq i}^n h_{ij} & i=j \\ -v_i v_j B_{ij} \cos(\delta_i^* - \delta_j^*) & i \neq j \end{cases} \quad (3.6)$$

B_{ij} = reactive part of the admittance between buses i and j .

If $H_{\ell\ell}^{-1}$ exists (by the assumption on stability of the equilibrium, $H_{\ell\ell}^{-1}$ is in fact positive definite) (3.3) can be reduced to

$$\begin{bmatrix} \Delta\dot{\delta} \\ \Delta\dot{\omega} \end{bmatrix} = \begin{bmatrix} 0 & I \\ -M^{-1}K & -M^{-1}D \end{bmatrix} \begin{bmatrix} \Delta\delta \\ \Delta\omega \end{bmatrix} \quad (3.7)$$

where

$$K \equiv H_{gg} - H_{g\ell} H_{\ell\ell}^{-1} H_{\ell g} = (k_{ij}). \quad (3.8)$$

Matrix K has several useful properties which can be deduced from the properties of the Jacobian H . First, due to (3.6) H and K are symmetric. From (3.6) it can be seen that matrix H has one zero eigenvalue with the corresponding eigenvector $v^T = (1, 1, \dots, 1)$. The same is true for the matrix K , namely $Kv_1 = 0$, where v_1 is the n -vector containing first n components of v . This property can be derived as follows. Let v_2 be n -vector containing last n components of v . Then, from $Hv = 0$ we have

$$v_2 = -H_{\ell\ell}^{-1} H_{\ell g} v_1 \quad (3.9)$$

so that

$$Kv_1 = (H_{gg} - H_{g\ell} H_{\ell\ell}^{-1} H_{\ell g}) v_1 = H_{gg} v_1 + H_{g\ell} v_2 = (H_{gg} \ H_{g\ell}) v = 0. \quad (3.10)$$

This property shows that each diagonal element of K equals the negative sum of the off-diagonal elements in the same row. Under the assumption

Assumption 3.4: $|\delta_i - \delta_j| < \pi/2$, if $B_{ij} \neq 0$ we have that the off-diagonal elements of H are negative, which due to the zero eigenvalue-eigenvector property means that the diagonal elements are positive. The same is true for K since then $H_{\ell\ell}^{-1}$ has all its elements positive* so that $-H_{g\ell} H_{\ell\ell}^{-1} H_{\ell g}$

* Matrix $H_{\ell\ell}$ is Minkowski matrix for which Theorem A.2 of [57] applies asserting that the elements of $H_{\ell\ell}^{-1}$ are positive.

is negative, and hence all the off-diagonal elements of K are negative as well. Due to (3.10) it means that the diagonal elements are positive.

Based on the properties of matrix $K = (k_{ij})$ it can be assumed that the elements k_{ij} are of the form (3.6). In this way we define an equivalent admittance matrix connecting generator buses only. Under Assumption 3.4 the off-diagonal elements of the reduced admittance matrix are of the same sign, and its diagonal elements are negative sums of the off-diagonal elements in the same row. An alternative way to get the same kind of model is to transform each load to an equivalent admittance, and then eliminate all load buses. In summary we will assume that the electromechanical model is in the form (3.7) in which k_{ij} elements have the form (3.6) for some equivalent admittance elements B_{ij} . This model has several properties which allow even further simplifications.

At δ^* and ω^* , the eigenvalues of (3.7) are of the following three types (see Figure 3.1 for an example):

1. a zero eigenvalue corresponding to the motion of all the machine angles,
2. a small negative real eigenvalue corresponding to the aggregate speed of all the machines, and
3. $(n-1)$ pairs of lightly damped oscillatory modes which typically range in frequency from $1/2$ to 2 Hz.

Models involving more details, such as excitation systems and governors would still contain the above set of eigenvalues, modified mostly in the damping and not in frequency [19]. Since the small damping constant D_i does not significantly affect the frequencies of the oscillatory modes [27], it can be

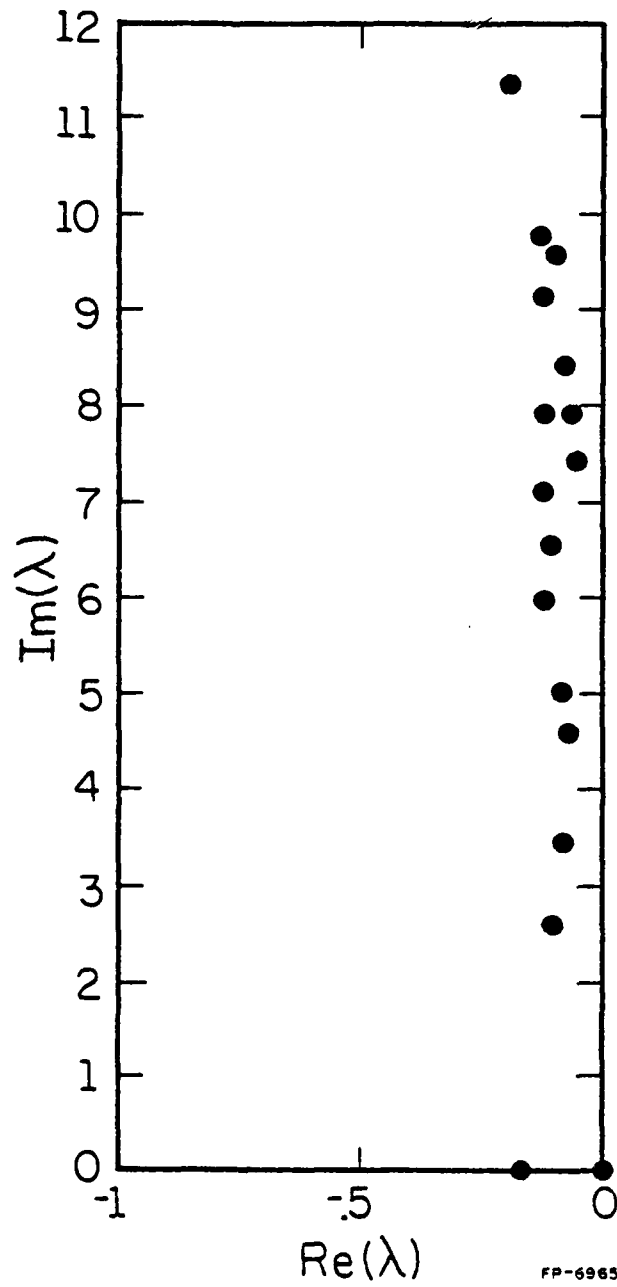


Figure 3.1. Eigenvalues of a 16 machine system [25].

neglected. See Figure 3.1 for a typical pattern of eigenvalues of (3.7).

Thus the model used in our approach is

$$\ddot{x} = -M^{-1}Kx \equiv Ax. \quad (3.11)$$

The properties of the A matrix are as follows:

(P1) A has zero eigenvalue whose eigenvector is

$$v_1^T = (1 \ 1 \ \dots \ 1). \quad (3.12)$$

Property (P1) follows from $Av_1 = 0$, which is due to (3.6) as the sum of each row in $A = (a_{ij})$ is

$$\sum_{j=1}^n a_{ij} = M_i^{-1} \sum_{j=1}^n k_{ij} = 0, \quad i = 1, 2, \dots, n. \quad (3.13)$$

(P2) A is diagonalizable because it is similar to the symmetric matrix

$$-M^{-1/2}KM^{-1/2} \quad (3.14)$$

where $M^{1/2}$ is the positive symmetric square root of M. Thus, all the eigenvalues λ_i of A are real. Furthermore, under assumption that the equilibrium of (3.2) and (3.3) is stable, they are all nonpositive [51].

(P3) If \bar{A} is the state matrix of the system (3.7), with damping neglected, then the relation between eigenvalues and eigenvectors of A and \bar{A} is

$$\bar{\lambda} = \pm \sqrt{\lambda_i}. \quad (3.15)$$

If x is an eigenvector of A corresponding to λ_i , then the two eigenvectors of \bar{A} are $(x^T, \pm \sqrt{\lambda_i} x^T)^T$. Because of such simple relations between eigenvalues and eigenvectors of $2n \times 2n$ matrix \bar{A} , and $n \times n$ matrix A, we choose to deal in our approach only with the lower order A matrix.

There are two ways of representing disturbances in such linearized models. In [19,21,23] the disturbance is modeled as an external input to either unreduced model (3.4) or the reduced (3.7). All the standard disturbances - generator outage, line switching and load shedding - are modeled as the equivalent change in load and generation. The duration of the external input equals the duration of the fault. Hence the model is

$$\dot{x} = \bar{A}x + Bu \quad 0 \leq t \leq t_c \quad (3.16)$$

$$\dot{x} = \bar{A}x \quad t > t_c \quad (3.17)$$

where

$$\bar{A} \text{ is the state matrix of (3.7) and } B = \begin{bmatrix} 0 & 0 \\ -M_1^{-1} - M^{-1} \begin{bmatrix} H_{gl} \\ I \end{bmatrix} (H'_{ll})^{-1} \end{bmatrix}$$

$$u = \text{input}; u = \begin{bmatrix} \Delta P_m \\ \Delta P_l \end{bmatrix}.$$

H'_{ll} = "22" block of the Jacobian H modified in structure to account for a line outage; otherwise equal to H_{ll} .

t_c = clearing time - duration of the disturbance.

In our approach disturbance is modeled as an initial condition at $t=t_c$ for the linearized system (3.11) around a postfault equilibrium point. In other words only the low order version of (3.4) is considered.

3.3. Review of Existing Coherency Methods

Coherency has been a fruitful approach to the model order reduction of power systems. The need for repeated simulation of larger and larger power systems has emphasized even more the role of this technique. A reflection of

this situation is the existence of a number of different approaches to coherency identification. In this section we give an overview of several characteristic approaches, in order to identify the limitations and gain insight into the problem.

In [37] the conditions for coherency of a group of machines are derived starting from the definition (3.1) and using (3.2), (3.3), and, in addition, the equations for the reactive power flow. The conditions are expressed in terms of machine internal voltages and interconnecting admittances as follows. A group of r machines in an n machine system is coherent if and only if

$$\begin{aligned} \text{a. } \frac{B_{ij}}{M_i} (V_i \cos \delta_{ir} - jV_i \sin \delta_{ir}) &= \frac{V_r}{M_r} B_{rj} \\ i &= 1, 2, \dots, r; \quad j = r+1, \dots, n \end{aligned} \quad (3.18)$$

b. the disturbance is outside the coherent area.

This condition indicates how strict requirements are to be satisfied for coherency to exist. One case when they are satisfied is when there are several machines on the same bus. To deal with the practical systems a less restrictive condition is needed. The one of reference [37] is given using the linearized model (3.16). If r machines are to be coherent, and if the corresponding states are the first r states of x in (3.16) then the condition for coherency is expressed as

$$\begin{aligned} \text{a. } \|\bar{A}_{12}\| &< \varepsilon \\ \text{b. } \|B_1 u\| &< \mu \end{aligned} \quad (3.19)$$

for some small numbers ε and μ . Matrices \bar{A}_{12} and B_1 are $r \times (n-r)$ "12" block of \bar{A} and $r \times 1$ block of B . In other words coherency is a result of weak

coupling of the group of r machines with the rest of the system and the disturbance is outside the group. The reference [37] does not contain an algorithm for identifying areas.

In [20,21] coherency is related to controllability observability of (3.16). The output is defined as follows. If a coherent area is to contain r machines, that is

$$y = \begin{bmatrix} I_{r-1,r-1} & \begin{matrix} -1 \\ \vdots \\ -1 \end{matrix} & 0 \end{bmatrix} x \equiv Cx \quad (3.20)$$

where x has been ordered so that first r components are the states of the coherent machines, then a necessary and sufficient condition for coherency is that

$$\text{Im } Q_c \subset \text{Ker } C \quad (3.21)$$

where Q_c is the controllability matrix $(B, \bar{A}B, \dots, \bar{A}^{n-1}B)$. This condition simply says that from any of the machine differences in the coherent area the disturbance should not be seen, either because the controllable modes are unobservable through C or because the observable modes are uncontrollable through B . In the case of nonideal coherency it is suggested to measure the distance between the two subspaces of (3.21) and define coherency when the distance is small. An algorithm for checking the condition (3.21) would be based on singular value decomposition [44] of several matrices of the same order as the order of the system, and is therefore inappropriate for large power systems.

The approach of [23] implicitly exploits the controllability-coherency relation. Two basic ideas are realized. First, that machines which

are coherent in the model (3.16), i.e. during the fault, will be coherent throughout the entire response period. Second, coherency is essentially defined with respect to the modes which are excited by the disturbance. Namely, eigenvectors of the modal matrix M from

$$x(t) = Mz(t) \quad (3.22)$$

are multiplied by the initial values of mode excitation, i.e. the matrix

$$\bar{M} = Mz(0) \quad (3.23)$$

where $z(0)$ is $2n \times 2n$ diagonal matrix with the i th diagonal entry equal to $z_i(0)$ is considered. Then two machines i and j are declared coherent if the difference $\|m_i - m_j\| < \epsilon$ for some small ϵ , where m_i and m_j are row vectors of \bar{M} . The method requires computation of all eigenvalues and both right and left eigenvectors of the matrix A . For large power systems this may require considerable computer time and memory.

Instead of normalizing all the eigenvectors, as in (3.23), the idea of using only a few preselected modes (a few eigenvectors of M) to define coherency has been explored in [26]. There the coherency of machines i and j with respect to mode k is defined as the requirement that

$$\text{angle}(m_{ik}, m_{jk}) < \epsilon < \pi/2 \quad (3.24)$$

where m_{ik} and m_{jk} are (in general) complex elements of the matrix M . For a real eigenvector this requirement means that the elements of the k -th eigenvector corresponding to the i -th and j -th machine have to be of the same sign. The criterion means that the machines i and j are accelerated (decelerated) by the power from the rest of the system for more than half a period of the k -th frequency. Coherency with respect to the group of modes is defined so

that the criterion (3.24) is satisfied with respect to each mode of the group.

The idea of using coherency for model order reduction has found overwhelming response from industry after it had been promoted in [41], and in particular after a complete computer program has recently been developed and its utility demonstrated on a number of large systems [19]. The method employed is a direct application of the definition (3.1), which means that to obtain system response, the integration is needed for each disturbance and then comparison of responses for each t on some time interval. A fast integration method (trapezoidal integration) is used to keep the numerical burden on the reasonable level. The method, however, does not provide any insight into the relation of coherent areas to the system parameters, as in the previous methods.

In all the previous methods coherent areas depend on the location of the fault. Therefore for each new fault reevaluation of the areas has to be made. In [39] an attempt has been made to overcome this difficulty, and to come up with the areas which can be used for more disturbances. A solution is found in a probabilistic approach. Namely, a set of disturbances, i.e., inputs u in the model (3.16) with given probabilities is used. A measure of coherency between machines i and j is computed as

$$c_{ij} = \sqrt{\frac{1}{T^p} \int_0^T (x_i - x_j)^2 dt} = \sqrt{e_{ij}^T S e_{ij}} \quad (3.25)$$

where p is selected to make c_{ij} finite for $T \rightarrow \infty$,

$$S = \frac{1}{T^p} \int_0^T E\{x(t)^T x(t)\} dt, \quad (3.26)$$

and e_{ij} is the vector of zero elements except i -th, which is 1 and j -th which is -1. It is easy to see that smaller values of c_{ij} indicate that machines i and j are coherent. Of particular interest is the case of the infinite time interval. Then S can be expressed as¹

$$S = A^T B (R + \mu \mu^T) B^T (A^I)^T \quad (3.27)$$

where A and B are defined by (3.16), μ is the expected value of u , and R is its covariance matrix. A^I is defined as

$$A^I = X \begin{bmatrix} \Lambda_1^{-1} & 0 \\ 0 & 0 \end{bmatrix} X^{-1} \quad (3.28)$$

where Λ_1 is a $2n-2$ diagonal matrix of nonzero eigenvalues of (3.16) and X is its matrix of right eigenvectors. For zero mean, independent identically distributed disturbance $R + \mu \mu^T = I$ and S of (3.27) depends only on the parameters of the system. This dependence is made explicit in [39] by writing part of (3.27) in terms of transformed matrix A , rather than via eigenvalues and eigenvectors. However, by using the above form to eliminate all the modes of the system which cause insignificant changes in S , it has been concluded in [39] that the eigenvalues of the reduced system, based on coherency and eigenvalues of the reduced system based on the modal method [15], are approximately the same.

This important connection between coherency and modal methods has also been indicated in [16] under the special condition that L of (2.11) has

¹This expression is different from [39] in that it is independent of the choice of reference machine whose choice may be a problem, but is in fact irrelevant for the existence of coherent areas as will be shown later in the chapter.

the structure in which each row has only one zero element equal to 1, and all other elements equal to zero.

Most of the presented coherency methods concentrate on the development of an alternative coherency criterion, in order to avoid direct simulation, implicitly required in Definition 3.1. Except for [19] none of the methods offer an algorithm for identifying coherent areas, which is efficient enough to be applied to large power systems. Most of them, except [39,26] would give areas which are valid for only one disturbance.

The coherency definition and the corresponding algorithm for identifying coherent areas, which will be given in the rest of this chapter, are aimed at overcoming the difficulties of the existing methods and retaining their good characteristics. We use the result of [16] directly to define the so-called ideal coherency. Systems with ideally coherent areas serve to give us an insight which we then use in analysis of realistic power systems, in much the same way as the descriptor variable system analysis of (1.11) serves to give insight into the behavior of singularly perturbed systems (1.9). A result of this approach is the new algorithm for identifying coherent areas, designed for application to large power systems. Analytical study reveals that so obtained coherent areas are almost independent on fault location and nonlinearities of the system.

3.4. Partial Coherency

Considering the definition of coherency (3.1) and the model (3.17) it is clear that coherency can be achieved only if the initial condition $x(0)$ is such that only r modes are excited, for some $r < n$. This is also clear from the coherency condition (3.21), for if $\dim \text{Im}(Q_c) = n$, this would

mean that there exists a single disturbance which would excite all the modes, but then C must be zero matrix which means that there is no coherency. In other words, each case of coherency is a partial coherency. In this section we will give a new formulation for the existence of partial coherency in terms of generalized Riccati equation. The coherency will be connected with the spectrum separation problem treated in Section 2.2. Let us first define partial coherency.

Definition 3.5: Given r eigenvalues of A in (3.11), σ_r . Then machines "i" and "j" are coherent with respect to σ_r (partially coherent) if for all t of interest, possible $t \in [0, \infty)$, and any initial condition $x(0)$, their angles $x_i(t)$ and $x_j(t)$ satisfy

$$x_i(t) - x_j(t) = z_{ij}(t) \quad (3.29)$$

where $z_{ij}(t)$ contains none of the modes from σ_r . A coherent area consists of all the machines coherent to each other.

We note that in this definition no machines from different areas can be coherent, that is, no coherent area can be divided into more areas.

Although Definition 3.1 does not require that the number of coherent areas equal the number of modes r , systems with this property, which will be called r -decomposable systems, are of particular importance. The study of r -decomposable systems is an essential step toward the analysis of more common "near-decomposable" systems, that is systems with near-coherent rather than coherent areas.

Definition 3.6: The machines "i" and "j" are near-coherent if in Definition 3.1 the contribution of the modes from σ_r in $z_{ij}(t)$ is small. A near-coherent

area consists of all machines which are near coherent to each other. An r -near-decomposable system consists of r near-coherent areas.

Our approach to the identification of coherent areas is to first consider this problem for r -decomposable systems. We show that in this idealized case the solution of the matrix Riccati equation (2.13), which separates the spectrum of A into σ_r and σ_r^2 , automatically groups the machines into areas. We then use this result to develop a grouping algorithm for near-decomposable systems.

We first study the definition (3.29). In each area i , consisting of n_i machines, there are only $n_i - 1$ independent functions $z_{ij}(t)$. We can form a basis of these functions for the areas by selecting arbitrarily one machine which we call reference machine, and forming the differences of all the other machines in the same area with respect to that machine. Doing so for all r areas we form $n - r$ angle difference functions $z_{ij}(t)$. If we denote by x^1 the vector of r machines selected as reference machines in the areas, and by x^2 the $n - r$ vector of the remaining machines, which we will call follower machines, then the z_{ij} variables making vector z can be written in terms of x variables as

$$z = x^2 - L_g x^1. \quad (3.30)$$

By comparing (3.30) with (3.29) it can be seen that the matrix L_g has in each row only one nonzero element which is equal to 1. For the row j , corresponding to the j -th follower machine, if the element 1 is in column i , that means that the j -th follower machine and the i -th reference machine are in the same area. This means that given x^1 , x^2 , and L_g the coherent areas are uniquely defined. Therefore we call the matrix L_g a grouping matrix.

since it groups the follower machines with the reference machines. However, when the areas are specified, there is not a unique choice of variables for x^1 and x^2 ; to each choice of x^1 and x^2 there corresponds a different L_g . As an illustration consider a three area five machine system. Given

$$\begin{aligned} x^1 &= (x_1, x_2, x_3)^T \\ x^2 &= (x_3, x_5)^T \\ L_g &= \begin{bmatrix} 1 & 0 & 0 \\ 0 & 1 & 0 \end{bmatrix} \end{aligned} \quad (3.31)$$

the three areas, which are composed of machines 1 and 3, machines 2 and 5 and machine 4, are uniquely defined. For the same areas a different choice of

$$\begin{aligned} x^1 &= (x_4, x_3, x_2)^T \\ x^2 &= (x_1, x_5)^T \end{aligned} \quad (3.32)$$

will result in a different L_g

$$L_g = \begin{bmatrix} 0 & 1 & 0 \\ 0 & 0 & 1 \end{bmatrix}. \quad (3.33)$$

Note the zero column in L_g of (3.31) or (3.33) indicates the presence of a single machine area. Equation (3.30) can be interpreted as a special case of the transformation (2.11)

$$\begin{bmatrix} x^1 \\ z \end{bmatrix} = \begin{bmatrix} I & 0 \\ -L & I \end{bmatrix} \begin{bmatrix} x^1 \\ x^2 \end{bmatrix} = T_L \begin{bmatrix} x^1 \\ x^2 \end{bmatrix}. \quad (3.34)$$

The substitution of (3.34) into (3.11) results in

$$\begin{bmatrix} \ddot{x}^1 \\ \ddot{z} \end{bmatrix} = \begin{bmatrix} B_1 & A_{12} \\ R(L) & B_1 \end{bmatrix} \begin{bmatrix} x^1 \\ z \end{bmatrix} \quad (3.35)$$

where B_1 , B_2 , and the Riccati equation $R(L)$ are given by (2.9), (2.10), and (2.13). To meet the definition (3.29) system (3.35) must have the following properties. First z has to contain only modes corresponding to σ_r^c , for any initial condition $x(0)$. That implies that $R(L) = 0$ with L being the solution corresponding to the spectrum σ_r . Next from (3.34) and (3.29) it follows that $L = L_g$. These observations allow an alternative formulation of coherency in terms of the generalized Riccati equation.

Theorem 3.7; In an n -machine system let x^1 be the angles of r noncoherent machines and x^2 be the angles of the other $n-r$ machines. This system is r -decomposable if and only if the solution L of $R(L) = 0$ corresponding to a given σ_r is a grouping matrix $L = L_g$.

Proof: According to Theorem 2.3, z will have only the modes corresponding to σ_r^c if $R(L) = 0$ such that $\text{Im} \begin{bmatrix} I \\ L \end{bmatrix}$ is the invariant subspace of A corresponding to σ_r . For the definition (3.29) to be satisfied this L must be equal to an L_g . Conversely, if a solution of $R(L) = 0$ exists and is L_g , it satisfies the definition (3.29).

Suppose now that the system is r -decomposable with respect to a given σ_r , but we do not know its areas. How can Theorem 3.3 help us find them? First, we make a choice of x^1 and x^2 , which in turn defines the corresponding equation $R(L) = 0$. If our x^1 does not contain coherent machines this equation will have the solution L which is the grouping matrix needed to define areas. If our x^1 contains coherent machines, the solution L will not exist. The negative outcome would mean that a new choice of x^1 would have to be made and a new equation $R(L) = 0$ is solved.

The situation is considerably more involved if this direct search is applied to a near-decomposable system due to the fact that L is no longer a grouping matrix. A further difficulty is that for any choice of machine angles x^1 , the solution L usually exists. In principle, one can make all reasonable choices of x^1 and form the set D defined next.

Definition 3.8: Given σ_r and a basis V of the corresponding invariant subspace of A . Consider $\hat{V} = PV = \begin{bmatrix} \hat{V}_1 \\ \hat{V}_2 \end{bmatrix}$, where P is any permutation matrix. Define $D = \{\hat{L} = \hat{V}_2 \hat{V}_1^{-1}\}$ for all P such that \hat{V}_1^{-1} exists.

If the system is indeed near-decomposable, the set D will contain at least one element sufficiently close to a grouping matrix L_g . One possible measure of the approximation between L and L_g is a norm of $\Delta = L - L_g$. The norm is defined as the maximum sum of absolute values of row elements, that is

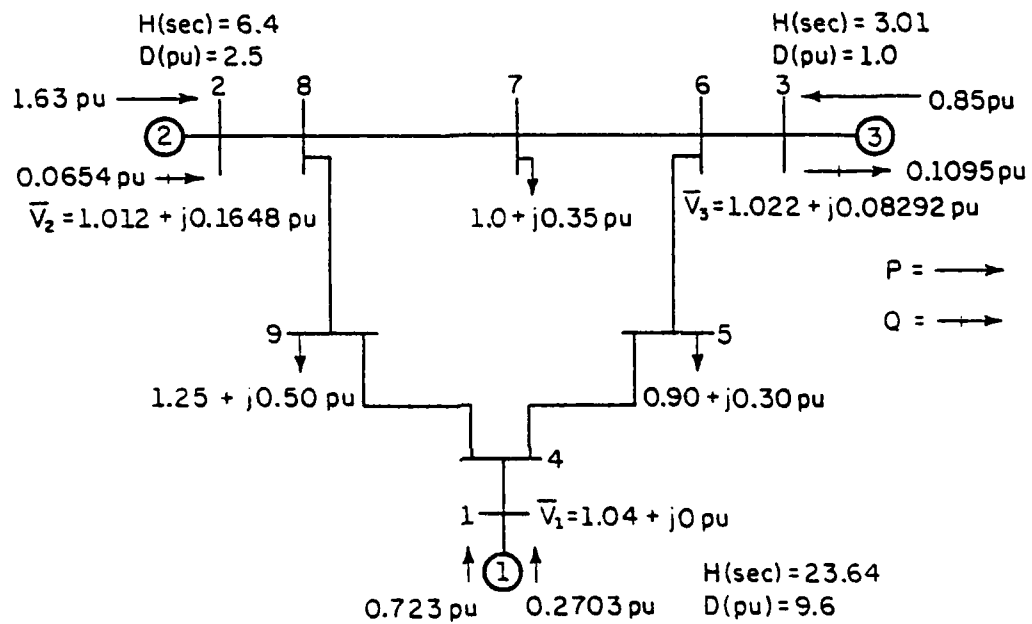
$$\|L\| = \max_i \sum_{j=1}^r |\ell_{ij}|, \quad L = (\ell_{ij}). \quad (3.36)$$

Thus if there exists a solution in D which is also a grouping matrix, that is, a decomposable system, then the norm $(L - L_g)$ is zero. In a near-decomposable system, one can search over all the solutions in D and find one which minimizes norm $(L - L_g)$. The systematic method for area identification in the next section avoids this exhaustive search. However, it is interesting to show an example of the search procedure. Let us decompose into two areas the simple three-machine system (Figure 3.2) whose model is

$$\ddot{x} = \begin{bmatrix} -14.3 & 5.43 & 8.83 \\ 14.3 & -49.4 & 35.1 \\ 58.4 & 81.4 & -140. \end{bmatrix} x. \quad (3.36)$$

Let the spectrum σ_2 consist of the two eigenvalues of smallest magnitude.

There are only three possible choices of reference machines for this example,



FP-6963

Line #	From	To	R(pu)	X(pu)	B/2(pu)
1	1	4	0.	0.0567	0.
2	4	5	0.017	0.092	0.079
3	5	6	0.039	0.170	0.179
4	3	6	0.	1.0586	0.
5	6	7	0.0119	0.1008	0.1045
6	7	8	0.0085	0.072	0.0745
7	8	2	0.	0.0625	0.
8	8	9	0.032	0.161	0.153
9	9	4	0.01	0.085	0.088

Figure 3.2. An example of the 3 machine system.

$x^1 = (x_1, x_3)^T$, $x^1 = (x_2, x_3)^T$, and $x^1 = (x_1, x_2)^T$ and two possible choices of L_g , $[0 \ 1]$ and $[1 \ 0]$. As our first choice of reference machines consider $x^1 = (x_1, x_3)^T$. Then the solution of the Riccati equation, which is for the given spectrum the dichotomic solution is

$$L_d = [-0.47 \quad 1.47]. \quad (3.37)$$

Of the two possible L_g matrices, the one with the best approximation of L_d is $L_g = [0 \ 1]$, with

$$\|L_d - L_g\| = 0.94. \quad (3.38)$$

The second choice of $x^1 = (x_2, x_3)^T$ will result in a dichotomic solution of the corresponding equation $R(L) = 0$

$$L_d = [-2.13 \quad 3.13]. \quad (3.39)$$

Of the two possible grouping matrices the one which is a better approximation of L_d is $L_g = [0 \ 1]$, with

$$\|L_d - L_g\| = 4.26. \quad (3.40)$$

The third possible choice of $x^1 = (x_1, x_2)^T$ will result in the dichotomic solution of the corresponding Riccati equation

$$L_d = [0.32 \quad 0.68] \quad (3.41)$$

which is best approximated with $L_g = [0 \ 1]$. This gives

$$\|L_d - L_g\| = 0.64. \quad (3.42)$$

The third choice of reference machines results in the solution L which can be better approximated by an L_g than for any other choice. The areas defined

by the resulting L_g are machine 1 in one area and machines 2 and 3 in the other area. There are several other observations that can be drawn from this example. First, by comparing (3.41) and (3.37) it can be seen that there is more than one choice of reference machines which result in the same area definition, although the grouping is most clearly displayed in the third case. The second choice of reference machines results in L_d with the largest norm. This is the case when the reference machines are taken from the same area. If this system was r -decomposable, we would not have had the solution at all.

In remark 2.8 it was pointed out that the spectrum separation and the modal method order reduction are equivalent problems. In Theorem 3.7 it was shown that r -decomposability can be expressed as the spectrum separation problem. Hence for r -decomposable systems all the three methods for reduced order modeling: modal method, spectrum separation, and coherency are directly related. After the aggregated model based on coherent areas is presented in Chapter 4, it will be shown that the modal method and this aggregated model based on coherency have the same eigenvalues. Therefore one of the tests for validity of areas can be the comparison of eigenvalues of B_1 and B_2 (3.35) with those of A where B_1 and B_2 are computed according to (2.9) and (2.10) by using L_g for L . For our three machine system $\sigma(B_1) = \{0, -28.6\}$, $\sigma(B_2) = \{-175\}$, and $\sigma(A) = \{0, -37, -166\}$, which is another indication that the areas are near-coherent.

The above direct search in the three machine example is presented only as a motivation for the systematic algorithm presented in the next section.

3.5. Grouping Algorithm

From the three machine example it is apparent that finding the areas consists of two interdependent tasks: first choosing the reference machines, and second associating the other machines to the reference machines. The approach used in the three machine example is to exhaust all possible choices of x^1 and L_g , that is for each L , a particular L_g was found to minimize norm $(L-L_g)$. The best choice of x^1 is the one corresponding to the smallest of these minima. When the order of the system is large, this exhaustive search would be computationally prohibitive. Due to the properties of the set D established next in Lemmas 3.5 and 3.6, the exhaustive search can be avoided. The algorithm presented in this section computes only one element of the set D , which does not necessarily minimize $\text{norm}(L-L_g)$, but still unambiguously determines the areas.

Lemma 3.9: Given σ_r such that $0 \in \sigma_r$. Then every element $L \in D$ defined by Definition 3.4 has the property

$$(a) \quad \sum_{j=1}^r l_{ij} = 1, \quad i = 1, 2, \dots, n-5, \quad (3.43)$$

that is the sum of row elements equals 1, for each row;

$$(b) \quad \|L\| \geq 1. \quad (3.44)$$

Proof: From the proof of Theorem 2.3, if u is an eigenvector of B_1 , then

$$v = \begin{bmatrix} u \\ L_d u \end{bmatrix} \quad (3.45)$$

is an eigenvector of A . In particular, if $V = V_0$, then from (P1)

$$v = v_o = \begin{bmatrix} u_o \\ L_d u_o \end{bmatrix} = \begin{bmatrix} 1 \\ \vdots \\ 1 \end{bmatrix}. \quad (3.46)$$

Thus (3.43) is obtained by writing $L_d u_o$ in scalar form. The (b) follows from (3.43) and the definition of the norm (3.36).

Notice that every L_g has the norm equal to 1. Hence the search for a grouping matrix due to (3.44) has to be based on the elements of D with the small norm. Based on (3.44) we can define a grouping error as follows.

Definition 3.10: Let L_m be an $L \in D$ with the smallest norm. Then a grouping error for a given L_g is

$$E = \|L_m - L_g\|. \quad (3.47)$$

From this definition it follows that $0 \leq E \leq \infty$, with $E=0$ if and only if the system is r -decomposable.

Using the connection between coherency and spectrum separation analyzed in the previous chapter, we can now analyze why some solutions to L have large norm. L is computed using (2.20) for a given basis matrix V . From the fact that $\begin{bmatrix} I \\ L_g \end{bmatrix}$ is also a valid basis of the invariant subspace corresponding to σ_r , it follows that any other basis will have identically the same row vectors in V corresponding to the machines in the same area. Geometrically, there will be r distinct groups of identical row vectors of V . In the case of near-coherency we will have, instead, r narrow nonoverlapping cones containing all the row vectors of V . Now it is clear that if reference machines, which give components of the vector x^1 , contain two machines from the same area, then the resulting V_1 will have two identical row vectors (in the case of r -decomposable systems, or near-identical in the case of r -near-decomposable systems) and hence the solution will not exist, or will have a

very large norm. That was the case with the second selection of reference machines in the example of the previous section. Since at the time of computing a basis V it is generally not known whether the selection of reference machines is good or not, the question is whether the effort spent on computing V (which is considerable) is lost. The following result answers the question.

Lemma 3.11: Given a subspectrum σ_r of A and a basis of the corresponding invariant subspace V . Then each element L of D is a solution of the Riccati equation corresponding to σ_r for the system with state vector $\bar{x} = Px$.

Proof: If V spans an invariant subspace of A then PV spans the invariant subspace corresponding to the same subspectrum of PAP^T . The result then follows from Theorem 2.3. This result shows that to find an L in D with a small norm we need to compute a basis V for a given state ordering, and then perform a suitable permutation of rows. In finding such a permutation we benefit from the geometrical interpretation of coherency requiring existence of narrow cones of row vectors in V . Hence, to ensure invertibility of V_1 we want to select r vectors from the r different cones. In this way we ensure invertibility and well conditioning of V_1 . To find this set of r rows, we use Gaussian elimination with complete pivoting. During the elimination, the rows and columns of V are permuted such that the $(1,1)$ entry of the resulting V is the largest entry in magnitude. Note that permuting the rows of V is equivalent to changing the ordering of the machines. This $(1,1)$ entry of V is used as the pivot for performing the first step of the Gaussian elimination. Then the largest entry is chosen from the remaining $(n-1) \times (r-1)$ submatrix of the reduced V and is used as the pivot for the next elimination step. The elimination terminates in r steps and the machines corresponding to the first

r rows of the final reduced V matrix are designated as the reference machines. In this Gaussian elimination process, rows having small entries will not be used as the pivoting row because these small entries are the result of elimination with almost identical rows already used as pivoting rows. Thus, this algorithm does not put two near-coherent machines together as reference machines.

For the set of reference machines found by the algorithm the corresponding L is readily computed from

$$V_1^T L^T = V_2^T \quad (3.48)$$

using the LU decomposition of V_1 obtained from the Gaussian elimination. The next step is to find an L_g approximating L , that is to find the machines belonging to each area.

From (3.47) we see that if row vectors of V_1 are understood as a basis for an r -dimensional space, then elements of L are coordinates of the row vectors of V_2 in this basis. Specifically, the elements of a j -th row of L , $l_{j1}, l_{j2}, \dots, l_{jr}$, are coordinates of the j -th vector in V_2 on v_1, v_2, \dots, v_r . If we now recall the geometrical image of coherent areas as consisting of narrow nonoverlapping cones of row vectors in V , and that the Gaussian elimination selects r vectors from r different cones, it becomes clear that in each row j of L , corresponding to a machine which belongs to some area k , there will be only one element close to 1, which is the projection of the j -th vector of V_2 on the basis vector v_k along the space spanned by vectors v_i , $i=1, 2, \dots, r$, $i \neq k$; all the other coordinates of this vector, i.e., all the other elements in the same row of L will be small.

Therefore to find an L_g from a computed L we proceed as follows. In each row of L we find the largest positive element, approximate it by one and approximate all other elements in the same row by zero. In view of the above analysis this is a suboptimal procedure for minimizing the norm of $L-L_g$, i.e., the grouping error of Definition 3.10. Although we cannot always claim that $\|L\| < \|L'\|$, $L' \in D$ (therefore the suboptimality of the algorithm), it is clear from the geometrical explanation that for near r -decomposable systems the algorithm gives a unique definition of areas. In other words if the "coherency cones" are sufficiently narrow, no matter which reference vectors are selected as long as there are r vectors from r different cones, the belonging of the other vectors to these cones is uniquely defined by the largest element in each row of L . In this case $\|L-L_g\| = O(\epsilon)$, where ϵ is the largest angle among two angles in the same cone. As the angles of the cones start increasing, the criterion for machine grouping based on the largest element in each row of L becomes less discriminative. For each follower machine we can define a discrimination factor as follows.

Definition 3.12: Given an $L \in D$ with the smallest norm, let i be the column index of the largest positive element and k be the column index of the second largest positive element in the same row. The discrimination factor for the follower machine j , DF_j is

$$DF_j = \left| \| \ell_j - e_i \| - \| \ell_j - e_k \| \right| \quad (3.49)$$

where ℓ_j is the j -th row of L and e_i is the i -th row of the $(r \times r)$ identity matrix.

The largest value of DF is 2, which is in the case of misplacing ideally coherent machines, and the smallest value is zero, which is in the

case when $v_j \in v_2$ has the same coordinates on both v_i and v_k , $v_i, v_k \in v_1$. Machines with the small discrimination factor should be given special consideration. First, they can be grouped based on approximating the second largest element in the row by one if that choice is more convenient for some reason (for example to achieve an area grouping consistent with the administrative boundaries of the areas). Second, in the case of network changes these are the machines most likely to change their area belonging.

We now summarize the grouping algorithm as follows:

- Step 1: Decide on the number of areas and spectrum σ_r .
- Step 2: Compute a basis matrix V for a given ordering of the x variables and σ_r .
- Step 3: Apply Gaussian elimination with complete pivoting to V and obtain the set of reference machines.
- Step 4: Compute L for the set of reference machines chosen in step 3.
- Step 5: Construct the matrix L_g and find the machines in each area.

The main computational load is in step 2. However, only a partial eigensubspace V of A is required and since A is similar to a symmetric matrix, eigenvalue-eigenvector computation is well conditioned [46]. The numerical aspects of the basis computation will be discussed in more detail in Section 4.8.

We illustrate this area selection procedure on a 48 machine system from [18]. The data are given in the reference. From the linearized system state matrix \bar{A} , we extract the $n \times n$ matrix A of (3.11) by eliminating rows of \bar{A} corresponding to $\dot{\delta}$ and columns corresponding to ω . This matrix is given in Appendix B. In the first step we specify that we want nine areas with

respect to the nine slowest modes. From this point on the algorithm proceeds automatically giving the following results. In step 2 a basis for the 9-dimensional slow subspace is computed. In step 3 the Gaussian elimination is performed and the set of reference machines is found to be 5, 39, 44, 34, 48, 41, 17, 29, 36. In Step 4 the solution L is found (for this selection of the spectrum it will be a dichotomic solution) and it is given in Table 3.1. The largest element in each row, those elements are underlined in Table 3.1, is used to identify the belonging of the corresponding machine to an area, i.e., this element is approximated by 1 and all other elements in the row by zero. As a result the following grouping of machines into areas is obtained:

Area 1: 1, 2, 3, 4, 5, 6, 7, 8, 9

Area 2: 39, 42

Area 3: 43, 44, 45, 46

Area 4: 34, 35

Area 5: 48

Area 6: 32, 37, 38, 40, 41

Area 7: 13, 14, 15, 16, 17, 18, 19, 20, 21, 22, 23, 24, 25, 26, 31, 47

Area 8: 10, 27, 28, 29, 30

Area 9: 11, 12, 33, 36.

The grouping error (3.47) normalized with the number of follower machines is 0.74. The average value of the elements of L approximated by one is .63 and the average value of elements of L approximated by zero is .05. In average, the discrimination factor is 0.85 (compared with the maximal value of 2). However, for some machines like 10, 14, 24, 25, 31, 32, 33, 37, 38, 42, and 47 the discrimination factor is much smaller than the average value. For example,

Table 3.1. Ld for the 48 machine system.

	5	39	44	34	48	41	17	29	36
1.	<u>0.56</u>	-0.00	-0.04	-0.01	-0.00	-0.00	0.05	0.42	0.02
2.	<u>0.60</u>	-0.00	-0.04	-0.01	-0.00	-0.00	0.05	0.38	0.02
3.	<u>0.83</u>	-0.00	-0.01	-0.01	0.00	-0.00	0.03	0.15	0.01
4.	<u>0.83</u>	-0.00	-0.01	-0.00	0.00	-0.00	0.03	0.14	0.01
6.	<u>0.84</u>	-0.00	-0.02	-0.01	-0.00	-0.00	0.03	0.15	0.01
7.	<u>0.83</u>	-0.00	-0.02	-0.01	-0.00	-0.00	0.03	0.16	0.01
8.	<u>0.85</u>	-0.00	-0.01	-0.01	0.00	-0.00	0.05	0.11	0.02
9.	<u>0.58</u>	-0.00	-0.01	-0.01	0.00	-0.01	0.10	0.30	0.04
10.	<u>0.18</u>	-0.00	0.03	-0.03	0.01	-0.01	0.28	<u>0.43</u>	0.13
11.	0.07	-0.01	-0.03	-0.15	0.00	-0.04	0.21	<u>0.28</u>	<u>0.66</u>
12.	0.08	-0.01	-0.02	-0.12	0.00	-0.03	0.21	0.27	<u>0.62</u>
13.	0.10	-0.00	-0.01	-0.03	0.00	-0.02	<u>0.51</u>	0.32	0.12
14.	0.11	-0.00	0.02	-0.02	0.01	-0.01	<u>0.46</u>	0.32	0.12
15.	0.04	-0.00	-0.01	-0.02	-0.00	-0.02	<u>0.78</u>	0.17	0.06
16.	0.02	0.01	-0.00	0.03	0.00	0.01	<u>0.77</u>	0.10	0.06
18.	0.02	0.00	0.00	0.02	0.01	0.01	<u>0.78</u>	0.09	0.06
19.	0.03	0.01	0.03	0.04	0.02	0.02	<u>0.67</u>	0.10	0.08
20.	0.03	0.01	0.02	0.03	0.02	0.01	<u>0.72</u>	0.10	0.06
21.	0.02	0.00	0.11	0.02	0.08	0.00	<u>0.63</u>	0.09	0.05
22.	0.03	0.00	0.09	0.02	0.07	0.01	<u>0.63</u>	0.10	0.06
23.	0.06	0.00	0.05	-0.00	0.01	-0.01	<u>0.62</u>	0.19	0.07
24.	0.09	0.00	0.21	-0.01	0.04	-0.00	<u>0.37</u>	0.24	0.06
25.	0.11	-0.00	0.17	-0.02	0.03	-0.01	<u>0.36</u>	0.30	0.07
26.	0.10	-0.00	0.09	-0.03	0.02	-0.02	<u>0.42</u>	0.33	0.09
27.	0.07	-0.00	0.12	-0.00	0.01	-0.00	0.05	<u>0.73</u>	0.02
28.	0.02	-0.00	0.03	-0.00	0.00	-0.00	0.01	<u>0.93</u>	0.00
30.	0.04	-0.00	0.06	-0.00	0.00	-0.00	0.02	<u>0.88</u>	0.01
31.	0.02	0.05	0.00	0.13	0.01	0.10	<u>0.48</u>	0.06	0.15
32.	0.00	0.24	-0.00	0.09	0.04	0.41	<u>0.16</u>	-0.01	0.07
33.	0.00	0.04	-0.00	0.28	0.00	0.10	0.25	0.02	<u>0.31</u>
35.	0.00	0.01	-0.00	<u>0.87</u>	-0.00	0.02	0.05	0.00	0.05
37.	0.00	0.32	0.01	<u>0.05</u>	0.09	<u>0.40</u>	0.09	-0.01	0.04
38.	0.00	0.38	0.00	0.04	0.06	<u>0.41</u>	0.08	-0.01	0.03
40.	0.00	0.28	-0.00	0.05	0.00	<u>0.56</u>	0.09	-0.01	0.03
42.	0.00	<u>0.47</u>	0.00	0.03	0.03	<u>0.39</u>	0.06	-0.01	0.02
43.	0.01	0.00	<u>0.73</u>	-0.00	0.11	0.00	0.02	0.13	0.00
45.	0.02	-0.00	<u>0.60</u>	-0.00	0.12	-0.00	0.18	0.07	0.02
46.	0.00	0.00	<u>0.89</u>	0.00	0.07	0.01	0.01	0.01	0.00
47.	0.02	0.00	0.26	0.01	0.21	0.00	<u>0.37</u>	0.08	0.04

for machine 33, $DF_{33} = 0.06$. All the machines with a small discrimination factor will be called critical machines. Note from Figure 3.3 that all the critical machines are border machines of their respective areas, but not all the border machines are critical machines. Despite the presence of the critical machines, the area grouping is good, as will be shown in Section 4.7 by some characteristic machine responses.

3.6. Area Variables and Intermachine Variables

In the previous section it was shown that the coherency is equivalent to the requirement that a grouping matrix achieves the spectrum separation. Then, the state variables associated with the subsystem with state matrix B_2 are z variables (3.29), i.e., intermachine variables within coherent areas. In this formulation the subsystem (x^1, B_1) is still coupled to the subsystem (z, B_2) . For the separate analysis of these two subsystems it is necessary to decouple them, and one way to do it is by using the transformation (2.52) introduced in Section 2.4,

$$\begin{bmatrix} y \\ z \end{bmatrix} = \begin{bmatrix} I & H \\ 0 & I \end{bmatrix} \begin{bmatrix} x^1 \\ z \end{bmatrix}. \quad (3.50)$$

Applying this transformation to (3.35) with L satisfying $R(L) = 0$ results in

$$\begin{bmatrix} \ddot{y} \\ \ddot{z} \end{bmatrix} = \begin{bmatrix} B_1 & P(H) \\ 0 & B_2 \end{bmatrix} \begin{bmatrix} y \\ z \end{bmatrix}. \quad (3.51)$$

As shown in Section 2.4, equation $P(H) = 0$ has always the solution, whenever $\sigma_r \cap \sigma_r^c = 0$. However, in this particular case even more can be concluded.

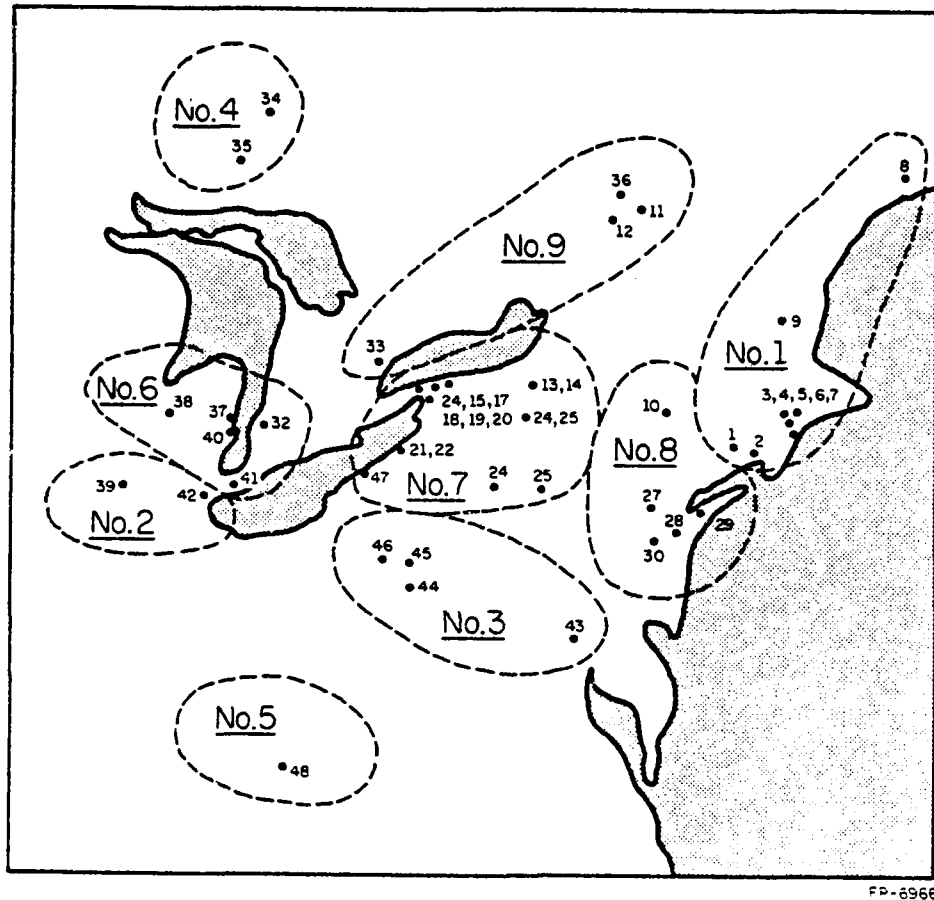


Figure 3.3. Coherent areas of the 48 machine system.

Lemma 3.13: Consider the matrix $A = -M^{-1}K$ of (3.11), where K is symmetric and M is the diagonal matrix of machine moments of inertia, whose $(r \times r)$ and $(n-r) \times (n-r)$ diagonal blocks are M_1 and M_2 , respectively. Then each solution L of $R(L) = 0$ corresponding to some σ_r , and the corresponding solution H of $P(H) = 0$ are related by

$$H = (M_1 + L^T M_2 L)^{-1} L^T M_2. \quad (3.52)$$

Proof: Let us first rewrite $R(L) = 0$ and $P(M) = 0$ as

$$[-L \quad I] A \begin{bmatrix} I \\ L \end{bmatrix} = 0 \quad (3.53)$$

$$[I \quad H] B \begin{bmatrix} -H \\ I \end{bmatrix} = 0. \quad (3.54)$$

Substituting $B = T_L A T_L^{-1}$ into (3.54) yields

$$\begin{aligned} [I-HL \quad H] A \begin{bmatrix} -H \\ I-LH \end{bmatrix} &= [I-HL \quad H] (-M^{-1}K) M^{-1} M \begin{bmatrix} -H \\ I-LH \end{bmatrix} \\ &= [(I-HL) M_1^{-1} H M_2^{-1}] A^T \begin{bmatrix} -M_1 H \\ M_2 (I-LH) \end{bmatrix} = 0. \end{aligned} \quad (3.55)$$

Pre- and post-multiplying (3.53) by $[M_2(I-LH)]^T$ and $[(I-HL)M_1^{-1}]^T$ and comparing to the transpose of (3.55), we obtain

$$H^T M_1 = (I-LH)^T M_2 L \quad (3.56)$$

which simplifies to (3.52).

The same relationship can be obtained by modal methods [16]. Under the conditions of this lemma the complete transformation from x to (y, z)

variables is

$$\begin{bmatrix} y \\ z \end{bmatrix} = \begin{bmatrix} M_a^{-1} M_1 & M_a^{-1} L^T M_2 \\ -L & I \end{bmatrix} \begin{bmatrix} x^1 \\ x^2 \end{bmatrix} \quad (3.57)$$

where

$$M_a = M_1 + L^T M_2 L. \quad (3.58)$$

If the system is r -decomposable then H has the same "zero-nonzero" pattern as L_g^T and we denote it by H_g . With L_g and H_g used in (3.57), an interesting interpretation of the physical meaning of y and z variables follows. First, notice from (3.58) that in this case M_a is the matrix of area inertias, i.e. the i -th entry contains the sum of moments of inertia of all the machines in the i -th area. Then from the first row of (3.57) we get immediately that y variables are familiar "area center of inertia" [41], given by

$$y_i = \sum_j M_j x_j / M_{ai}, \quad \text{for all } j \text{ in area } i. \quad (3.59)$$

In summary, in the case of r -decomposable systems by dividing the system into coherent areas, it is possible to construct directly two low order subsystems, one describing the dynamics of intermachine oscillations within coherent areas, and the other describing the interarea dynamics. For the r -near-decomposable system we still apply the same transformation (3.59) and (3.30). We will get the two subsystems which are weakly coupled, rather than completely decoupled. The same is true for models with damping and nonlinear models. When the spectrum defining coherency is given as r slowest eigenvalues of A , the procedure will result in y variables being the slow states and z variables being the fast states of the system. For the r -near-decomposable systems, their basic slow, i.e., fast character will be retained, which means that by means

of coherency the mixed state model (3.11) is transformed into singularly perturbed form. In [25] it was shown that application of singular perturbation on the transformed model gives excellent results in terms of eigenvalue approximation of the reduced subsystems compared with the full system eigenvalues. More properties of the slow coherency will be given in the next chapter.

4. SLOW COHERENCY, WEAK COUPLING, AND NONLINEAR EQUIVALENTS

4.1. Introduction

In this chapter we show that only if coherency is defined with respect to the slowest modes of the linearized system (3.11), the resulting areas are weakly coupled, i.e., weaker than for any other partial coherency. The area boundaries are in this case relatively insensitive to small loads and parameter changes. These two factors taken together indicate certain robustness of area boundaries, making them useful for nonlinear system analysis. Possibilities for using slow coherency for analysis of nonlinear models are discussed and conclusions verified on a 48 machine system. Benefits in numerical identification of coherent areas resulting from using slow coherency are discussed at the end.

There is no previous published work on the relation between coherency and weak coupling, as well as the analytical study of the sensitivity of area boundaries to parameter changes. However, the use of linear coherency for aggregation of nonlinear models is implicit, or alluded to in [16,19,41,43]. Other uses of slow coherency considered in this chapter [45], which exploit the connection between time scales and coherency, are based on singular perturbation theory.

4.2. Electromechanical Equivalent of Area Dynamics

As a preparation for exposition of the main result of this chapter concerning a relation between slow coherency and weak coupling between areas, we first study aggregated models of the linearized system (3.11). This

analysis is extended to nonlinear models in Section 4.6. Once areas are identified, their aggregation is intuitively appealing to a power system expert [19,41]. Each area is represented by one generator, those are then suitably interconnected to preserve the total power interchange between areas. The resulting interconnection matrix is generally nonsymmetric [19]. In this section we proceed differently. We use analytical tools of Chapter 3 to establish aggregated models and their properties. One of the results is that the aggregated model has the same structure as in previous approaches, but the interconnection matrix is symmetric, so that it can be modeled as a passive network without phase shifters. The result is given in the following lemma.

Lemma 4.1: Let the coherency in the system (3.11) be defined with respect to a spectrum σ_r containing zero eigenvalue, and let $L_g : R(L_g) = 0$ define corresponding areas. Then

(i) the aggregated model of (3.11) which reproduces area dynamics is defined by

$$y = Sx \quad (4.1)$$

where

$$S = (I - H_g L_g + H_g). \quad (4.2)$$

(ii) The aggregated state matrix $F = B_1 = A_{11} + A_{12} L_g$ can be factored as

$$B_1 = M_a^{-1} K_a \quad (4.3)$$

where M_a is the diagonal matrix of area inertias (3.50) and K_a is a symmetric matrix defined as

$$K_a = (I \quad L_g^T) K \begin{pmatrix} I \\ L_g \end{pmatrix}. \quad (4.5)$$

(iii) B_1 is a function of connections between machines in different areas only and not a function of connections between machines in the same area, i.e.

$$k_{ija} = \begin{cases} \sum_{p \in I(i)} \sum_{q \in I(j)} k_{pq}, & i \neq j \\ -\sum_{\ell=1}^r k_{i\ell}, & i = j \end{cases}. \quad (4.5)$$

Before giving the proof let us emphasize the following. In the standard aggregation approaches [6,7], the main concern is to obtain a low order model which reproduces a given spectrum. In application to the electromechanical model of power systems, once L_g and the corresponding H are known, more can be achieved. Namely, the complete decomposition of the system into two subsystems is possible in such a way that one subsystem reproduces the given subspectrum, and the other subsystem reproduces the complementary subspectrum.

Proof: (i) The form of S follows from (3.55) and (3.50). In comparison to the general form of aggregation matrix given in [5], $S = P(I \ 0)X^{-1}$, it can be seen that in this case $P = X_r$, i.e., it is the r -dimensional principal submatrix of the modal matrix X .

(ii) Again with reference to the general form of the aggregated state matrix [4], $F = B_1 = SAS^+$, we see from (2.7) that the r.h. side inverse S^+ is $S^+ = (I \ L_g)^T$. Using the particular form of the solution $H_g = M_a^{-1} L_g^T M_2$ (as given in (2.50)), we get $S = M_a^{-1} (I + L_g)^T M$ from which the result follows immediately.

(iii) The result (4.5) follows by noting the specific "zero-one" structure of L_g and the fact that the diagonal elements of K are the negative sums of off-diagonal elements. The above properties are best illustrated by an example.

Example 4.1: For the (hypothetical) system in Figure 4.1, the matrices M and K are as given below. We will find a grouping matrix for this system, and then analyze the corresponding aggregated model B_1 .

$$M = \text{diag}(5, 1, 4, 1, 1)$$

$$K = \begin{bmatrix} -5 & 2 & 0 & 2 & 1 \\ 2 & -3 & 1 & 0 & 0 \\ 0 & 1 & -4 & 1 & 2 \\ 2 & 0 & 1 & -3 & 0 \\ 1 & 0 & 2 & 0 & -3 \end{bmatrix}$$

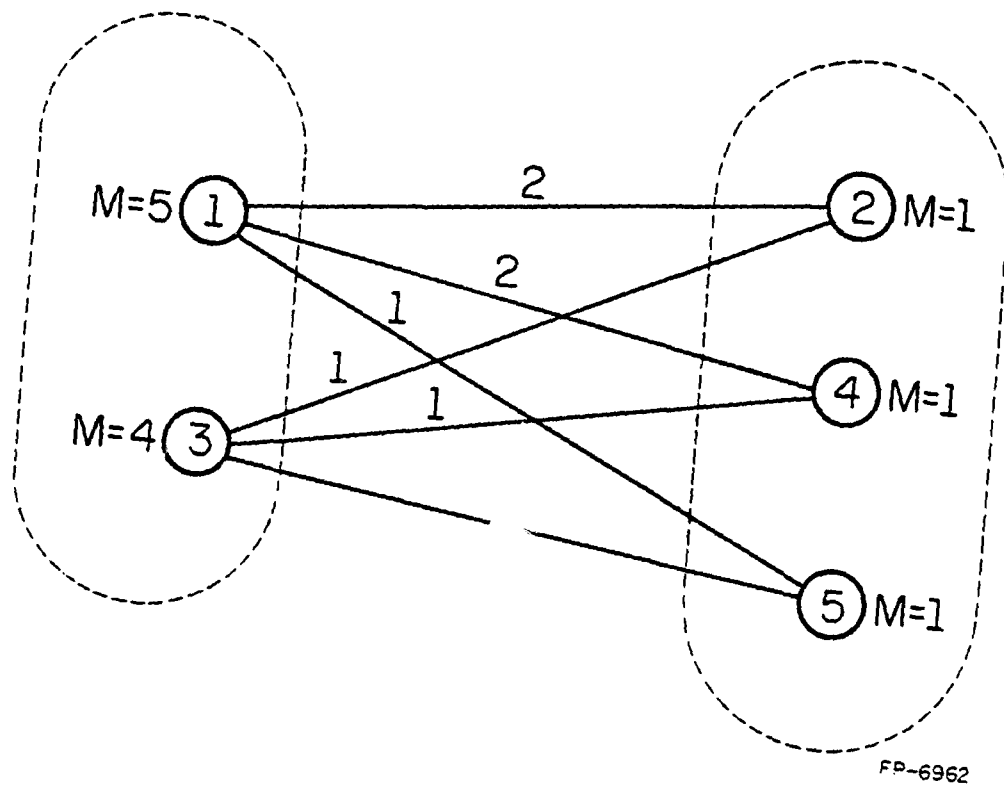
If $r = 2$ and $\sigma_2 = \{0, \lambda_5\}$, then

$$L_g = \begin{bmatrix} 1 & 0 \\ 0 & 1 \\ 0 & 1 \end{bmatrix}$$

satisfies Riccati equation (2.13) and defines coherent areas as indicated in the figure by the dotted lines. The matrix H_g is given by

$$H_g = M_a^{-1} L_g^T M_2 = \begin{bmatrix} \frac{4}{9} & 0 & 0 \\ 0 & \frac{1}{3} & \frac{1}{3} \end{bmatrix}.$$

Then from (2.9) B_1 is



FP-6962

Figure 4.1. Ideally coherent system.

$$B_1 = A_{11} + A_{12}L_g = \begin{bmatrix} M_1 & 0 \\ 0 & M_2 \end{bmatrix}^{-1} \begin{bmatrix} -(k_{12}+k_{14}+k_{15}) & k_{12}+k_{14}+k_{15} \\ k_{21} & -k_{21} \end{bmatrix}$$

$$= \begin{bmatrix} 5 & 0 \\ 0 & 1 \end{bmatrix}^{-1} \begin{bmatrix} -5 & 5 \\ 3 & -3 \end{bmatrix},$$

which gives a nonsymmetric interconnection matrix. However, by (4.3) the same B_1 can be written as

$$B_1 = \begin{bmatrix} M_1+M_3 & 0 \\ 0 & M_2+M_4+M_5 \end{bmatrix} \begin{bmatrix} -k_{12a} & k_{12a} \\ k_{21a} & -k_{21a} \end{bmatrix}$$

$$k_{12a} = k_{21a} = k_{12} + k_{14} + k_{15} + k_{32} + k_{34} + k_{35}$$

$$B_1 = \begin{bmatrix} 9 & 0 \\ 0 & 3 \end{bmatrix}^{-1} \begin{bmatrix} -9 & 9 \\ 9 & -9 \end{bmatrix},$$

i.e., in terms of the symmetric interconnection matrix. The initial conditions for machines are computed using the transformation (3.52) with the particular values for L_g and H_g .

4.3. Structural Conditions for Coherency

Using the fact that in the case of coherency L_g and H_g satisfy Riccati (2.13) and Lyapunov equations (2.49), respectively, allows alternative formulation of the coherency directly in terms of network and machine parameters. The following lemma states the result.

AD-A125 845

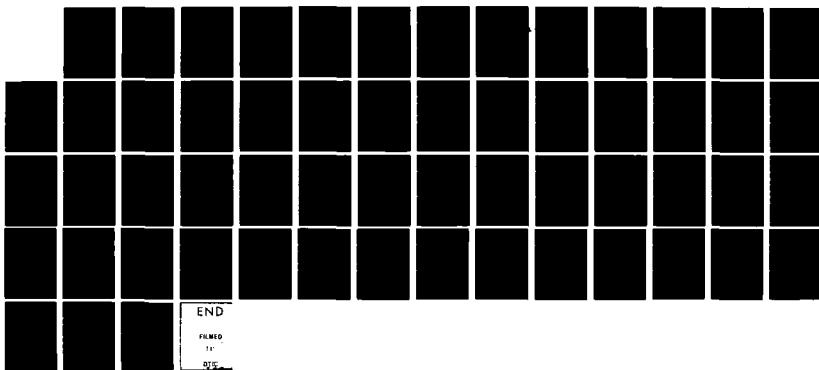
TIME SCALES COHERENCY AND WEAK COUPLING(U) ILLINOIS
UNIV AT URBANA DECISION AND CONTROL LAB B AVRAMOVIC
OCT 80 DC-40 N00014-79-C-0424

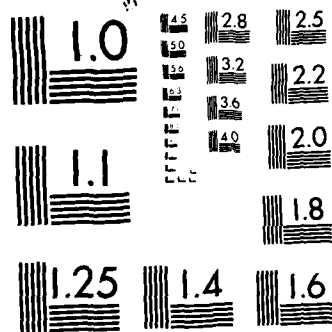
2/2

UNCLASSIFIED

F/G 12/1

NL





MICROCOPY RESOLUTION TEST CHART
NATIONAL BUREAU OF STANDARDS-1963-A

Lemma 4.2: A necessary and sufficient condition for a system (3.11) to be divided into r coherent areas according to Definition 3.1 is that

$$(i) \quad \sum_{\ell \in I(i)} \left(\frac{v_k v_{\ell} b_{k\ell} \cos \theta_{k\ell}}{M_k} - \frac{v_j v_{\ell} b_{j\ell} \cos \theta_{j\ell}}{M_j} \right) = 0 \quad (4.6)$$

$$i = 1, 2, \dots, r; \quad j = r+1, \dots, n$$

or equivalently

$$(ii) \quad \frac{M_{ai}}{M_i} \sum_{\ell \in I(k)} v_i v_{\ell} b_{i\ell} \cos \theta_{i\ell} =$$

$$\frac{M_{ak}}{M_j} \sum_{\ell \in I(i)} v_{\ell} v_j b_{j\ell} \cos \theta_{\ell i} \quad (4.7)$$

$$i = 1, \dots, r; \quad j = r+1, \dots, n.$$

For simplicity of notation it is assumed $k = k(j)$ to mean the representative machine of the area containing j .

Proof: Condition (4.6) follows from (2.13) directly by inserting L_g for L , and (4.7) follows from (2.49) by inserting L_g and H_g for L and H .

Similar conditions were also obtained in [21] using a different approach. These conditions are interesting in that they emphasize the role of network and machine parameters in forming areas. For most networks and loading conditions cosine terms in (4.6) and (4.7) can be approximated by 1. Then the two conditions say that if

$$d_{ji} = \sum_{\substack{\ell \in I(i) \\ j \neq \ell}} \frac{v_j v_{\ell} b_{j\ell}}{M_j}, \quad i = 1, 2, \dots, r \quad (4.8)$$

$$j = r+1, \dots, n$$

is defined as electromechanical distance of machine j from the area i , then

all the machines in the coherent area k have the same distance to a given area i , where $i, k = 1, 2, \dots, r$.

For the 48 machine system of Section 3.5, Table 4.1 gives the average variation of this distance for each of the nine areas. The conditions of the lemma guarantee partial coherency, but they do not take explicitly into account the spectrum corresponding to the coherency.

4.4. Weak Coupling Between Areas

So far we have considered partial coherency with respect to any prespecified spectrum σ_r , with the only restriction that it had to contain the zero eigenvalue. In this section, as well as in Section 4.5, we will show that the slow coherency, i.e., the case when σ_r contains r slowest eigenvalues of (3.11), has particularly useful properties.

The basis for the following analysis is the result of Section 4.2, which establishes a link between coherency defining spectrum and the strength of connections between areas. Before stating the new result, we introduce several definitions, similar to the definition of the electromechanical distance (4.8).

Definition 4.3: The electromechanical connection between areas i and j is defined as

$$D_{ij} = M_{a_i}^{-1} \sum_{p \in I(i)} \sum_{q \in I(j)} k_{pq}, \quad i \neq j \quad (4.9)$$

$$i, j = 1, 2, \dots, r.$$

Table 4.1. Average violation of the criterion (4.6) for the 48 machine system.

Area →	1	2	3	4	5	6	7	8	9
↓									
1	.09	-	-	-	-	-	-	.02	-
2	-	.04	-	-	-	.07	-	-	-
3	-	-	.13	-	.02	-	.01	.06	-
4	-	-	-	-	-	-	-	-	-
5	-	-	-	-	-	-	-	-	
6	-	.03	-	-	-	.05	.02	-	.01
7	.01	-	.03	-	.01	.01	.09	.02	.01
8	.03	-	.01	-	-	-	.07	.10	.02
9	-	-	-	.01	-	.01	.02	.01	0

The electromechanical connection of machine i to the system is

$$D_i = \sum_{\substack{j=1 \\ j \neq i}}^r D_{ij}. \quad (4.10)$$

The total interconnection of the system is

$$D_T = \sum_{i=1}^r D_i. \quad (4.11)$$

Assuming that the \cos terms in k_{pq} are approximately 1, then all these connection measures are basically measures of electromechanical distance. We also define

Definition 4.4: The measure of the maximal strength of the aggregated model is

$$m_s = \max_x \frac{X^T K_a X}{X^T M_a X}, \quad (4.12)$$

which is the biggest ratio of the potential over the kinetic energy in the aggregated model.

We are now ready to characterize different types of coherency.

Lemma 4.5: Suppose that in the system (3.11) there are several different $L_g: R(L_g)=0$, each corresponding to a different spectrum σ_r . Suppose that one σ_r contains r slowest eigenvalues of the system, i.e., it defines slow coherency. Then,

(i) the total interconnection of the system, D_T , is the smallest for the slow coherency case;

(ii) the maximal strength of interconnections, m_s , is the smallest for the slow coherency case.

Proof: The proof uses the relation between eigenvalues of σ_r and area interconnections established in Lemma 4.1, and various definitions of eigenvalues.

(i) This property is established using $\text{Tr} B_1 = \sum_{i=1}^r \lambda_i, \lambda_i \in \sigma_r$, the form of diagonal elements of B_1 which are given by (4.5), and the fact that this trace is the smallest for the slow coherency case. (ii) This property can be derived using eigenvalue definition via the Raleigh-quotient [27] and the fact that the largest of the slow eigenvalues, which is equal to m_s , is the smallest in the case of slow coherency. The results of the lemma indicate that slow coherence has the property to divide the system into weakly coupled areas so that the total sum of interconnections is minimized. Since for a given system the total sum of connections between machines is equal to the total sum of interconnections between areas and the sum of connections inside areas, it follows that the slow coherency also maximizes the total sum of internal connections in the areas. This property will be further clarified later on in this section. With this result an interpretation of the slow coherency can be the following: it is a result of groups of machines being strongly coupled inside the groups and weakly coupled between the groups. The results concerning the slow coherency are global, that is, for the whole system rather than for each individual subsystem, although as we will see later on the weak coupling property can be stated as the average property of each subsystem, which is also observed on the example system. Table 4.2 gives interconnection patterns for the 48 machine system divided into 9 areas based on slow coherency. Entry t_{ij} in the table gives relative electromechanical connection between areas i and j , where scaling is done with the total connection of area i , i.e., $t_{ij} = D_{ij}/D_i$. Entries less than 1% in magnitude are denoted by -. Several observations can be made from the table.

Table 4.2. Interconnection strength between coherent areas of the 48 machine system.

	1	2	3	4	5	6	7	8	9
1	(41)	-	-	-	-	-	1.5	9	-
2	-	(34)	-	-	3.5	26	1	-	-
3	-	-	(65)	-	9	-	3	12	-
4	-	-	-	(47)	-	4	7	-	32
5	-	3	34	-	(100)	17.5	3	3	-
6	-	20	1	-	7.5	(31)	4	-	3
7	1	-	17.5	-	9	2	(24.5)	7	6
8	4	-	5	-	-	-	7	(83)	3
9	2	-	-	7	-	5	14	7	(40)

(i) In all cases $t_{ii} > t_{ij}$, i.e., connections inside areas are stronger than the connections between areas.

(ii) The cases of stronger interconnections (for example " t_{26} ") are the cases where some machines in areas 2 and 6 are grouped based on rows of L_d which were not close to zero-one pattern, see Table 3.1.

(iii) The state matrix A has the same block-diagonal structure as Table 4.2, if the rows are ordered so that all the machines in area 1 come first, then all the machines in area 2, and so on.

These interconnection properties reflect on the characteristics of the fast dynamics, determined by the matrix B_2 of (3.10). In the remainder of this section we will study the properties of B_2 . From equation (3.10)

$B_2 = A_{22} - L_g A_{12}$. Using L_g we can easily derive that the elements of B_2 are given by

$$b_{ij} = \begin{cases} a_{pq} - a_{k(p),q} & i \neq j \\ - \sum_{\substack{\ell=1 \\ \ell \neq p}}^{n_1} a_{p\ell} - a_{k(p),p} & i=j, \quad p=i+r, \quad q=j+r \end{cases} \quad (4.13)$$

From (2.7), (2.9), and (2.10)

$$\text{tr } B_2 = \text{tr } A - \text{tr } B_1 \quad (4.14)$$

it is easy to see that $\text{tr } B_2$ contains the total sum of connections between machines inside coherent areas. Since in the case of slow coherency

$$\frac{|\text{tr } B_2|}{r} > \frac{|\text{tr } B_1|}{r}, \quad (r < \frac{n}{2}) \quad (4.15)$$

it follows that the average connection strength within areas is higher than the average interconnection strength. To state this simpler: on the average,

connections are stronger between machines inside the same area than between machines from different areas. A consequence of this property is that the matrix B_2 is also block-diagonally dominant, as is A . Its diagonal blocks, of size equal to the number of follower machines in the areas, are functions of elements of A corresponding to the connections of machines inside areas, see (4.15), and off-diagonal blocks are functions of interconnection elements of A . Hence the diagonal blocks have larger norms than their off-diagonal blocks. When the interconnection table is formed for B_2 , the same way Table 4.2 is formed for A , the entries in the table are almost identical to those for A .

4.5. Sensitivity of Area Boundaries to Parameter Changes

In this section we will show that in the case of slow coherency areas are not only weakly coupled as established in the previous section, but also area boundaries are relatively insensitive to small changes of network parameters. The first step in this study is to evaluate the changes in the steady state matrix A , for small changes in network parameters. A similar problem has been treated in power system analysis within so-called security analysis. Security analysis is concerned with the problem of fast computation of the equilibrium state after some given disturbance. These methods, surveyed in [42], are numerical in nature, despite the fact they use various forms of sensitivity relations to achieve necessary effectiveness. There are two characteristics which distinguish the approach in this section from the security analysis approach. First, our ultimate goal is to evaluate the change of L_g after a change in network parameters, and second, we will use the analytical, rather than numerical approach, with the purpose of gaining

insight into the behavior of area boundaries. For that reason we will consider only the change of admittance elements (which may model a line outage, for example).

Outage of a line between nodes i and j affects matrix A in two ways: first, it directly changes admittance $y_{ij}, y_{ji}, y_{ii}, y_{jj}$, and second, it changes the equilibrium angles $\delta_i, i=1,2,\dots,n$. Angle changes can be analyzed from the DC load flow equations [52]

$$P = B \cdot \theta \quad (4.16)$$

with

P - $n-1$ vector of active power injections into the nodes
of the system

B - admittance matrix, reactive part

θ - $n-1$ vector of angle differences $\delta_i - \delta_n, i=1,2,\dots,n-1$.

After a line outage B changes to

$$B' = B + \Delta B \quad (4.17)$$

where

$$\Delta B = \Delta b_{ij} e_{ij} e_{ij}^T \quad (4.18)$$

Δb_{ij} - the change in admittance of the line (i,j)

e_{ij}^T - row vector with all zero elements except the i -th, which is 1 and the j -th which is -1.

For small Δb_{ij} the change in equilibrium angles can be found as [42]

$$\Delta \theta = -B^{-1} \Delta B \theta. \quad (4.19)$$

Using the symmetry of B a bound for the change in θ can be established as

$$\|\Delta \theta\| \leq \Delta b_{ij} (\delta_i - \delta_j) \frac{1}{\min |\lambda(B)|}. \quad (4.20)$$

This expression shows several facts: (i) in systems working close to their static stability boundaries, even small changes in parameters can cause big changes in equilibrium angles, (ii) parameter changes in higher loaded lines, and (iii) bigger parameter changes can cause bigger equilibrium changes.

In the rest of this analysis we assume that parameter changes are small so that the linear analysis can still be applied after the disturbance. Hence in determining sensitivity of area boundaries we concentrate on the effect of the admittance change (4.17). We want to see the effect of this change on the change in $L_g = L_d$. We approach the problem by studying how the slow subspace of A changes. From $L_g = L_d$ it follows that $V_0 = \begin{bmatrix} I \\ L_g \end{bmatrix}$ is a basis of the slow subspace of A . To find a first order variation of this subspace corresponding to the disturbed matrix $A' = M^{-1}(B + \Delta B)$ we use Lemma 2.11 and apply only one simultaneous iteration to A' with V_0 as the initial condition. To make the slowest spectrum dominant prior to applying the simultaneous iterations, we shift the spectrum of A , as well as the spectrum of A' , for some μ to the right. This is possible in this case since all eigenvalues of A are real and in the left hand side of the complex plane, by assumption. The result on the variation of L_g is given in the following lemma.

Lemma 4.6: Suppose that for the system (3.11) cos terms in (3.6) are approximately 1, and that there exists $L_g = L_d$ s.t. $R(L_g) = 0$. Then for a sufficiently small perturbation ΔB of the type (4.17)

- (i) if i and j belong to the same area, the first order variation of L_d is zero
- (ii) if i and j belong to different areas, the first order variation of L_d is zero except for rows i and j .

Proof: Let $A' = A + \Delta A = M^{-1}(B + \Delta B)$. Due to the linear convergence of the simultaneous iterations (SI), one suitably defined SI may be used to obtain a first order variation of the slow subspace of A when perturbed as $A + \Delta A$. For that we have to make SI converge to the slow subspace of A' . This we do by using (2.40) and $A'' = A' + \mu I$, $\mu \geq \max |\lambda(A)|$, instead of A . The initial guess is $V_0 = \begin{bmatrix} I \\ L_g \end{bmatrix}$, which is a basis of the slow subspace of A . After SI, $V_1 = A'' V_0$. Using $(M^{-1}B + \mu I) \begin{bmatrix} I \\ L_g \end{bmatrix} = \begin{bmatrix} I \\ L_g \end{bmatrix} (B_1 + \mu I)$ and the fact that $(B_1 + \mu I)$ is nonsingular, we can write

$$V_1 = [V_0 + \Delta V] \quad (4.21)$$

where

$$\Delta V = \Delta b_{ij} M^{-1} e_{ij} e_{ij}^T \begin{bmatrix} I \\ L_g \end{bmatrix} (B_1 + \mu I)^{-1}. \quad (4.22)$$

In case (i), $e_{ij} V_0 = 0$ because i and j belong to the same coherent area. In case (ii), it can be seen from (4.22) that the conclusion follows directly. Hence, the lemma indicates that for small parameter changes of the type (4.17) all machines remain in their predisturbance areas, except possibly the terminal machines i and j . An easy extension of the above argument can be used to show that if ΔB is modeled to account for parameter changes of more than one line within one coherent area and no changes in the others, the only nonzero rows in the matrix ΔV are those corresponding to the machines in the affected area. This means that in the case of a disturbance only machines in the affected areas may migrate from this area, and probably only the boundary machines. Due to the weak coupling between areas the situation as assumed above may model a line outage within a coherent area.

A natural question which arises after this analysis is how can the predisturbance areas be used in the determination of areas after a disturbance. There are several possibilities.

(i) When the allowed computation time is minimal and the disturbance is small, the predisturbance areas can be used.

(ii) The first order variation formula (4.22) can be used to decide how to group borderline machines. Any decision about dislocating machines can be checked via the criterion (4.6) (only for the affected area and the machines in it).

(iii) Use the exact matrix A' (from a load flow or static state estimator) and V_0 as initial guess to perform necessary number of SI. A simplification in this approach can be obtained if far from disturbance areas are replaced by their slow equivalent derived in Section 4.2. This is equivalent to some sort of condensation used in structural mechanics [45].

The following example using the 48 machine system confirms the expected robustness of area boundaries with respect to the parameter and load changes, and hence indicates that area boundaries will have to be changed only infrequently. The example corresponds to applying the alternative (iii) above for finding areas of the network with different configurations. Three network configurations are considered. For each the exact L_d is computed using the corresponding linearized state matrix. The areas are obtained by approximating this L_d by an L_g as explained in Chapter 3.

Case one is the nominal configuration of the system, which has been considered so far. For this system, L_d is given in Table 3.1. The corresponding

areas are given in Figure 3.7. Case two is the same network, but after switching a line in area 1 [45] following a disturbance in the area. The third case is similar to case two, but with a line disconnected in area 7. Inspection of the elements of L_d for all the three cases shows that none of the machines changes its area belonging except for the machines 1 and 2, which in case 2, instead of being grouped with the area 1, become a part of area 7. The rows of L_d corresponding to three characteristic machines, machines 1, 2, and 9, are given in Table 4.3 for the three network configurations. The discrimination factors for machines 1, 2, and 9, also given in the table, are considerably smaller than the average value of DF (for case one), which is 0.85. It is interesting that the reference machines in all three cases remain the same.

4.6. Use of Slow Coherency in Nonlinear System Analysis

Weak coupling between areas in the case of slow coherency and insensitivity of area boundaries to small parameter changes indicate the possibility of using coherent areas of the linearized model (3.11) for the nonlinear system analysis. Existing coherency methods [19] use, in fact, the linearized model to identify coherent areas, and use them for nonlinear system analysis. In this section we will analyze aggregation of the nonlinear model using the block diagonalizing transformation for the linearized one. This analysis is along the lines of the approach in Section 2.5, except that here we take explicitly into account the specific structure of L_g and H_g . Later in the section we discuss different possibilities for approximate system analysis based on the division of the system into slow coherent areas.

Table 4.3. Variation of L_d (machines 1, 2, and 3) with the change in network configuration.

AREA MAC		1	2	3	4	5	6	7	8	9	DF
1	a	.56	0	-0.04	-0.01	0	0	0.05	0.42	0.02	.28
	b	.38	0	-.09	-0.01	0	0	.06	.64	.02	.52
	c	.56	0	-.03	-.01	0	0	.06	.42	.02	.28
2	a	0.60	0	-0.04	-0.01	0	0	0.05	0.38	0.02	.44
	b	.40	0	-.09	-0.01	0	0	.06	.63	.02	.46
	c	.59	0	-.03	-0.01	0	0	.05	.37	.02	.44
9	a	0.58	0	-0.01	-0.01	0	0	0.10	0.30	0.04	.56
	b	.54	0	-.03	-0.01	0	0	0.10	.37	.04	.34
	c	.58	0	0	-0.01	0	0	0.10	.30	.04	.56

a - predisturbance network

b - disturbance in area 1

c - disturbance in area 7

The nonlinear model (3.3) reduced to machine terminals is rewritten here for convenience.

$$\ddot{\delta} + M^{-1} D \dot{\delta} = M^{-1} (P_m - P_e(\delta)) \quad (4.23)$$

Similarly to the approach in Section 2.5, we apply the transformation

$$\delta = \delta^0 + T \begin{bmatrix} y \\ z \end{bmatrix} \quad (4.24)$$

using slow and fast deviations around the equilibrium, y and z , respectively, and the block-diagonalizing transformation of the linearized model T from (2.52). In component form (4.24) becomes

$$\begin{aligned} \delta_i &= \delta_i^0 + y_i - \sum_{\ell \in J(i)} \frac{M_\ell}{M_{ai}} z_\ell, & i \in \mathcal{R} \\ \delta_i &= \delta_i^0 + y_k - \sum_{\ell \in J(k)} \frac{M_\ell}{M_{ak}} z_\ell, & i \in \mathcal{A} \end{aligned} \quad (4.25)$$

where

$k = k(i)$ - representative machine for the area containing i

$J(i) = I(i) - \{i\}$

$M_{ai} = \sum_{\ell \in I(i)} M_\ell$.

After some manipulations with the transformed variables in (4.23), we get

$$\ddot{y}_i + D_{ai} \dot{y}_i + \sum_{j \in J(i)} D_j \dot{z}_j = P_{mai} - P_{eai}, \quad i = 1, 2, \dots, r \quad (4.26)$$

$$\begin{aligned} \ddot{z}_j + \left(\frac{D_j}{M_j} - \frac{D_k}{M_k} \right) y_j(k) + \left(\frac{D_k}{M_k} - \frac{D_j}{M_j} \right) \sum_{\ell \in J(k)} \frac{M_\ell}{M_{ak}} \dot{z}_\ell \\ + \frac{D_j}{M_j} \dot{z}_j = \left(\frac{P_{mj}}{M_j} - \frac{P_{mk}}{M_k} \right) + \left(\frac{P_{ej}}{M_j} - \frac{P_{ek}}{M_k} \right) \quad j \in \mathcal{A} \end{aligned} \quad (4.27)$$

where

$$P_{mai} = \sum_{\ell \in I(i)} P_{m\ell} \quad (4.28)$$

$$D_{ai} = \sum_{\ell \in I(i)} D_{\ell} \quad (4.29)$$

$$P_{eai} = \sum_{\ell \in I(i)} P_{ei}. \quad (4.30)$$

Equation (4.26) describes the area motion, while equation (4.27) describes the intermachine motion. For small variation around the equilibrium point, these two equations are decoupled. We assume that even for large excursions around equilibrium, variables y basically determine area motion and variables z the intermachine motion. We now analyze in more detail the area motion. Writing power output of area i , P_{eai} as the sum of intra- and interarea load flow, we get (after a few manipulations) the accelerating power of the area in the form

$$\begin{aligned} F_{ai}(y, z) &\equiv P_{mai} - P_{eai} = \\ &= - \sum_{\substack{\ell=1 \\ \ell \neq i}}^r \left[\sum_{j \in I(i)} \sum_{s \in I(\ell)} b_{js} \sin(\delta_{js}^0 + \psi_{js}(z)) \right] \cos y_{i\ell} \\ &\quad + \sum_{\substack{\ell=1 \\ \ell \neq i}}^r \sum_{j \in I(i)} \sum_{s \in I(\ell)} b_{js} \sin \delta_{js}^0 \\ &\quad - \sum_{j \in I(i)} \sum_{\ell \in I(i)} b_{j\ell} \sin(\delta_{j\ell}^0 + \psi_{j\ell}(z)) \\ &\quad - \sum_{\substack{\ell=1 \\ \ell \neq i}}^r \left(\sum_{j \in I(i)} \sum_{s \in I(\ell)} b_{js} \cos(\delta_{js}^0 + \psi_{js}(z)) \right) \sin y_{i\ell} \\ &\equiv \bar{P}_{mai}(y, z) - \bar{P}_{eai}(y, z) \end{aligned} \quad (4.31)$$

where

\bar{P}_{mai} - the first three terms in (4.31)

\bar{P}_{eai} - the fourth term in (4.31)

$$\Psi(z) = \begin{pmatrix} H \\ I+LH \end{pmatrix} z, \quad \Psi_{ij} = \Psi_i - \Psi_j.$$

From the linear system analysis, the following is true.

Proposition 4.7: Assume L_g and H_g satisfy (2.13) and (2.49), for system (3.11). Then:

$$(i) \quad \bar{P}_{mai}(0,0) = 0 \quad (4.32)$$

$$(ii) \quad d_z F_{ai}(0,z) = 0 \quad (4.33)$$

$$(iii) \quad d_y \bar{P}_{mai}(y,0) = 0. \quad (4.34)$$

Proof: (i) and (iii) follow directly from (4.31). The property (ii) follows from the block diagonalizing property of the transformation T for the linearized model.

Based on these properties we make

Assumption 4.8: The terms $\Psi(z)$ have a small effect on y and can be neglected in (4.26) and (4.31).

With this assumption the model for area dynamics can be realized as a machine-impedance system, as explained in Section 4.2, but with time varying input $\bar{P}_{mai}(y,0)$. The other possibility exploited in [43] is to sacrifice the symmetry of the network for the advantage of having the constant mechanical input. In this model, accelerating power is written as

$$F_{ai}(y,0) = - \sum_{\substack{\ell=1 \\ \ell \neq i}}^r Y_{i\ell} \sin(y_{i\ell} + \alpha_{i\ell}) + P_{mai} \quad (4.35)$$

where

$$Y_{il}^2 = g_{il}^2 + b_{il}^2 \quad (4.36)$$

$$g_{il} = \sum_{j \in I(1)} \sum_{s \in I(l)} b_{js} \sin \delta_{js}^0 \quad (4.37)$$

$$b_{il} = \sum_{j \in I(1)} \sum_{s \in I(l)} b_{js} \cos \delta_{js}^0 \quad (4.38)$$

$$\alpha_{il} = \arctan \frac{g_{il}}{b_{il}}. \quad (4.39)$$

In this model power input is constant and each line requires one phase shifter, which eliminates admittance symmetry. Let us now analyze the intermachine dynamics. In equation (4.27) the following is assumed.

Assumption 4.9: The contribution of $(\frac{D_j}{M_j} - \frac{D_k}{M_k}) \cdot (\cdot)$ is smaller than the contribution of $\frac{D_j}{M_j} \dot{z}_j$ in equation (4.27) so that it can be neglected.

Then, the equation of intermachine motion becomes

$$(\ddot{\delta}_j - \ddot{\delta}_k) + \frac{D_j}{M_j} (\dot{\delta}_j - \dot{\delta}_k) = P_{md} - P_{ed} \quad (4.40)$$

where

$$P_{md} = \frac{P_{mj}}{M_j} - \frac{P_{mk}}{M_k} \quad (4.41)$$

$$P_{ed} = \frac{P_{ej}}{M_j} - \frac{P_{ek}}{M_k}. \quad (4.42)$$

Equations (4.40)-(4.42) hold for any partial coherency. However, in the case of slow coherency further simplification is possible by using the weak coupling between areas. In this case it can be assumed that the fast variables are excited (different from zero) only in the area in which the disturbance has occurred. The model for fast dynamics now becomes

$$\begin{aligned}
\ddot{\delta}_{jk} + \frac{D_j}{M_j} \dot{\delta}_{jk} = & P_{md} + \frac{1}{M_j} \sum_{\substack{\ell \in I(k) \\ \ell \neq j}} b_{j\ell} \sin(\delta_{jk} - \delta_{\ell k}) \\
& + \frac{1}{M_k} \sum_{\substack{\ell \in I(k) \\ \ell \neq k}} b_{k\ell} \sin \delta_{\ell k} - P_o \quad j \in \mathcal{J}_k
\end{aligned} \tag{4.43}$$

where

\mathcal{J}_k - is the set of all follower machines in the affected area k
and P_o is artificially added to satisfy the equilibrium
condition ($\ddot{\delta}_{jk} = \dot{\delta}_{jk} = 0$).

Equation (4.43) can be solved independently from the equation for the slow dynamics. However, the solution angles are with respect to the reference machine angle, which becomes known only after the slow subsystem (4.26), (4.31) is solved and the transformation (4.25) is used.

4.7. 48 Machine Example

This section starts with a brief discussion of the results already given for the 48 machine system in various sections of Chapters 3 and 4. In addition we will also use system responses to illustrate some of the developed theoretical points.

In Section 3 the 48 machine system has been divided into nine areas, based on nine slow modes and the corresponding L_d approximated by an L_g . Our choice of slow coherency, rather than any other coherency was motivated by the weak coupling property of the areas, demonstrated in Table 4.2 and the robustness of area boundaries, demonstrated in Table 4.3. These properties of slow coherent areas, derived on a linearized model, will be further substantiated in this section by using system responses of the nonlinear model.

First we check the definition of slow coherency as given by equation (3.29). For that purpose a fault is applied in area one followed by switching off a line. The definition of areas is kept the same as in the predisturbance linearized system. Exact nonlinear responses are obtained and then the slow coherency definition checked by forming the differences of responses of machines inside the areas. As expected the area with the most excited intermachine motions is the disturbed area, i.e. the area one. Some z variables for this area are given in Figure 4.1 (see also [45]), and their slow components are given in Figure 4.2. It can clearly be seen that the difference variables contain some slow dynamics; basically all the individual machine responses agree in their slow motion. In our definition of slow coherency we tolerate an arbitrary magnitude of z variables. This is one of the key differences with the other coherency definitions [19], which restrict the magnitude of z also. In this particular example for all the machines of area one to be in the same coherent area according to the latter criterion the tolerance should be (see Figure 4.1) about 25° , but with this tolerance it may as well happen that many areas collapse into one area. With our approach of identifying areas based on approximation of L_d by an L_g , we avoid a need for specifying the above tolerance criterion, which may, as indicated above, significantly affect the found areas.

The next figures also illustrate the robustness of area boundaries to parameter changes, which for the linear case was illustrated by Table 4.3. For this purpose a fault was applied in area 7, followed by switching a line in the same area [45]. We now give, for the sake of comparison, the responses of machines in area 7. Figure 4.3 contains machine angle differences and

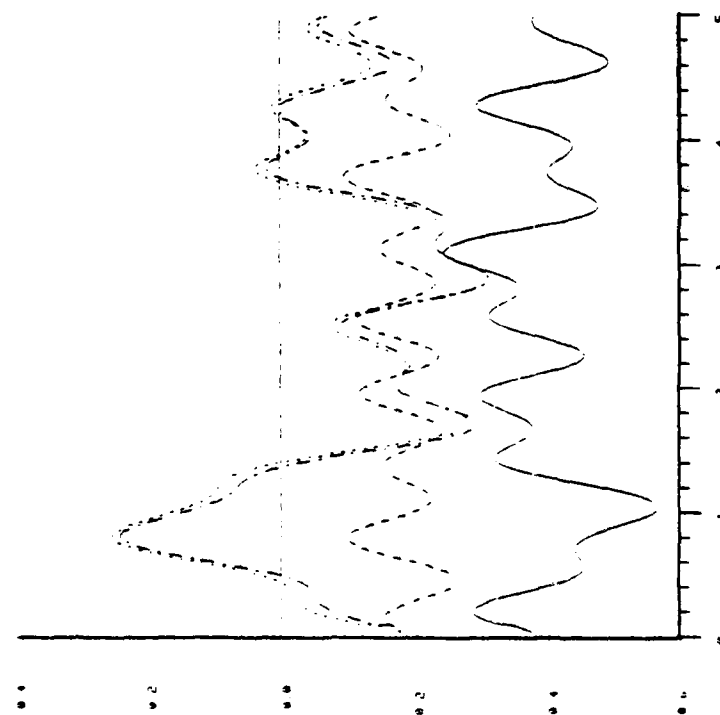


Figure 4.1. Difference variables of machines in area 1.

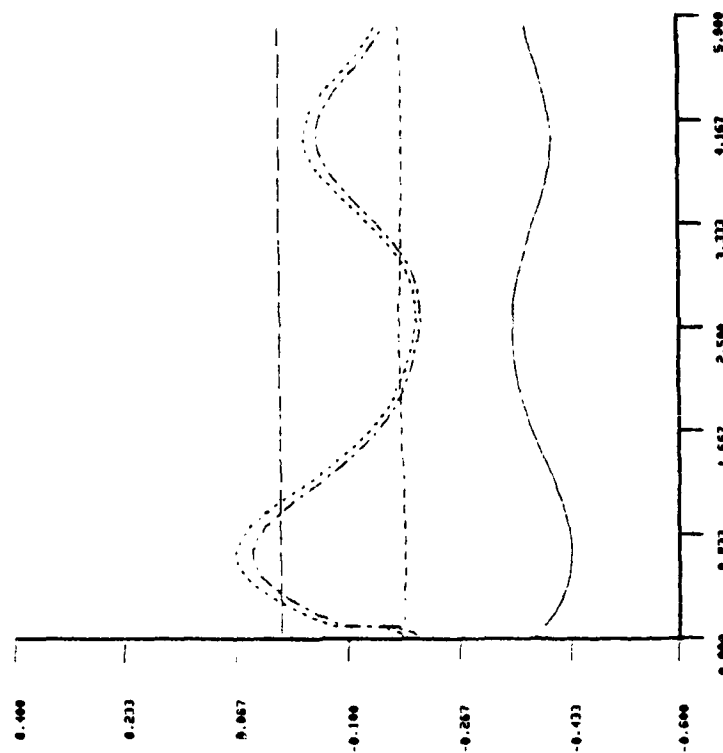


Figure 4.2. Slow components in the difference variables for area 1.

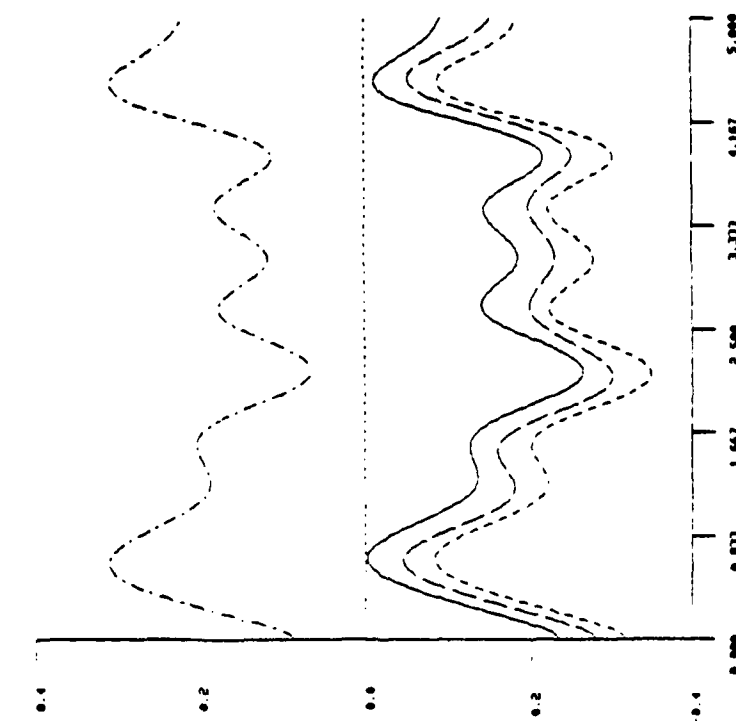


Figure 4.3. Machine angle differences for area 7 after a disturbance in the area.

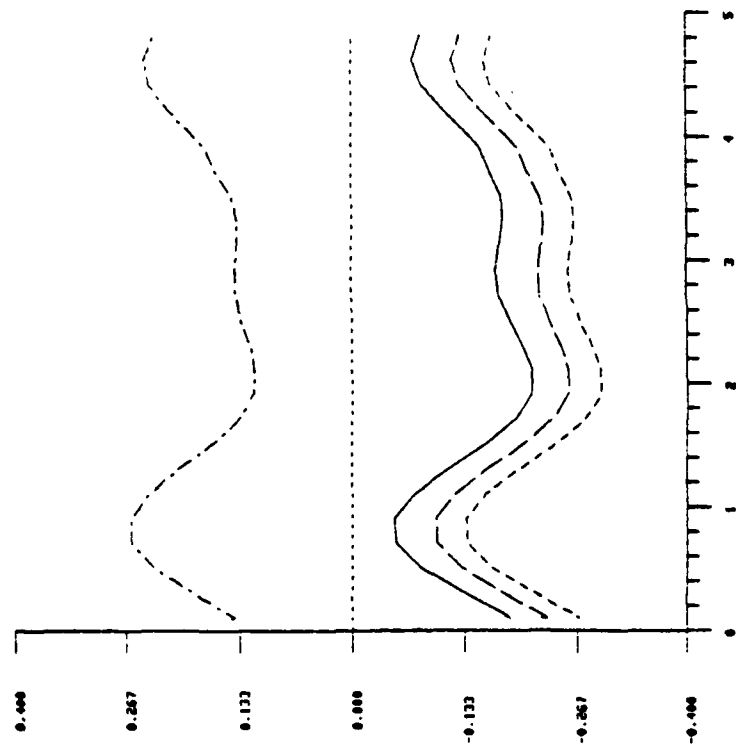


Figure 4.4. Slow components of machine angle differences in area 7.

Figure 4.4 contains their slow components. Again as in the previous case the definition of slow coherency is satisfied for area 7 as well as for all other areas.

The third group of figures illustrates results of various approximations in the simulation of the nonlinear model.

Approximation 1 (A1): In this approximation the singular perturbation approach, similar to the one in Chapter 2, was applied to the model (4.26), (4.27). Namely, the fast system (4.27) is assumed to be stable for each value of $y(t)$ and infinitely fast, so that the set of equations containing differential equations (4.26) and algebraic equations (4.27) obtained by setting $\ddot{z}(t) = \dot{z}(t) = 0$ is solved. Since these equations describe the slow dynamics, a large integration step size can be used. However, the number of equations is still n . From Figure 4.5a it can be seen that the individual machine responses are well approximated.

Approximation 2 (A2): The weak coupling between areas, which implies the weak coupling between the fast subsystems in different areas, suggests using the differential equations for the area affected by the disturbance, only, and algebraic equations for all the other areas. The number of differential equations equals r + the number of the free machines in the affected area. Again, the total number of equations equals n . Inclusion of the fast dynamics in the affected area improves the accuracy of the responses over the previous case, as can be seen by comparing Figure 4.5a and Figure 4.5b. The difference between the exact response and A2 is only due to the fast dynamics outside the affected area.

Approximation 3 (A3): This approximation differs from A2 in that outside the affected area a constant $z(t) = z(0^-)$ is used. However, more

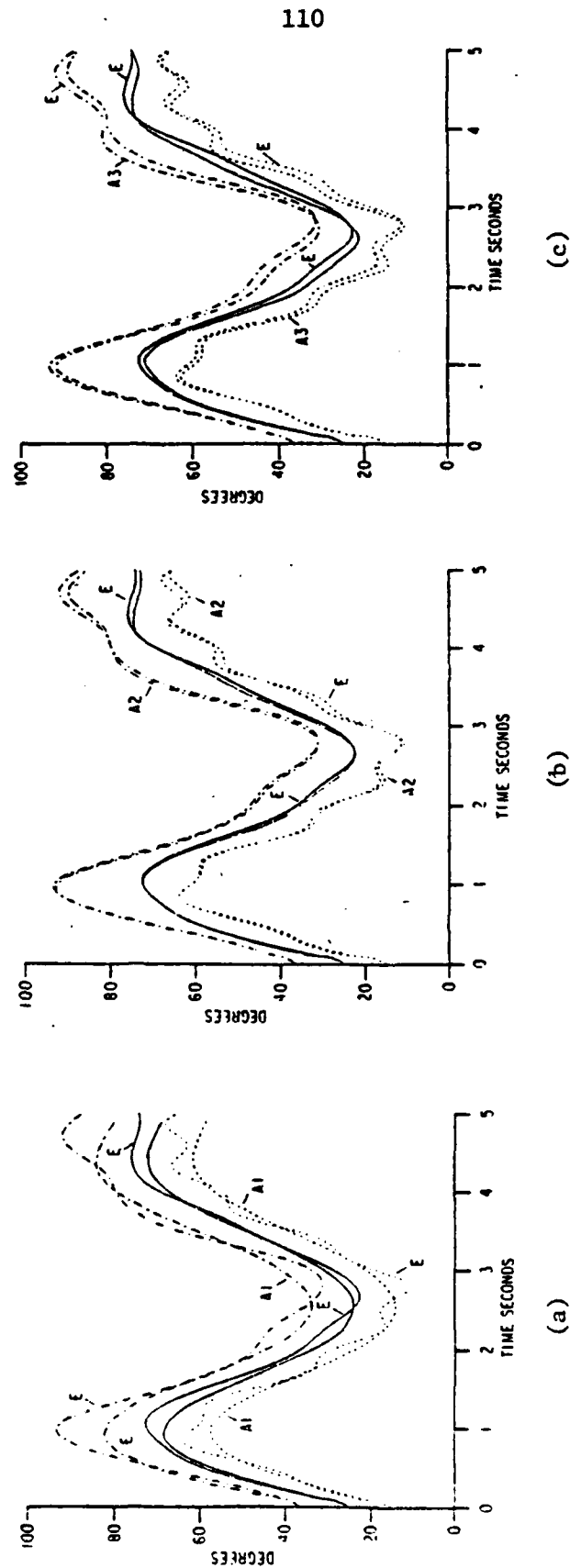


Figure 4.5. Exact individual machine responses in area 1 vs. different approximations. A1-algebraic equation for the difference variables; A2-differential equations for the difference variables in area 1 only, algebraic elsewhere; A3-differential equations for the difference variables in area 1 and constant values for the other areas.

appropriate would be to use $z(t) = z(\infty)$, but this requires solving an additional load flow. The results given in Figure 4.5c indicate that this approximation is somewhat worse than A2.

As a conclusion to this series of experiments, it follows that the approximation A3 seems to be a compromise between accuracy and integration cost. Note however, that these simulations cannot indicate only the instability due to the fast dynamics outside the affected area because in all the approximations it was assumed that the fast dynamics, i.e., intermachine motion is stable. Due to the weak coupling between areas this does not appear to be a serious limitation. Therefore a justifiable approach to the system stability would be to use the dynamic equations for the area dynamics, and the fast dynamics for the affected area only.

4.8. Numerical Aspects of the Slow Coherency Algorithm

Slow coherency proves to be easier to identify numerically than other types of coherency. In view of the grouping algorithm of Section 3.5, this is to say that it is somewhat easier to find a basis for the slow eigenspace than for any other arbitrary eigenspace (excluding the fast eigenspace which is physically unrealistic to be used for coherency definition). This section is devoted to the discussion of various methods for computing a basis for the slow subspace, with the emphasis on large and very large systems. By large systems we mean systems in which the computation of all eigenvalues and eigenvectors is expensive, but their state matrix A can still be manipulated in the core of an available computer. Very large systems will be those in which the state matrix cannot be processed in core; computation

of all eigenvalues and eigenvectors is almost impossible. Independently of the system size there are two factors that make computation of V easier.

(i) Matrix A is similar to a symmetric matrix (3.14). This means that special programs can be used which are faster and more economical in memory use than the programs for general matrices.

(ii) Arbitrary basis of the slow eigenspace can be used, rather than the eigenvector basis. In the case of identical or very close eigenvalues, eigenvectors are very sensitive to parameter changes (numerical error, say), while the space they span is not. Therefore any basis of that subspace can be used. Most of the existing eigenvector programs compute efficiently an arbitrary basis corresponding to a multiple eigenvalue and then spend most of the time trying to compute exact eigenvectors.

For the large systems there are already available production programs [46] which compute V . The conclusion [46] is that if, roughly, $r < \frac{n}{4}$, which can be considered satisfied in coherency identification, then the special purpose programs for partial eigensolutions are superior to the ones that compute all eigenvalues and eigenvectors. Following recommendations of [46], the bisection method seems to be a desirable choice. In this method the frequency range defining coherency, rather than the number of slow modes, should be specified.

Alternatively, a very simple method of Chapter 3, based on Riccati iterations (2.41), can be used. For this method an initial guess of reference machines needs to be made. Good guesses result in faster convergence to the solution; poor guesses may require many more iterations, as is evident from Figure 4.6. Curve a corresponds to a good choice of reference machines,

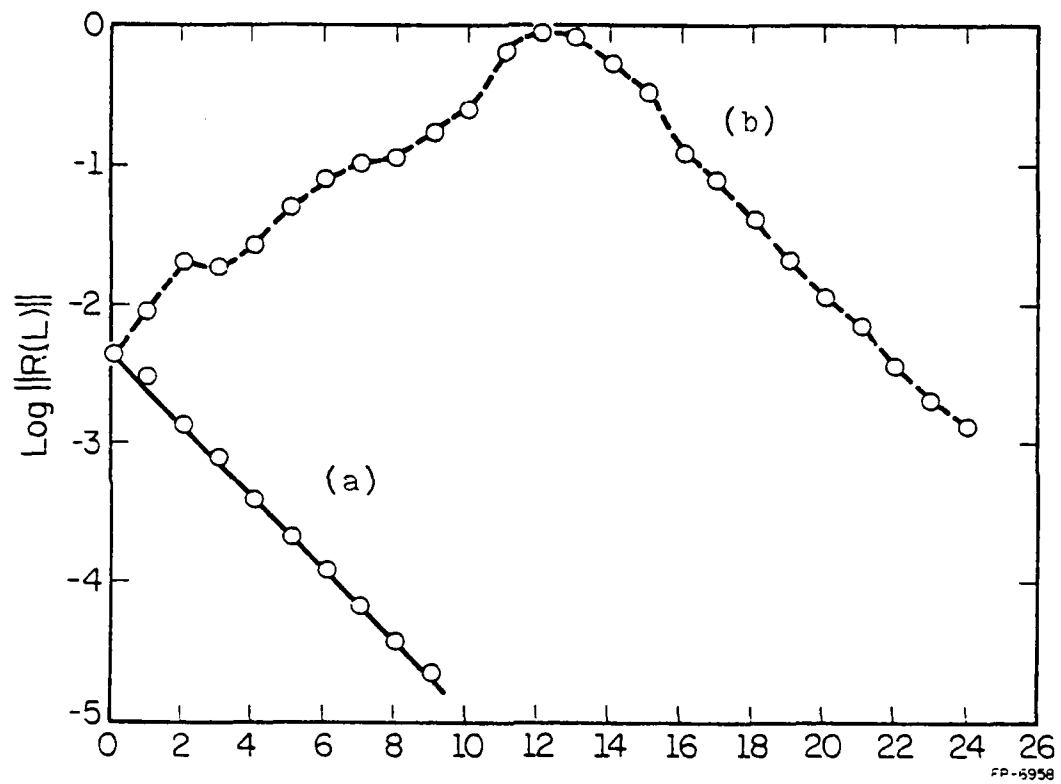


Figure 4.6. Behavior of Riccati iterations for the 48 machine system; (a) a good guess of reference machines, (b) a poor guess of reference machines.

in fact to those that are found by the grouping algorithm. Curve b corresponds to selecting machines 13 and 47 instead of 17 and 29 in the above choice. In this case machines 13 and 47 both belong to the same area (area 7) and area 8 does not have any reference machine. If this were the ideal coherency case, the algorithm would not have converged at all.

Computation of partial eigensystems for very large systems is still an area of active research [47,48,32]. Almost all the methods of this group, of which we will mention only a few, have inner product $a^T x$ as a basic in core operation. Methods with this property are simultaneous iteration methods [49,32], modified simultaneous iteration methods [48], Lanczos method [49], and modified inverse method [47]. All of these methods have basically the linear rate of convergence. Some acceleration is possible by using Tchebishev's transformation [49]. Also, all of these methods can take advantage of the sparsity in programming the inner-product. However, in the model (3.11), the state matrix A is dense. We now show, on the example of simultaneous iterations, that it is possible to use the original sparse Jacobian (3.4), instead of the reduced one. The result is given in the following lemma.

Lemma 4.10: Let J be the Jacobian of the unreduced load flow system in which the first n rows correspond to the generator nodes and the last m rows to the load nodes. Let

$$J = \begin{pmatrix} A & B \\ C & D \end{pmatrix}, \quad J = J^T, \quad A \in \mathbb{R}^{n \times n} \quad (4.44)$$

and assume D^{-1} exists. Then

$$JV^{k+1} = EV^k \quad (4.45)$$

where

$$V^k = \begin{bmatrix} V_1 \\ V_2 \end{bmatrix}^k, \quad V_1 \in R^{n \times n} \quad (4.46)$$

$$E = \begin{bmatrix} M & 0 \\ 0 & 0 \end{bmatrix} \quad (4.47)$$

generates for sufficiently large k a basis of the r -dimensional slow eigenspace of $M^{-1}(A-BD^{-1}C) \equiv M^{-1}K$, where K is given by (3.8), in the form of the matrix V_1 of (4.46).

Proof: Writing (4.45) in expanded form, solving for V_2 from the second equation, and substituting in the first equation, gives in view of Lemma 2.11 the claimed result.

Use of the sparse Jacobian (4.44) rather than the reduced one as in (3.11), can result in substantial savings in computation time, as is already shown in related approaches, see for example [56].

4.9. Summary of the Chapter

In this chapter we have shown that the equivalent for the area dynamics in the linearized model can be realized by a symmetric network connecting r generators, each representing one area. In the nonlinear model the same structure can be retained under very mild assumption, but with time varying mechanical input, or alternatively, asymmetric network and constant input. It is concluded further that for most networks and loading conditions, the coherency is largely determined by network parameters

and machine inertias, rather than by loading conditions. The most important result is that in the case of slow coherency areas are weakly coupled. Furthermore, in this very case the area boundaries are relatively insensitive to small parameter changes. The weak coupling and robustness of area boundaries are a basis for using areas obtained in the analysis of the linearized model for the nonlinear system analysis. Several approximations based on the use of slow coherency and singular perturbations on the nonlinear model are demonstrated to be accurate and efficient. Numerical aspects of the slow coherency are discussed in light of the existing methods and research trends in the field. A sparse formulation of the numerical algorithm for computing slow basis is given.

5. SUGGESTIONS AND CONCLUSIONS

5.1. Suggestions for Further Research

In chapter 4 we gave several uses of the coherency. First we have considered aggregation of linear and nonlinear power system models. Then by using slow coherency we were able to transform the mixed state electromechanical power system model into the singularly perturbed form. Finally, we illustrated several uses of the model in the singularly perturbed form as well as the weak coupling between coherent areas in the simulation of the nonlinear model. A simulation of the system is usually undertaken for the purpose of checking its stability. We now want to discuss possible uses of coherency and in particular slow coherency in the direct stability analysis of power systems. In order to do so we will first sketch the background of the direct stability analysis.

One of the main objectives in the stability studies of power systems is to determine the so called critical clearing time t_c . This is the time defined for each fault and represents the maximal duration of the fault for which post disturbance system (which may have different structure than the original one) remains stable. Large t_c indicates that the system is stronger (more robust) with respect to the given disturbance. Critical clearing time is then used in the design of protective equipment (local controls). The problem of determining the critical clearing time is, however, almost identical to the problem of determining the domain of attraction around postdisturbance equilibrium - or stability domain in short.

Stability analysis of power systems at the present time is basically conducted using simulation of system responses for given disturbances [59]. Such methods enable use of detailed models of system

components (machines and transmission elements) and offer flexibility in using different configurations of the same network. However there are some disadvantages: (a) computation time is large, becoming prohibitive for very large systems, (b) experience needed in interpreting responses in order to conclude instability and (c) no advantage from previous simulations can be gained when analyzing the same network for different fault locations. An alternative is to perform a direct stability analysis based on Liapunov theory [53]. The electromechanical model (3.2), (3.3), in which the load nodes are eliminated and the admittances between the remaining generator busses are suitably altered as discussed in section 3.2, is typically used in such studies. By further manipulations [53] the model can be written in the form

$$\begin{aligned} \dot{x} &= Ax + B f(y) \\ y &= Cx \end{aligned} \quad (5.1)$$

where $x^T = (\omega_1, \omega_2, \dots, \omega_n, \delta_1 - \delta_N, \delta_2 - \delta_N, \dots, \delta_{n-1} - \delta_N)$,

$$f_i(y) = V_p V_q B_{pq} [\sin(y_i + \delta_{pq}^0) - \sin \delta_{pq}^0] \quad (5.2)$$

The relation between indexes i , p and q and the form of matrices A , B and C are given in [53]. For the model (5.1) of the postdisturbance network the form of a Liapunov function

$$V(x) = x^T P x + 2 \int_0^y f^T(u) Q du \equiv V_c + V_p \quad (5.3)$$

and the necessary definitnes conditions are given in [62]. From (5.3)

the classical transient energy function [61] is obtained with $P = \begin{bmatrix} M & 0 \\ 0 & 0 \end{bmatrix}$

and $Q = I$. Having selected a Liapunov function, the next step is to

find the critical value $V(x) = V_c$, such that if $V(x) < V_c$ for some x , then the system is said to be stable. In [60] it is shown that V_c equals the minimum potential energy over all the unstable equilibrium points of the system (5.1), i.e.

$$V_c = \inf_{x \in U} V(x) \quad (5.4)$$

where U is the set of all the unstable equilibrium points for the system (5.1). With known V_c computation of the critical clearing time for each disturbance proceeds as follows. When the system is subjected to the disturbance, its response is simulated and the function $V(x)$ of (5.3) is evaluated along the trajectory. The time at which $V(x) = V_c$ is the critical clearing time. From this description it is clear that the direct methods are in fact the combination of a simulation and a direct stability analysis. An inherent difficulty in the direct methods, however, is computation of V_c , because the number of unstable equilibrium points of (5.1) is $O(2^n)$, where n is the number of generators in the network, and to find each of this points requires solving the set of $(n-1)$ nonlinear (load flow) equations. Therefore the utility of the method critically depends on the way of computing V_c ; its effectiveness is to be measured against possible savings in computer time over the direct simulation. There are also other problems summarized below which have resulted in certain scepticism from power industry toward the application of these methods [Disc. on 61].

(a) The methods have proven useful for small order systems (several machines, say); for one machine infinite bus system exact stability boundary can be obtained.

(b) Depending on the fault location they can give overly conservative results when applied to large systems [56]; if parts of the same system are aggregated, better results can be obtained [56].

(c) Most of the results for large systems are reported for the electro-mechanical model and the line conductances neglected. Inclusion of the more detailed machine models and the conductances is followed by the difficulty in finding an "appropriate" Liapunov function.

Despite the shortcomings, the need for direct stability methods which would complement simulation, exists. The utility of the approach is seen in the planning stage or on-line security assessment where it would be used to select some critical disturbances for further study. Here the initial effort spent on computing V_c would be well compensated by the repeated use of the same V_c for different faults resulting in the same postdisturbance network. These methods also offer a basis for studying the effect of parameter changes on systems stability. In response to this need, and in an attempt to overcome (some of) the shortcomings, there have recently appeared several major contributions to the problem of direct transient stability studies.

First, in [63] it was shown that the potential function (the integral part of $V(x)$ in (5.3)) is smooth around equilibrium points. Using this property of the potential function and generalizing the case of one machine infinite bus system, in which δ^0 is the stable equilibrium, then the smaller of $(\pm\pi - 2\delta^0)$ is the unstable equilibrium with the smallest potential energy. Approximations of the unstable equilibrium points of the following type have been suggested by several authors (See [53] for an overview)

$$\delta_k = (\delta_1^o, \delta_2^o, \dots, u_k, \dots, \delta_{n-1}^o), k = 1, 2, \dots, n-1$$

$$u_k = \text{sign}[P_k - \frac{M_k}{M_1 + M_2 + \dots + M_N} (P_1 + \dots + P_n)] J_1 - \delta_k^o \quad (5.5)$$

where superscript "o" denotes equilibrium values, and u_k is an approximation of the angle corresponding to the k-th machine becoming unstable. Variants exist [53] to account for several machines becoming unstable. Now the search for V_c in (5.4) can be carried out over the set U whose elements are of the form (5.5). This set may still be large (it has n elements if only one machine at a time is considered to become unstable, but combinations often have to be considered as well) so that selecting the right element remains a serious task. It is interesting to note, however, that when the separation of a system into groups under a given disturbance is known, then the V_c computed as the potential energy at the points of the type (5.5) corresponding to these groups gives favorable results. A major step forward in finding V_c for a given disturbance has been made in [54,55].

The main idea is that V_c is the potential energy at the unstable equilibrium point which is in the direction of the systems motion (the motion is considered in the space of angles δ). The direction is determined at the time when the kinetic energy is maximal. This implies that the system continues to move basically in the direction established during the fault, even after the fault is cleared. As a consequence the method proves to be very effective for the so called first swing instability, which is when δ grows without changing signs. On the other hand it is often inaccurate for multiswing instability, in which case the system

oscillates several times before becoming unstable. In this case the assumption of unidirectional motion is not satisfied, and a different unstable equilibrium has to be found in order to compute appropriate V_c . A group of methods with sound analytical background, but less satisfying practical results so far, is centered around the use of vector Lyapunov function approach [53,57,43]. The essence of the method is to [58]: (a) decompose the system into suitable subsystems, (b) find stability domain of subsystems ignoring the interconnections, (c) impose (linear) bound on interconnections and (d) find the stability region of the overall system [57].

For the methods to be successfully applied it is essential that the subsystems are weakly coupled [57,58]. The main reasons for the conservativeness are : (a) in bounding interconnections it is assumed that they all act simultaneously in the way which is the worst for the systems stability, and (b) nonlinear interconnection terms of the form $s = [\sin(x+a) - \sin a]$ are usually bounded by $\mathcal{E}x \leq s \leq \cos a \cdot x$, where \mathcal{E} has to satisfy two contradictory requirements: for a large region of stability to be obtained it has to be as small as possible, but for the matrix $A(\mathcal{E})$, from $\dot{V} = A(\mathcal{E})V^T$ where V is the vector of subsystem Liapunov functions, to have all the eigenvalue positive, \mathcal{E} has to be as large as possible. It may happen, therefore, that for a given \mathcal{E} , which is a design parameter, suitable $A(\mathcal{E})$ does not exist; then \mathcal{E} has to be increased, resulting ultimately in the reduction of the region of stability. The methods, however, can be very attractive when the decomposition of the system into weakly coupled subsystems can be made.

With this somewhat longer introduction into the complex and unresolved problem, we are now ready to consider coherency in the framework of the direct stability analysis. Our consideration is basically oriented toward listing problems for further research.

For the methods based on vector Liapunov function approach the decomposition of the system into areas based on slow coherency seems to be the best choice because of the weak coupling between areas established in chapter 4. If the problem consists of finding the "slow" stability i.e. the stability of the interarea motion, assuming that the fast intermachine oscillations within areas are stable, then the vector Lyapunov function approaches appear to be applicable. However, when the stability of the overall system, including the intermachine oscillations, is of interest (which is the most usual case), then there are several options. One is to study separately the fast and the slow stability using models (4.26) and 4.43). For analyzing the fast stability, a method along the lines of [54,55] will have to be used. The other way is to aggregate all the areas outside the area in which a disturbance is applied and study the whole composite system [43].

In summary, the coherency can help in three ways. First, coherency based aggregation reduces the order of the system. Second, when slow coherency is used, the areas are weakly coupled, and third, the machines in the coherent areas have a sort of symmetry (homogeneity) in coupling (4.6). The last property may imply that the criterion (5.4), with U containing unstable points (5.5) corresponding to the generators in the area affected by a disturbance, may not be too conservative.

Among other applications of the coherency decomposition and possible extensions of the work we mention the following.

The electromechanical model without damping was used in the previous analysis under the assumption that small damping does not affect frequency of the system. However the effects of the more complete machine models on the identity of coherent areas should be investigated.

Numerical aspects of the simulation algorithm for weakly nonlinear systems, the algorithm for identifying coherent areas and the use of the decomposition for analysis and design still deserve a lot of attention.

When the slow coherency is used for system decomposition, the areas are weakly coupled. It is felt that this property and a similar approach can be used for the decomposition of a power system for use in steady state (load flow) type studies.

5.2. Conclusions

In this thesis the properties and some uses of coherency in electromechanical models of power systems have been considered. It has been shown that the coherency can be treated in the framework of the spectrum separation problem. This property was essential in defining the new efficient algorithm for the decomposition of power systems into coherent areas.

When the coherency is defined as the so called slow coherency, then the areas are weakly coupled and insensitive to small parameter changes. This is a justification for using linearized model for defining areas, and then using those areas in the nonlinear model.

For the class of r -decomposable power systems with respect to the slow modes the subsystem whose states are so called center of inertia variables is the true slow subsystem and the subsystem with inter-machine variables within areas as states is the true fast subsystem. Applying the area and intermachine variable transformation to near r -decomposable systems transforms the mixed state electro-mechanical model into the singularly perturbed form. Use of the standard singular perturbation approaches to the simulation of such models was illustrated on several examples. Analysis of the reduced order models has revealed the sources of approximations used in going from the exact subsystems to the commonly used aggregated models, both in the linear and the nonlinear case.

The numerical algorithm for identifying coherent areas is designed with the idea to be applicable for large power systems, and hence it consists of well conditioned steps and modest use of computer time and memory. Together with the weak coupling property of the resulting areas the method offers a useful way of decomposing a power system into subsystems which can then be used in various applications.

REFERENCES

1. E. J. Davison, "A Method for Simplifying Linear Dynamic Systems," IEEE Trans. on Automatic Control, Vol. AC-12, pp. 213-214, April 1967.
2. S. S. Lamba and S. V. Rao, "On Suboptimal Control Via the Simplified Model of Davison," IEEE Trans. on Automatic Control, Vol. 19, No. 4, pp. 448-450, August 1974.
3. M. J. Balas, "Modal Control of Certain Flexible Dynamic Systems," SIAM J. Control and Optimization, Vol. 16, No. 3, pp. 450-462, May 1978.
4. J. Hickin and N. K. Sinha, "Aggregation Matrices for a Class of Low-Order Models for Large-Scale Systems," Electronics Letters, Vol. 11, No. 9, p. 186, May 1975.
5. G. Michalesco, J. M. Siret, and P. Bertrand, "Aggregated Models for High-Order Systems," Electronic Letters, Vol. 11, pp. 398-399, July 1975.
6. M. Aoki, "Control of Large-Scale Dynamic Systems by Aggregation," IEEE Trans. on Automatic Control, Vol. AC-13, No. 3, pp. 246-253, June 1968.
7. M. Aoki, "Some Approximation Methods for Estimation and Control of Large Scale Systems," IEEE Trans. on Automatic Control, Vol. AC-23, No. 2, pp. 173-181, April 1978.
8. P. V. Kokotovic, R. E. O'Malley, P. Sannuti, "Singular Perturbations and Order Reduction in Control Theory - An Overview," Automatica, Vol. 12, pp. 123-132, 1976.
9. D. G. Luenberger, "Dynamic Equations in Descriptor Form," IEEE Trans. on Automatic Control, Vol. AC-22, pp. 312-321, 1977.
10. J. D. Cobb, "Descriptor Variable and Generalized Singular Perturbed Systems; a Geometric Approach," Ph.D. Dissertation, University of Illinois, Urbana, 1980.
11. P. V. Kokotovic, J. J. Allemong, J. R. Winkelman, J. H. Chow, "Singular Perturbations and Iterative Separation of Time Scales," Automatica, Vol. 16, pp. 23-44, 1980.
12. P. V. Kokotovic, "A Riccati Equation for Block-Diagonalization of Ill-Conditioned Systems," IEEE Trans. on Automatic Control, Vol. AC-20, pp. 812-814, 1975.
13. L. Anderson, "Decomposition of Two-Time-Scale Linear Systems," Proc. JACC, Philadelphia, pp. 153-163, 1978.

14. B. Avramovic, "Subspace Iteration Approach to the Time Scale Separation," Proc. of the 18th IEEE Conf. on Decision and Control, Florida, pp. 684-687, 1979.
15. J. Medanic, "The Geometric Properties and Invariant Manifolds of the General Riccati Equation," in Report DC-28: Multimodeling and Control of Large Scale Systems, Coordinated Science Laboratory, University of Illinois, Urbana, IL, pp. 3.108-3.117, 1979.
16. F. Saccomano, "Dynamic Modeling of Multimachine Electric Power Systems," Symposium on Mathematical Methods for the Analysis of Large Systems, Praga, 1974.
17. F. Marconato, F. Mariani, F. Saccomano, "Application of Simplified Dynamic Models to the Italian Power Systems," Proc. of 8th PICA Conf., Minneapolis, Minnesota, 1973.
18. W. W. Price, et al., "Testing of the Modal Dynamic Equivalent Technique," IEEE Trans. on Power Apparatus & Systems, Vol. PAS-97, pp. 1366-1372, 1978.
19. R. Podmore, "Identification of Coherent Generators for Dynamic Equivalents," IEEE Trans. Power Apparatus & Systems, Vol. PAS-97, pp. 1344-1354, 1978.
20. F. F. Wu and N. Narasimhamurthy, "Coherency Identification for Power System Dynamic Equivalents," Memorandum No. UCB/ERL M77/57, University of California, Berkeley.
21. S. Sastry and P. Varaiya, "Coherence and Alert State for Interconnected Power Systems," Memorandum No. UCB/ERL M79/57.
22. S. T. Lee and F. C. Schweppe, "Distance Measures and Coherency Recognition for Transient Stability Equivalents," IEEE Trans. on Power Apparatus and Systems, Vol. PAS-92, pp. 1550-1557, 1973.
23. M. A. Pai and R. P. Adgaonkar, "Identification of Coherent Generators Using Weighted Eigenvectors," IEEE Paper A79022-5, presented at PES Winter Meeting, New York, 1979.
24. E. G. Castro-Leon and A. H. El-Abiad, "Bibliographi on Power System Dynamic Equivalents," Workshop on Dynamic Equivalents for Stability Studies, IEEE PES Summer Meeting, Los Angeles, Calif., July 1978.
25. B. Avramovic, P. V. Kokotovic, J. R. Winkelman, J. H. Chow, "Area Decomposition for Electromechanical Models of Power Systems," to be presented at IFAC Symposium on Large Scale Systems: Theory and Applications, Toulouse, France, 1980.
26. A. D. Bhatt, H. G. Kwatny, and V. E. Mablekos, "A Coherency Concept for Construction of Power System Equivalents," presented at the 1976 International Conference on Information Sciences and Systems, Patras, Greece, 1976.

27. F. R. Gantmacher, The Theory of Matrices, Chelsea, New York, 1964.
28. Kalman, R. E., "Contributions to the Theory of Optimal Control," Bol. Soc. Mat. Mex., Vol. 5, pp. 102-119, 1960.
29. M. Athans and P. L. Falb, Optimal Control, McGraw-Hill, 1966.
30. K. Martensson, "On the Matrix Riccati Equation," Information Science, Vol. 3, pp. 17-49, 1971.
31. F. F. Wu and N. Narasimhamurthy, "On the Riccati Equation Arising from the Study of Singularly Perturbed Systems," Proc. JACC, San Francisco, U.S.A., pp. 1244-1247, 1977.
32. G. W. Stewart, "Simultaneous Iteration Method for Computing Invariant Subspaces of Non-Hermitian Matrices," Numer. Math., Vol. 25, pp. 123-136, 1976.
33. D. L. Kleiman, "On an Iterative Technique for Riccati Equation Computations," IEEE Trans. on Automatic Control, Vol. 13, p. 114, 1968.
34. J. J. Allemong, "A Singular Perturbation Approach to Power System Dynamics," Ph.D. Dissertation, University of Illinois, Urbana, 1978.
35. E. J. Davison, "An Algorithm for the Computer Simulation of Very Large Dynamic Systems," Automatica, Vol. 9, pp. 665-675, 1973.
36. R. F. Sincovec, et.al., "Solvability of Large Scale Descriptor Systems," Final Report prepared for the Department of Energy, 1979.
37. U. Di Caprio, R. Marconato, "Structural Coherency Conditions in Multimachine Power Systems," Presented at the 8th IFAC World Congress, Helsinki, 1978.
38. G. W. Stewart, Introduction to Matrix Computation, Academic Press, 1973.
39. J. Lowler, R. A. Schleuter, P. Rushe, D. L. Hachett, "Modal-coherent equivalents derived from an RMS coherency measure," IEEE Paper F79 663-6, presented at PES Summer Meeting, Vancouver, Canada, 1979.
40. P. M. Anderson, A. A. Fouad, Power System Control and Stability, Iowa State University Press, Ames, Iowa, 1977.
41. K. N. Stanton, "Dynamic Energy Balance Studies for Simulation of Power Frequency Transients," 1971 PICA Proc., pp. 173-179, 1971.
42. A. S. Debs and A. R. Benson, "Security Assessment of Power Systems," System Engineering for Power: Status and Prospects, Conf. Report, Henniker, New Hampshire, pp. 144-173, 1975.

43. L. J. Grujic, M. Darwish and J. Fantin, "Coherence, Vector Liapunov Functions and Large-Scale Power Systems," Int. J. System Sci. Vol. 10, No. 3, pp. 351-362, 1979.
44. G. H. Golub and C. T. Reinch, "Singular Value Decomposition and Least Squares Solution," Numer. Math., pp. 403-420, 1970.
45. J. R. Winkelman, J. H. Chow, B. C. Bowler, B. Avramovic and P. V. Kokotovic, "An Analysis of Interarea Dynamics of Power Systems," to appear in IEEE Trans. on Power Apparatus and Systems.
46. Wilkinson, J. H. C. Reinch, Linear Algebra, Springer-Verlag, New York, 1971.
47. In Wan Lee, "Solution Techniques for Large Eigenvalue Problems in Structural Dynamics," Ph.D. Thesis, University of Illinois, 1979.
48. A. Sameh and J. Wisniewski, "A Modified Simultaneous Iteration Algorithm for $Ax = \lambda Bx$," presented at the International Conference on Electrical Power Problems: The Mathematical Challenge, March 1980, Seattle, Washington.
49. A. Jennings, "Matrix Computation for Engineers and Scientists," John Wiley & Sons, 1978.
50. C. W. Gear, Numerical Initial Value Problems in Ordinary Differential Equations, Englewood Cliffs, N.J.: Prentice-Hall, 1971.
51. U. D. Caprio and F. Saccomanno, "Non-Linear Analysis of Multimachine Electric Power Systems," Ricerche di Automatica, Vol. 1., No. 1, Sept. 1970.
52. B. Stott and O. Alsac, "Fast Decoupled Load Flow," IEEE Trans. on Power Apparatus and Systems, Vol. PAS 93, pp. 868, 1974.
53. M. A. Pai, "Stability of Large Scale Power Systems," in the book M. Singh, A. Titli, Large Scale Systems Engineering Applications, North Holland, 1979.
54. T. Athay et.al., "A Practical Method for the Direct Analysis of Transient Stability," IEEE Trans. on Power Apparatus and Systems, Vol. PAS 98, pp. 573-584, 1979.
55. N. Kakimoto, et al., "Transient Stability Analysis of Electric Power Systems via Lure' Type Lyapunov Function, Parts I and II," Trans. IEE of Japan, Vol. 98, No. 5/6, 1978.
56. Systems Control, Inc., Final Report "Transient Energy Stability Analysis," in Proc. of Systems Engineering for Power: Emergency Operating State Control, Davos, Switzerland, 1979.

57. D. Siljak, Large Scale Dynamic Systems, North Holland, 1978.
58. M. Araki, "Stability of Large Scale Nonlinear Systems - Quadratic Order Theory of Composite System Method Using M-Matrices," IEEE Trans. on Automatic Control, Vol. AC-23, No. 2, pp. 129-142, 1978.
59. B. Stott, "Power System Step by Step Stability Calculations," Proc. of IEEE International Symp. on Circuits and Systems, pp. 839-857, 1977.
60. J. L. Willems and J. C. Willems, "The Application of Lyapunov Methods to the Computation of Stability Regions of Multi-Machine Power Systems," IEEE Trans. on Power Apparatus and Systems, Vol. PAS-89, pp. 795-801, 1970.
61. A. A. Fouad, "Stability Theory-Criteria for Transient Stability," ERDA Symp. on System Engineering for Power, August 1975.
62. J. B. Moore and B. D. O. Anderson, "A Generalization of the Popov Criterion," J. Franklin Institute, pp. 488-492, 1968.
63. F. S. Prabhakara and A. H. El-Abiad, "A Simplified Determination of Transient Stability Regions for Lyapunov Methods," IEEE Trans. on Power Apparatus and Systems, Vol. PAS-94, No. 2, pp. 672-689, 1975.

APPENDIX A. ONE MACHINE INFINITE BUS MODEL [34]

Notation

AVR - automatic voltage regulator

E_{fd}, V_R, R_f - voltage regulator states

e'_q, e'_d - flux decay states

Ω, δ - swing model states

Subscripts

d - direct axis quantities

q - quadrature axis quantities

f - main field quantities

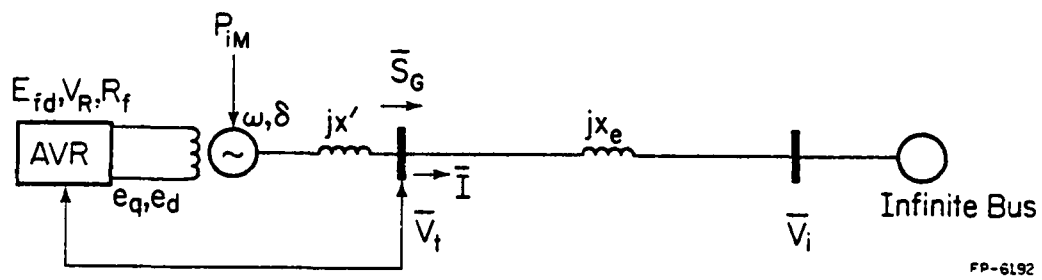


Figure A.1. One machine infinity bus system.

Full Model

$$\dot{e}'_q = \frac{1}{T_{d0}} \{ - [1 + (x_d - x')Y] e'_q - (x_d - x')YV_i \sin\delta + E_{fd} \}$$

$$\dot{R}_f = \frac{1}{T_F} (-R_f + \frac{K_F}{T_F} E_{fd})$$

$$\dot{e}'_d = \frac{1}{T'_{d0}} \{ (x_q - x') YV_i \cos\delta - [1 + (x_q - x')Y] e'_d \}$$

$$\dot{\delta} = 377 (\Omega - 1)$$

$$\Omega = \frac{1}{2H} \left[\frac{P_{in}}{\Omega} - D(\Omega - 1) - YV_i (e'_q \cos\delta + e'_d \sin\delta) \right]$$

$$\dot{E}_{fd} = \frac{1}{T_E} \{ - [K_E + S_E(E_{fd})] E_{fd} + V_R \}$$

$$\dot{V}_R = \frac{1}{T_A} [K_A (R_f - \frac{K_F}{T_F} E_{fd} - V_t + V_{Ref}) - V_R]$$

$$V_t = [(1 - x'Y)^2 (e_q'^2 + e_d'^2) + 2(1 - x'Y)(x'YV_i)(e'_d \cos\delta) + (x'YV_i)^2]^{1/2}$$

$$S_E(E_{fd}) = A_{sat} \exp [(B_{sat})(E_{fd})]$$

$$Y = \frac{1}{x' + x_e}$$

For the example of chapter 2 the parameters have the following values

$$\begin{array}{ll}
 H = 5.0 \text{ sec} & T_A = 0.06 \text{ sec} \\
 D = 2.0 \text{ pu} & T_E = 0.5 \text{ sec} \\
 x_d = 1.2 \text{ pu} & T_F = 1.0 \text{ sec} \\
 x_q = 1.0 \text{ pu} & K_A = 25 \\
 x' = 0.25 \text{ pu} & K_E = -0.0445 \\
 x_e = 0.25 \text{ pu} & K_F = 0.16 \\
 T'_{d0} = 5.0 \text{ sec} & A_{\text{sat}} = 0.001123 \\
 T'_{q0} = 0.50 \text{ sec} & B_{\text{sat}} = 0.3043
 \end{array}$$

The operating point is defined by

$$\begin{array}{l}
 \bar{V}_i = 1. + j0. \text{ p.u.} \\
 \bar{V}_t = 1. + j0.2 \text{ p.u.} \\
 \bar{S}_g = 0.8 + j0.1608 \text{ p.u.} \\
 V_{\text{Ref}} = 1. \text{ p.u.}
 \end{array}$$

With these parameters linearization of the model gives the following state matrix

$$\begin{bmatrix}
 -0.58 & 0 & 0 & -0.269 & 0 & 0.2 & 0 \\
 0 & -1.0 & 0 & 0 & 0 & 0.16 & 0 \\
 0 & 0 & -5.0 & 2.12 & 0 & 0 & 0 \\
 0 & 0 & 0 & 0 & 377 & 0 & 0 \\
 -0.141 & 0 & 0.141 & -0.2 & -0.28 & 0 & 0 \\
 0 & 0 & 0 & 0 & 0 & 0.0838 & 2.0 \\
 -173 & 417 & -116 & 40.9 & 0 & -66.7 & -16.7
 \end{bmatrix}$$

APPENDIX B. MATRIX A OF $\ddot{\delta} = A\delta$ FOR THE 48 MACHINE SYSTEM

[illegible]

[illegible]

	25	26	27	28	29	30	31	32
1.	0.001	0.001	0.038	0.000	0.000	0.000	0.001	0.000
2.	0.001	0.001	0.032	0.000	0.000	0.000	0.001	0.000
3.	0.000	0.000	0.014	0.000	0.000	0.000	0.000	0.000
4.	0.001	0.001	0.026	0.000	0.000	0.000	0.001	0.000
5.	0.000	0.000	0.003	0.000	0.000	0.000	0.000	0.000
6.	0.000	0.000	0.011	0.000	0.000	0.000	0.000	0.000
7.	0.000	0.000	0.012	0.000	0.000	0.000	0.000	0.000
8.	0.000	0.000	0.009	0.000	0.000	0.000	0.000	0.000
9.	0.002	0.001	0.035	0.000	0.000	0.000	0.001	0.000
10.	0.005	0.005	0.075	0.000	0.000	0.000	0.005	0.001
11.	0.001	0.002	0.012	0.000	0.000	0.000	0.003	0.001
12.	0.002	0.002	0.018	0.000	0.000	0.000	0.004	0.001
13.	0.002	0.005	0.023	0.000	0.000	0.000	0.009	0.001
14.	0.005	0.018	0.038	0.000	0.000	0.000	0.012	0.001
15.	0.001	0.002	0.005	0.000	0.000	0.000	0.011	0.002
16.	0.001	0.001	0.003	0.000	0.000	0.000	0.026	0.003
17.	-0.000	-0.000	-0.003	0.000	0.000	0.000	0.023	0.004
18.	0.001	0.001	0.003	0.000	0.000	0.000	0.024	0.003
19.	0.001	0.002	0.005	0.000	0.000	0.000	0.041	0.005
20.	0.001	0.001	0.004	0.000	0.000	0.000	0.029	0.004
21.	0.001	0.001	0.003	0.000	0.000	0.000	0.016	0.002
22.	0.002	0.001	0.004	0.000	0.000	0.000	0.024	0.003
23.	0.007	0.006	0.014	0.000	0.000	0.000	0.015	0.002
24.	0.044	0.028	0.046	0.000	0.000	0.000	0.012	0.001
25.	-0.259	0.036	0.035	0.000	0.000	0.000	0.005	0.001
26.	0.027	-0.208	0.025	0.000	0.000	0.000	0.005	0.001
27.	0.001	0.001	-0.170	0.041	0.017	0.021	0.001	0.000
28.	0.000	0.000	0.239	-0.241	0.000	0.000	0.000	0.000
29.	0.000	0.000	0.194	0.001	-0.196	0.000	0.000	0.000
30.	0.000	0.000	0.300	0.001	0.000	-0.303	0.000	0.000
31.	0.001	0.001	0.003	0.000	0.000	0.000	-0.258	0.025
32.	0.000	0.000	0.000	0.000	0.000	0.000	0.015	-0.169
33.	0.000	0.000	0.001	0.000	0.000	0.000	0.043	0.017
34.	0.000	0.000	0.000	0.000	0.000	0.000	0.007	0.004
35.	0.000	0.000	0.000	0.000	0.000	0.000	0.010	0.005
36.	0.000	0.000	0.001	0.000	0.000	0.000	0.007	0.003
37.	0.000	0.000	0.000	0.000	0.000	0.000	0.006	0.066
38.	0.000	0.000	0.000	0.000	0.000	0.000	0.005	0.048
39.	0.000	0.000	0.000	0.000	0.000	0.000	0.000	0.001
40.	0.000	0.000	0.000	0.000	0.000	0.000	0.003	0.029
41.	0.000	0.000	0.000	0.000	0.000	0.000	0.001	0.005
42.	0.000	0.000	0.000	-0.000	-0.000	-0.000	0.003	0.027
43.	0.001	0.000	0.077	0.000	0.000	0.000	0.000	0.000
44.	0.000	0.000	0.003	0.000	0.000	0.000	0.000	0.000
45.	0.004	0.003	0.007	0.000	0.000	0.000	0.002	0.000
46.	0.000	0.000	0.006	0.000	0.000	0.000	0.000	0.001
47.	0.006	0.004	0.011	0.000	0.000	0.000	0.021	0.003
48.	0.000	0.000	0.001	0.000	0.000	0.000	0.000	0.001

	33	34	35	36	37	38	39	40
1.	0.000	0.000	0.000	0.000	0.000	0.000	0.000	0.000
2.	0.000	0.000	0.000	0.000	0.000	0.000	0.000	0.000
3.	0.000	0.000	0.000	0.000	0.000	0.000	0.000	0.000
4.	0.000	0.000	0.000	0.000	0.000	0.000	0.000	0.000
5.	0.000	0.000	0.000	0.000	0.000	0.000	0.000	0.000
6.	0.000	0.000	0.000	0.000	0.000	0.000	0.000	0.000
7.	0.000	0.000	0.000	0.000	0.000	0.000	0.000	0.000
8.	0.000	0.000	0.000	0.000	0.000	0.000	0.000	0.000
9.	0.000	0.000	0.000	0.001	0.000	0.000	0.000	0.000
10.	0.002	0.000	0.000	0.004	0.000	0.000	0.000	0.000
11.	0.004	0.000	0.000	0.029	0.000	0.000	0.000	0.000
12.	0.006	0.000	0.000	0.045	0.000	0.000	0.000	0.000
13.	0.003	0.000	0.000	0.002	0.000	0.000	0.000	0.000
14.	0.005	0.000	0.000	0.004	0.000	0.000	0.000	0.000
15.	0.003	0.000	0.000	0.001	0.000	0.000	0.000	0.000
16.	0.008	0.001	0.001	0.002	0.001	0.000	0.000	0.001
17.	-0.003	0.000	-0.000	0.001	0.000	0.000	0.000	0.000
18.	0.006	0.000	0.001	0.001	0.001	0.000	0.000	0.000
19.	0.013	0.001	0.001	0.002	0.001	0.001	0.001	0.001
20.	0.009	0.001	0.001	0.002	0.001	0.000	0.000	0.001
21.	0.005	0.000	0.000	0.001	0.000	0.000	0.000	0.000
22.	0.008	0.000	0.001	0.001	0.001	0.000	0.000	0.001
23.	0.005	0.000	0.000	0.001	0.000	0.000	0.000	0.000
24.	0.004	0.000	0.000	0.002	0.000	0.000	0.000	0.000
25.	0.002	0.000	0.000	0.002	0.000	0.000	0.000	0.000
26.	0.002	0.000	0.000	0.001	0.000	0.000	0.000	0.000
27.	0.000	0.000	0.000	0.000	0.000	0.000	0.000	0.000
28.	0.000	0.000	0.000	0.000	0.000	0.000	0.000	0.000
29.	0.000	0.000	0.000	0.000	0.000	0.000	0.000	0.000
30.	0.000	0.000	0.000	0.000	0.000	0.000	0.000	0.000
31.	0.063	0.004	0.006	0.010	0.005	0.003	0.003	0.004
32.	0.013	0.001	0.002	0.002	0.036	0.017	0.016	0.022
33.	-0.172	0.013	0.020	0.034	0.004	0.002	0.002	0.003
34.	0.036	-0.127	0.067	0.006	0.001	0.000	0.000	0.001
35.	0.048	0.057	-0.139	0.007	0.001	0.001	0.001	0.001
36.	0.037	0.002	0.003	-0.076	0.001	0.000	0.000	0.000
37.	0.005	0.000	0.001	0.001	-0.280	0.044	0.042	0.030
38.	0.004	0.000	0.000	0.001	0.068	-0.316	0.064	0.040
39.	0.000	0.000	0.000	0.000	0.002	0.002	-0.013	0.001
40.	0.003	0.000	0.000	0.001	0.021	0.018	0.021	-0.142
41.	0.001	0.000	0.000	0.000	0.006	0.005	0.009	0.003
42.	0.002	0.000	0.000	0.000	0.035	0.023	0.091	0.027
43.	0.000	0.000	0.000	0.000	0.000	0.000	0.000	0.000
44.	0.000	0.000	0.000	0.000	0.000	0.000	0.000	0.000
45.	0.001	0.000	0.000	0.000	0.000	0.000	0.000	0.000
46.	0.000	0.000	0.000	0.000	0.001	0.000	0.000	0.000
47.	0.007	0.000	0.001	0.001	0.001	0.000	0.000	0.000
48.	0.000	0.000	0.000	0.000	0.001	0.001	0.001	0.000

	41	42	43	44	45	46	47	48
1.	0.000	0.000	0.000	0.001	0.001	0.000	0.000	0.000
2.	0.000	0.000	0.000	0.001	0.001	0.000	0.000	0.000
3.	0.000	0.000	0.000	0.001	0.001	0.000	0.000	0.000
4.	0.000	0.000	0.000	0.001	0.001	0.000	0.000	0.000
5.	0.000	0.000	0.000	0.000	0.000	0.000	0.000	0.000
6.	0.000	0.000	0.000	0.000	0.001	0.000	0.000	0.000
7.	0.000	0.000	0.000	0.001	0.001	0.000	0.000	0.000
8.	0.000	0.000	0.000	0.000	0.001	0.000	0.000	0.000
9.	0.000	0.000	0.000	0.001	0.002	0.001	0.000	0.000
10.	0.000	0.000	0.001	0.003	0.005	0.001	0.001	0.001
11.	0.000	0.000	0.000	0.001	0.002	0.000	0.000	0.000
12.	0.000	0.000	0.000	0.001	0.002	0.000	0.000	0.000
13.	0.000	0.000	0.000	0.001	0.003	0.001	0.001	0.001
14.	0.000	0.000	0.001	0.002	0.004	0.001	0.001	0.001
15.	0.000	0.000	0.000	0.001	0.003	0.001	0.001	0.001
16.	0.000	0.000	0.000	0.001	0.002	0.000	0.001	0.001
17.	0.000	0.000	-0.000	0.001	0.003	0.000	0.002	0.001
18.	0.000	0.000	0.000	0.001	0.003	0.000	0.002	0.001
19.	0.000	0.000	0.000	0.002	0.006	0.001	0.004	0.003
20.	0.000	0.000	0.000	0.001	0.005	0.001	0.004	0.002
21.	0.000	0.000	0.000	0.004	0.021	0.003	0.021	0.011
22.	0.000	0.000	0.000	0.004	0.021	0.003	0.020	0.011
23.	0.000	0.000	0.001	0.005	0.011	0.002	0.002	0.002
24.	0.000	0.000	0.005	0.025	0.059	0.011	0.006	0.007
25.	0.000	0.000	0.002	0.012	0.032	0.006	0.003	0.003
26.	0.000	0.000	0.001	0.005	0.013	0.002	0.001	0.001
27.	0.000	0.000	0.009	0.022	0.002	0.005	0.000	0.003
28.	0.000	0.000	0.000	0.000	0.000	0.000	0.000	0.000
29.	0.000	0.000	0.000	0.000	0.000	0.000	0.000	0.000
30.	0.000	0.000	0.000	0.000	0.000	0.000	0.000	0.000
31.	0.002	0.002	0.000	0.001	0.002	0.000	0.001	0.002
32.	0.012	0.011	0.000	0.001	0.000	0.001	0.000	0.003
33.	0.002	0.001	0.000	0.000	0.000	0.000	0.000	0.001
34.	0.000	0.000	0.000	0.000	0.000	0.000	0.000	0.000
35.	0.000	0.000	0.000	0.000	0.000	0.000	0.000	0.000
36.	0.000	0.000	0.000	0.000	0.000	0.000	0.000	0.000
37.	0.024	0.026	0.000	0.002	0.000	0.002	0.000	0.025
38.	0.031	0.032	0.000	0.002	0.000	0.001	0.000	0.016
39.	0.002	0.003	0.000	0.000	0.000	0.000	0.000	0.001
40.	0.022	0.014	0.000	0.001	0.000	0.001	0.000	0.006
41.	-0.060	0.006	0.000	0.002	0.000	0.001	0.000	0.016
42.	0.036	-0.264	0.000	0.001	0.000	0.001	0.000	0.009
43.	0.001	0.000	-0.478	0.267	0.010	0.064	0.000	0.049
44.	0.000	0.000	0.005	-0.052	0.003	0.034	0.000	0.005
45.	0.000	0.000	0.004	0.070	-0.228	0.057	0.015	0.021
46.	0.002	0.000	0.011	0.325	0.022	-0.405	0.001	0.032
47.	0.000	0.000	0.003	0.034	0.203	0.025	-0.769	0.116
48.	0.003	0.000	0.001	0.006	0.001	0.003	0.000	-0.020

VITA

Bozidar Avramovic was born in Pranjani, Yugoslavia in 1949. He received the Diploma of Electrical Engineering and the Master of Science degree in Electrical Engineering from the University of Belgrade, Yugoslavia, in 1973 and 1978, respectively.

From June 1973 until March 1974 he was with the System Analysis Group of Brown Boveri & Cie, Baden, Switzerland, where he was involved in the development of a Power System State Estimator and a package of programs for sparse matrices. From 1974 until June 1977 he was with the System Analysis Group of the Institute Mihailo Pupin, Yugoslavia. His responsibilities were in the development of the Power System Security Analysis Methods. Since 1977 he has been with the Decision and Control Laboratory at the Coordinated Science Laboratory, University of Illinois, where he has been working on the analysis of large scale systems and power systems in particular.

Mr. Avramovic is a member of the Institute of Electrical and Electronics Engineers.

PUBLICATIONS

1. J. Medanic and B. Avramovic, " ϵ -Coupling Method for the Solution of Load-Flow Problems in Power Systems," Proc. IEE, Vol. 122, No. 8, August 1975.
2. B. Avramovic, "Analysis of Power Systems in Normal and Alert States," Proc. of the Symp. on Power System Analysis, JUGEL, October 1975.
3. J. Medanic, B. Avramovic, M. Ilic, and V. Todorovic, "Methodology for Power System Security Analysis," final report to the Serbian Power Association (ZEPS), Belgrade, 1977.
4. B. Avramovic, "An Approach to the Solution of the Load Flow Equations," M.S. thesis, University of Belgrade, 1978.
5. B. Avramovic, "Subspace Iteration Approach to the Time Scale Separation," Proc. of the 18th IEEE Conf. on Decision and Control, Fort Lauderdale, Florida, December 1979, pp. 684-687.
6. B. Avramovic, P. V. Kokotovic, J. R. Winkelman, and J. H. Chow, "Area Decomposition for Electromechanical Models of Power Systems," 2nd IFAC Symp. on Large Scale Systems, Toulouse, France, 1980; also to appear in Automatica, November 1980.
7. P. V. Kokotovic, B. Avramovic, J. H. Chow, and J. Winkelman, "Singular Perturbations and Multitime Analysis of Power Systems," presented at the International Conf. on Electric Power Problems: The Mathematical Challenge, Seattle, Washington, March 1980.
8. J. Winkelman, J. Chow, B. Bowler, B. Avramovic, and P. Kokotovic, "An Analysis of Interarea Dynamics of Multimachine Systems," to appear in IEEE Trans. on Power Apparatus and Systems; also accepted for presentation at 1980 Summer Meeting, Minneapolis, Minnesota, July 13-18, Paper #80 SM 533-0.

3-8

DT